Robust Evidence of Unidentified Anomalous Phenomena

in Pre-Satellite Era Night-Sky Images

Marik von Rennenkampff

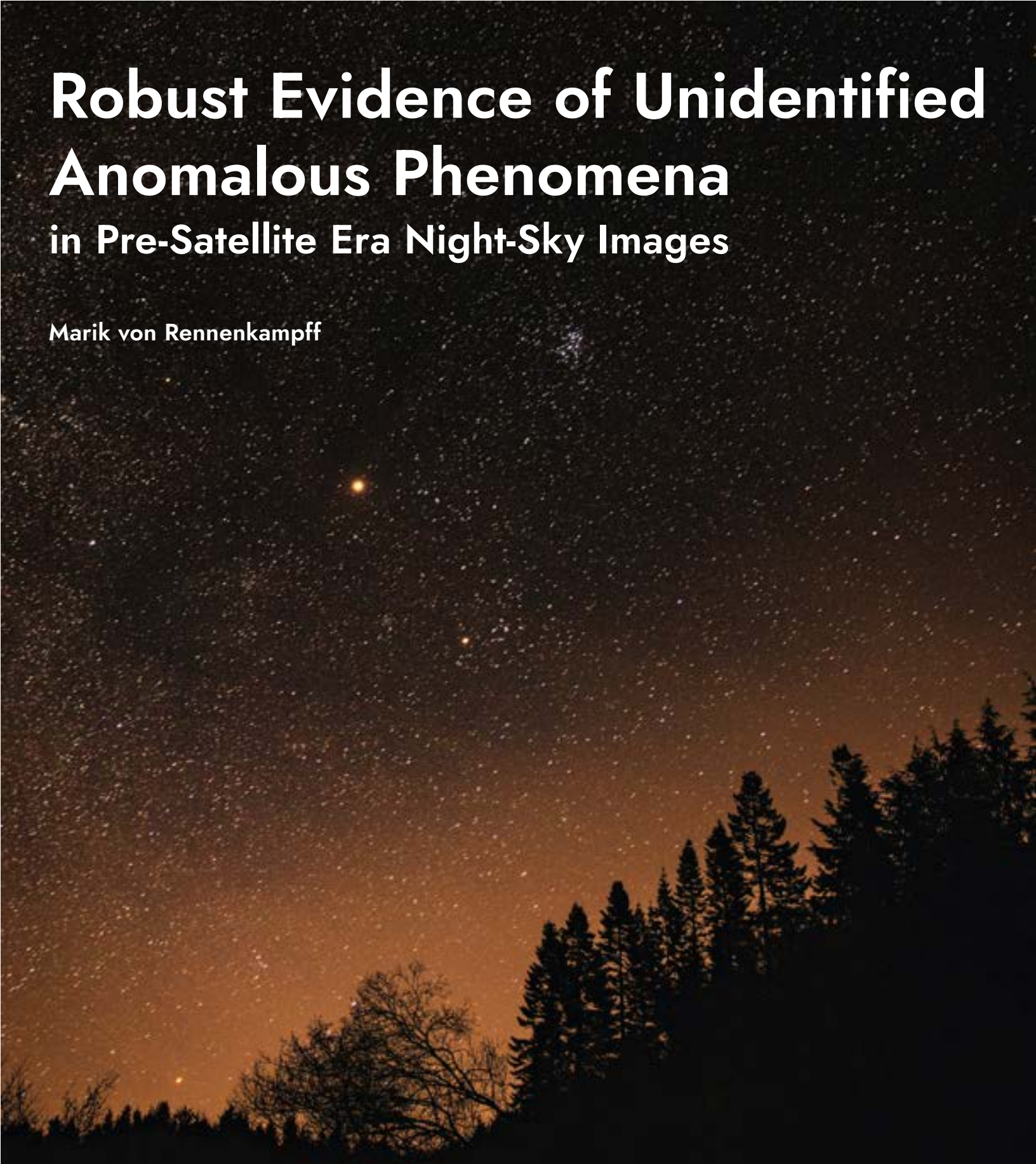

The Sol Foundation Science and Policy Briefings
No. 1

Contents

Executive Summary

Swedish astronomer Beatriz Villarroel has recently shown that photographs of surveys of the night sky taken between 1949 and 1957, in the pre-satellite era, contain hundreds of thousands of temporary star-like points of light, called "transients," that do not appear in other images of the sky. By using the Earth's shadow as a filter, Villarroel and her colleagues have demonstrated with exceptionally high statistical confidence that tens of thousands of these "transients" are not optical artifacts or defects. Instead, they are likely brief (<1 second) glint-like reflections of the sun off objects of unknown origin with flat, highly reflective surfaces. These objects must be at least several hundred kilometers, and most likely tens of thousands of kilometers, above Earth. These scientists also discovered a statistically significant association among (1) observations of such "transients," (2) nuclear tests, and (3) historical UAP reporting. Villarroel and her colleagues outline these findings and methodologies in three peer-reviewed papers, published in three respected, widely cited, independent scientific journals. This briefing summarizes these findings as well as their implications for continued congressional engagement with UAP, particularly through the sweeping transparency measures in the Schumer–Rounds UAP Disclosure Act (SA 3111) and companion legislation in the House of Representatives.

1. First Paper: "Aligned, Multiple- Transient Events in the First Palomar Sky Survey"[1]

Villarroel and her colleagues employ an innovative method, using the Earth's shadow (umbra) as a filter, to find star-like "transients" in the sky. They find a remarkably statistically significant ($21.9\sigma^2$) lack of transients in the Earth's shadow compared to the rest of the sky. This indicates the presence of thousands of light-reflecting objects high above Earth in the pre-satellite era.

Critically, the "Earth shadow" test eliminates photographic defects and other instrumental errors as explanations for the transient glints. Moreover, the optical nature of the transients indicates that the phenomena that caused them must have been at least "several hundred kilometers" above the Earth's surface. This rules out aircraft, high-altitude balloons, and other man-made objects as explanations for the transients. These star-like flashes are associated with very flat and highly reflective surfaces (e.g., glass, mirrors, certain polymers) of objects orbiting Earth. Natural objects such as asteroids, in contrast, produce streaks in photographic astronomical surveys due to their rough and matte surfaces.

In several instances, multiple transients appear to form a line. This suggests linear movement by an object or multiple objects traveling in formation. The most statistically significant alignment of transients coincides with the July 1952 Washington, D.C., UAP incidents. These incursions, which occurred over two successive weekends and involved pilot observations corroborated by radar tracks from multiple stations, caused significant concern in the Truman White House and senior Air Force leadership.[3] In early 1953, as a direct result of the July 1952

Washington, D.C., incidents, the US government's executive branch adopted a formal policy of "debunking" UAP sightings, regardless of witness credibility or supporting data.[4]

Historical Note: The most authoritative US government analyses of UAP from 1947–1952 (i.e., contemporaneous with the astronomical observations of transients in Paper 1) describe disc-shaped "metallic," "silver," and "light reflecting" objects with a "round top" and a "flat bottom."[5] This morphology is ideally suited to reflect sunlight in the manner suggested in Villaorrel's first paper. Notably, the modern UAP era formally began on June 24, 1947, when pilot Kenneth Arnold observed a "bright flash" of sunlight reflecting from one of nine disc-like objects flying in formation over Washington state.[6]

2. Second Paper: "Transients in the Palomar Observatory Sky Survey (POSS-I) May Be Associated with Nuclear Testing and Reports of Unidentified Anomalous Phenomena"[7]

In a second paper, Villarroel, first author Steven Bruehl, and their colleagues find a statistically significant correlation among: (1) observations of transients, (2) nuclear tests, and (3) historical UAP reports. These findings add empirical evidence to a long, well-documented nexus between UAP and nuclear weapons. They also provide robust empirical support for historical UAP reporting by eyewitnesses, which has long been dismissed by skeptics for lacking data.

This analysis compares more than 100,000 transients observed during a period in the pre-satellite era (1949–1957) to contemporaneous nuclear tests. Bruehl and Villarroel find that transients are 45 percent more likely to be observed on dates within one day of a nuclear test than on dates not associated with a nuclear test. The strongest statistical link between transient observations and nuclear tests is detected on the date immediately after a nuclear test.

Bruehl and Villarroel also find a statistically significant association, beyond chance, between the number of transients observed on a given date and eyewitness UAP reports (based on a comprehensive historical database of such reports) on the same date.

Importantly, dates with: (1) no eyewitness UAP reports and (2) which were not within one day of a nuclear test are associated with the fewest total observed transients.

In contrast, dates with: (1) at least one eyewitness UAP report and (2) within one day of a nuclear test displayed the highest total number of transients.

These statistically significant correlations bolster the case for the association between UAP and nuclear weapons and energy, as well as the reliability of many eyewitness reports of UAP. These findings also constitute further evidence that transients are not photographic or optical artifacts, but rather glint-like reflections of the sun off objects of unknown origin in orbit above Earth.

Note on UAP and Nuclear Weapons: Declassified and unclassified US government records, contemporaneous newspaper reporting, and credible witness accounts already show a robust, decades-long link between UAP activity and nuclear weapons and assets. Readers are encouraged to review Robert Hastings's comprehensive study of the UAP–nuclear nexus, *UFOs and Nukes.*[8]

3. Third Paper: "A Cost-Effective Search for Extraterrestrial Probes in the Solar System"[9]

A third paper presents novel and innovative techniques to search for extraterrestrial artifacts near Earth. Scientists place particular emphasis on methods of observation that are uncontaminated by thousands of man-made satellites and millions of reflective pieces of space debris. These include: (1) examining pre-Sputnik astronomical images and surveys,[10] (2) utilizing space-based telescopes, (3) prioritizing analysis and examination of unknown objects based on color and reflectivity characteristics,[11] and (4) using the Earth's shadow as a filter to identify self-luminous objects in orbit.

4. Policy Implications and Recommendations

While Congress and the executive branch are rightly concerned with the national security implications of present-day UAP reports, Villarroel and her colleagues' findings are a stark reminder that UAP activity dates back several decades and has been of concern to the Department of Defense and Intelligence Community for as long as it has been reported. As Senator Chuck Schumer stated in a December 13, 2023, colloquy with Senator Micheal Rounds, "the United States government has gathered a great deal of information about UAPs over many decades but has refused to share it with the American people."[12]

Villarroel's peer-reviewed scientific discoveries additionally provide empirical support to the core allegation of the Schumer–Rounds UAP Disclosure Act: that a surreptitious, decades-old classified program has retrieved and attempted to reverse-engineer UAP vehicles outside of congressional and even relevant executive branch oversight. Public testimony from former intelligence officials and contractors, some of which undoubtedly informed the Disclosure Act, indicates that elements of the executive branch began retrieving UAP in the 1940s and 1950s. As unlikely as it may seem, astronomical surveys indicate the presence of thousands of unknown light-reflecting objects in orbit above Earth during the same period.

With peer-reviewed empirical evidence now corroborating historical UAP reporting, it is imperative that senators and members of Congress support the sweeping transparency measures in the bipartisan UAP Disclosure Act, as well as similar legislation. We urge Congress to make haste in executing its constitutional responsibility to govern federal efforts concerning this matter of world-historical importance.

About the Author

Marik von Rennenkampff is a notable public commentator and analyst of UAP affairs. He served as an appointee in the US Department of Defense during the Obama administration and later worked in the US State Department. He delivers the Sol Briefing, the Sol Foundation's monthly update on UAP news, and has been a regular contributor to The Hill.

Notes

1. Villarroel, Beatriz, et al. "Aligned, Multiple-Transient Events in the First Palomar Sky Survey." Publications of the Astronomical Society of the Pacific 137, no. 10 (2025): 104504. https://doi.org/10.1088/1538-3873/ae0afe. For a firsthand account of the Truman White House's reaction to the 1952 Washington, D.C., incidents and the Air Force's public response, see Edward Ruppelt, The Report on Unidentified Flying Objects (Doubleday/Cosimo Classics, New York, 2011 [1956]).

2. In astronomy and physics, a 3σ result is considered "evidence," while a 5σ result constitutes a "discovery."

3. Carlson, Peter. "50 Years Ago, Unidentified Flying Objects From Way Beyond the Beltway Seized the Capital's Imagination." Washington Post, 20 July 2002. https://www.washingtonpost.com/archive/lifestyle/2002/07/21/50-years-ago-unidentified-flying-objects-from-way-beyond-the-beltway-seized-the-capitals-imagination/59f74156-51f4-4204-96df-e12be061d3f8/.

4. Central Intelligence Agency. "Report of Meetings of Scientific Advisory Panel on Unidentified Flying Objects." 18 January 1953. https://www.cia.gov/readingroom/docs/CIA-RDP79B00752A000300100010-4.pdf. https://www.cia.gov/readingroom/docs/CIA-RDP81R00560R000100030027-0.pdf.

5. Twining, Nathan F. "AMC Opinion Concerning 'Flying Disks.'" 23 September 1947. https://s3.documentcloud.org/documents/20797978/twining-memo.pdf; US Air Force. "Analysis of Flying Object Incidents in the United States." 10 December 1948. https://documents2.theblackvault.com/documents/100-203-79.pdf.

6. For Kenneth Arnold's "bright flash," see Lee, Russell. "1947: Year of the Flying Saucer." Smithsonian National Air and Space Museum, 24 June 2022. https://airandspace.si.edu/stories/editorial/1947-year-flying-saucer.

7. Bruehl, Steven, and Beatriz Villarroel. "Transients in the Palomar Observatory Sky Survey (POSS-I) May Be Associated with Nuclear Testing and Reports of Unidentified Anomalous Phenomena." Scientific Reports (Nature) 15 (2025): 34125. https://doi.org/10.1038/s41598-025-21620-3.

8. Robert Hastings, UFOs and Nukes: Extraordinary Encounters at Nuclear Weapons Sites, 2nd ed.

(self-pub., CreateSpace, 2017). For a brief overview of this phenomenon, see Marik von Rennenkampff, "The Shocking History of UFOs and Nuclear Weapons." The Hill, 15 April 2024. https://thehill.com/opinion/technology/4588030-the-shocking-history-of-ufos-and-nuclear-weapons/amp/.

9. Beatriz Villarroel et al. "A Cost-Effective Search for Extraterrestrial Probes in the Solar System." Monthly Notices of the Royal Astronomical Society (2025): staf1158. https://doi.org/10.1093/mnras/staf1158.

10. See the first and second papers discussed here.

11. Long-term exposure of metallic objects to the effects of space will cause reddening and decreased reflectivity.

12. Senate Democrats. "Majority Leader Schumer and Republican Senator Mike Rounds Floor Colloquy on Unidentified Anomalous Phenomena Provisions in the NDAA and Future Legislation on UAPs." 13 December 2023. https://www.democrats.senate.gov/newsroom/press-releases/majority-leader-schumer-and-republican-senator-mike-rounds-floor-colloquy-on-unidentified-anomalous-phenomena-provisions-in-the-ndaa-and-future-legislation-on-uaps.

Bibliography

Bruehl, Steven, and Beatriz Villarroel. "Transients in the Palomar Observatory Sky Survey (POSS-I) May Be Associated with Nuclear Testing and Reports of Unidentified Anomalous Phenomena." Scientific Reports 15 (2025): 34125. https://doi.org/10.1038/s41598-025-21620-3.

Carlson, Peter. "50 Years Ago, Unidentified Flying Objects From Way Beyond the Beltway Seized the Capital's Imagination." Washington Post, 20 July 2002. https://www.washingtonpost.com/archive/lifestyle/2002/07/21/50-years-ago-unidentified-flying-objects-from-way-beyond-the-beltway-seized-the-capitals-imagination/59f74156-51f4-4204-96df-e12be061d3f8/.

Central Intelligence Agency. "Report of Meetings of Scientific Advisory Panel on Unidentified Flying Objects." 18 January 1953. https://www.cia.gov/readingroom/docs/CIA-RDP79B00752A000300100010-4.pdf.

Hastings, Robert. UFOs & Nukes: Extraordinary Encounters at Nuclear Weapons Sites. 2nd ed. Self-published, CreateSpace, 2017.

Lee, Russell. "1947: Year of the Flying Saucer." Smithsonian National Air and Space Museum, 24 June 2022. https://airandspace.si.edu/stories/editorial/1947-year-flying-saucer.

Ruppelt, Edward. The Report on Unidentified Flying Objects. Doubleday/Cosimo Classics, New York, 2011 [1956].

Senate Democrats. "Majority Leader Schumer and Republican Senator Mike Rounds Floor Colloquy on Unidentified Anomalous Phenomena Provisions in the NDAA and Future Legislation on UAPs." 13 December 2023. https://www.democrats.senate.gov/newsroom/press-releases/majority-leader-schumer-and-republican-senator-mike-rounds-floor-colloquy-on-unidentified-anomalous-phenomena-provisions-in-the-ndaa-and-future-legislation-on-uaps.

Twining, Nathan F. "AMC Opinion Concerning 'Flying Discs.'" 23 September 1947. https://s3.documentcloud.org/documents/20797978/twining-memo.pdf

US Air Force. "Analysis of Flying Object Incidents in the United States." 10 December 1948. https://documents2.theblackvault.com/documents/100-203-79.pdf.

Villarroel, Beatriz, Enrique Solano, Hichem Guergouri, et al. "Aligned, Multiple-Transient Events in the First Palomar Sky Survey." Publications of the Astronomical Society of the Pacific 137, no. 10 (2025): 104504. https://doi.org/10.1088/1538-3873/ae0afe.

Villarroel, Beatriz, Wesley A. Watters, Alina Streblyanska, Enrique Solano, Stefan Geier, and Lars Mattsson. "A Cost-Effective Search for Extraterrestrial Probes in the Solar System." Monthly Notices of the Royal Astronomical Society (2025): staf1158. https://doi.org/10.1093/mnras/staf1158.

von Rennenkampff, Marik. "The Shocking History of UFOs and Nuclear Weapons." The Hill, 15 April 2024. https://thehill.com/opinion/technology/4588030-the-shocking-history-of-ufos-and-nuclear-weapons/amp/.

The Sol Foundation
www.thesolfoundation.org
information@thesolfoundation.org

Executive Leadership: Dr. Garry Nolan, Dr. Peter Skafish, Maura Mindrila, and Jonathan Berte

Design: Isaac Lopez, Monarch Digital

Publications of the Astronomical Society of the Pacific, 137:104504 (22pp), 2025 October https://doi.org/10.1088/1538-3873/ae0afe

Aligned, Multiple-transient Events in the First Palomar Sky Survey

Beatriz Villarroel[1], Enrique Solano[2,3], Hichem Guergouri[4], Alina Streblyanska[5], Stephen Bruehl[6], Vitaly M. Andruk[7], Lars Mattsson[1], Rudolf E. Bär[8], Jamal Mimouni[9], Stefan Geier[5,10], Alok C. Gupta[11], Vanessa Okororie[12], Khaoula Laggoune[13], Matthew E. Shultz[14], and Robert A. Freitas, Jr.[15]

[1] Nordita, KTH Royal Institute of Technology and Stockholm University, Hannes Alfvéns väg 12, SE-106 91 Stockholm, Sweden
[2] Departamento de Astrofísica, Centro de Astrobiología (CSIC/INTA), PO Box 78, E-28691, Villanueva de la Cañada, Spain
[3] Spanish Virtual Observatory, Spain
[4] Science of the Matter Division. Research Unit in Scientific Mediation, CERIST, Constantine, Algeria
[5] Instituto de Astrofísica de Canarias, Avda Vía Láctea S/N, La Laguna, E-38205, Tenerife, Spain
[6] Department of Anesthesiology, Vanderbilt University Medical Center, 701 Medical Arts Building, 1211 Twenty-First Avenue South, Nashville, TN 37212, USA
[7] Main Astronomical Observatory Observatory of the NAS of Ukraine, 27, Akademika Zabolotnoho St., Kyiv, 03143, Ukraine
[8] Institute for Particle Physics and Astrophysics, ETH Zurich, Wolfgang-Pauli-Strasse 27, CH-8093 Zurich, Switzerland
[9] Department of Physics, University of Constantine-1, LPMPS & CERIST, Constantine, Algeria
[10] Gran Telescopio Canarias (GRANTECAN), Cuesta de San José s/n, 38712 Breña Baja, La Palma, Spain
[11] Aryabhatta Research Institute of Observational Sciences (ARIES), Manora Peak, Nainital, 263 001, India
[12] Center for Basic Space Science, National Space Research and Development Agency, Enugu, Nigeria
[13] Sirius Astronomy Association, Algeria
[14] Department of Physics and Astronomy, University of Delaware, USA
[15] Institute for Molecular Manufacturing, Palo Alto, CA, USA
Received 2025 June 8; revised 2025 September 23; accepted 2025 September 24; published 2025 October 17

Abstract

Old, digitized astronomical images taken before the human spacefaring age offer a rare glimpse of the sky before the era of artificial satellites. In this paper, we present the first optical searches for artificial objects with high specular reflections near the Earth. We follow the method proposed in Villarroel et al. and use a transient sample drawn from Solano et al. We use images from the First Palomar Sky Survey to search for multiple (within a plate exposure) transients that, in addition to being point-like, are aligned along a narrow band. We provide a shortlist of the most promising candidate alignments, including one with $\sim 3.9\sigma$ statistical significance. These aligned transients remain difficult to explain with known phenomena, even if rare optical ghosting producing point-like sources cannot be fully excluded at present. We explore remaining possibilities, including fast reflections from highly reflective objects in geosynchronous orbit, or emissions from artificial sources high above Earth's atmosphere. We also find a highly significant ($\sim 22\sigma$) deficit of POSS-I transients within Earth's shadow when compared with the theoretical hemispheric shadow coverage at 42,164 km altitude. The deficit is still present though at reduced significance ($\sim 7.6\sigma$) when a more realistic plate-based coverage is considered. This study should be viewed as an initial exploration into the potential of archival photographic surveys to reveal transient phenomena, and we hope it motivates more systematic searches across historical data sets.

Unified Astronomy Thesaurus concepts: Search for extraterrestrial intelligence (2127); Transient detection (1957); Surveys (1671); Solar system astronomy (1529)

1. Introduction

Digitized sky surveys have broadened the time window in which we can study changes in the sky. Programs such as the Digital Access to a Sky Century at Harvard (DASCH; Grindlay et al. 2012), the Digital Sky Survey[16] (DSS), the Ukraine Virtual Observatory (JDA UkrVO; Vavilova et al. 2012; Vavilova et al. 2017), and *Carte du Ciel*, provide images of the sky spanning not just a few decades but, in some cases, over 150 yr.

While photographic plates are no longer used for large astronomical surveys—having been replaced by significantly faster and more sensitive CCDs—the archival images still serve important scientific purposes. For example, they allow studies of long-term variability of astronomical sources over timescales of decades or even a century, assuming the object is bright enough to be detected.

Another use of these archives is to search for vanishing stars and other transients. In the Vanishing and Appearing Sources during a Century of Observations (VASCO; Villarroel et al. 2016, 2020) project, images of the sky taken in the early

[16] https://archive.stsci.edu/cgi-bin/dss_form/

1950s, prior to the first anthropogenic satellite, are compared with modern surveys to identify possible sources that may have disappeared. VASCO employs two complementary approaches: first, an automated procedure (Solano et al. 2022) that searches digitized image data from the First and Second Palomar Sky Surveys (POSS-I and POSS-II) for transients; and second, a citizen science project (Villarroel et al. 2022b) where volunteers classify potentially interesting objects. These efforts are facilitated by the Spanish Virtual Observatory[17] and its software tools. The VASCO program has resulted in the cataloging of many thousands of unknown transients, visible only within a single plate exposure (Solano et al. 2022; Villarroel et al. 2022b).

An intriguing finding from the VASCO project was presented in Villarroel et al. (2021): nine faint, star-like objects that appeared and vanished simultaneously on a 1950s POSS-I plate. The central transient was first identified during the visual vetting of 24,000 candidates with small cutout images of fix size, yielding ∼100 vanishing star-candidates, see Table 2 of Villarroel et al. (2020). In a subsequent follow-up of these 100 transients, the image containing nine transients was discovered. The nine transients were not visible on another plate taken half an hour earlier, nor on a third plate six days later. All known astrophysical explanations were considered but deemed implausible. The surface density of such transients was too high to be attributed to any known natural phenomenon. Whether this was due to unknown contamination on the plate with coincidentally star-like defects or a genuine astronomical observation remains unresolved. If real, one explanation could be that they were caused by solar reflections off flat, highly reflective objects in geosynchronous orbit (GSO) around the Earth. Nevertheless, the nine transients on their own are ambiguous, particularly since they are located near the plate edge, where defects are known to accumulate (Hambly & Blair 2024) and where other round objects can also be found. Yet the finding prompts a provocative question: could some of the objects long dismissed as plate defects actually represent reflections or emissions from artificial sources? And, more generally, can pre-Sputnik plates serve as a search domain for non-human artificial objects?

Finding such objects in pre-Sputnik data, would represent a significant discovery with far-reaching implications for both astronomy and humanity, including the possibility of non-terrestrial artifacts (NTAs). It also bears directly on the scientific investigation of Unidentified Anomalous Phenomena (UAPs), formerly known as Unidentified Flying Objects ("UFOs")—a subject that, after decades of stigma, is now gaining serious academic attention, as highlighted in the recent review by Knuth et al. (2025) in *Progress in Aerospace*. Clarifying the origin of these transient events is therefore not only of astrophysical interest but also of potential importance for one of the most enigmatic and consequential questions facing science today.

To add to the intrigue, Solano et al. (2023) recently reported a bright triple transient event occurring on 1952 July 19, found among a set of ∼5000 short-lived POSS-I transients (Solano et al. 2022). This highly curated data set, in which diagnostics based on photometry and morphometric parameters have been carefully applied to the sample to reduce false positives (e.g., plate defects), suggests that the phenomenon of multiple transients can be found even when stringent diagnostic criteria are applied. As in the earlier case with the nine transients, the objects appeared and vanished within a single 50 minutes exposure. Their brightness ($r \sim$ 15–16 mag) makes contamination less likely. Notably, this particular event coincides in time with one of the most extensively documented aerial anomalies in historical records: the Washington D.C. "UFO flap" of 1952 July, which unfolded over two consecutive weekends (July 18–19 and 26–27). While this may be a coincidence, the temporal proximity invites further scrutiny—especially given the rarity of both phenomena. In a separate study Bruehl & Villarroel (2025), we investigate possible statistical associations between historical UAP reports and VASCO transients, and find preliminary evidence of a temporal correlation at the $\sim 3\sigma$ level. While such a finding does not imply causation, it raises the possibility that certain anomalous aerial observations recorded in the pre-satellite era may have had physical counterparts observable in deep-sky imaging.

Given the unusual nature and potential implications of these events, it is essential to test the hypothesis that some transients arise from reflective artificial objects in Earth orbit, and that certain point-like features long dismissed as plate defects may in fact be solar reflections from artificial surfaces. Searches for extraterrestrial probes were proposed as early as the 1960s (Bracewell 1960), but to date only a few searches for NTAs have been attempted or proposed (Freitas & Valdes 1980; Valdes & Freitas 1983; Freitas & Valdes 1985; Haqq-Misra & Kopparapu 2012).

In a previous white paper, Villarroel et al. (2022a) proposed a methodology to search for solar reflections from artificial objects in GSO using photographic plates from before the satellite era (pre-1957). One key signature is the presence of several point-like transients that are aligned along a line within a single exposure. A statistical framework was also developed to assess the significance of such alignments.

In this paper, we carry out that test. We apply the published methodology and statistical framework to a published sample of POSS-I transients from Solano et al. (2022).

We identify several promising candidates and examine them in detail in Section 5. Assuming the events are real, we use the aligned transients to infer the possible geometry and surface density of reflective objects near GSO. We also perform a statistical test to evaluate whether sunlight is required to

[17] http://svo.cab.inta-csic.es

produce these transients, based on their detection rate within Earth's shadow. Finally, we discuss prospects for detecting similar objects in modern digital sky surveys.

2. Plate Defect or Technosignature?

One of the core challenges in our work is the contamination of photographic plates by artifacts that may mimic astronomical sources. Apparent transient events in these plates often present a case of degeneracy—where genuine astrophysical signals and mundane defects can appear strikingly similar. Certain plate defects are known to resemble stellar profiles (Greiner et al. 1990), and distinguishing them from authentic observations remains a nontrivial task, even when full-width-half-maximum (FWHM) comparisons are applied. Moreover, defects can cluster near plate edges, and vignetting or uneven development may further confound interpretation. Nevertheless, visual inspection and photometric profile analysis remain indispensable tools in this early phase of exploration.

Rigorous diagnostics with quantitative measurements are central to any search for genuine transients in photographic plates, as overly permissive criteria inevitably admit large amounts of noise. For that reason, we shall use carefully selected transient samples in Solano et al. (2022), which average 167 transients per plate and have been matched to several modern surveys to remove variable stars, asteroids, and comets.

It is scientifically untenable to assume that all candidates are either authentic transients or all defects. A reasonable working assumption is that both populations are present in some unknown proportion. From this perspective, even a single authentic detection among many contaminants would validate the effort and warrant continued search.

This degeneracy is intrinsic to any attempt at identifying NTAs in archival material. Two primary examples illustrate this problem:

1. *Narrower FWHMs and rounder profiles.* Hambly & Blair (2024) interpret slightly more concentrated, round profiles as signs of spurious detections and makes an example with Villarroel et al. (2021). However, atmospheric seeing and short-lived (sub-second to few-second) optical events are also expected to produce narrower FWHMs than long-exposed stars (Tokovinin 2002; Villarroel et al. 2025a). Thus, profile sharpness alone cannot conclusively distinguish between artifact and astrophysical origin. We note, in passing, that Hambly & Blair (2024) have not attempted to apply their analysis to the triple transient reported by Solano et al. (2023), which might have provided a more stringent test of their conclusions.
2. *Spatial distributions.* A high number density of transient-like features in one region could be mistaken for evidence of poor plate quality. But the number density of transients on a plate is not diagnostic. If NTAs exist in coordinated swarms, these swarms could span tens of square degrees, easily covering entire plates, while a grid of NTAs could cover the entire sky.[18] In ambiguous and uncertain cases—such as the plate analyzed in Villarroel et al. (2021)—additional transients or artifacts may surround the nine candidates (see Supplementary Information of mentioned paper). Their presence illustrates the degeneracy problem: authentic events may coexist on the same plate as numerous star-like defects, which makes it essential to apply independent diagnostics such as alignment statistics and Earth's shadow tests.

Because of the ambiguity in these early cases, we advocated for more targeted searches in Villarroel et al. (2022a), emphasizing particularly multiple transients aligned along a line—where statistical analysis can decisively test whether such configurations occur by chance.

Moreover, the temporal correlations between the 1950s transients and both the Washington 1952 UFO events and 124 U.S., Soviet, and British nuclear weapons tests deserve serious attention. Even if individual events remain uncertain, Bruehl & Villarroel (2025) shows statistically significant correlations between subsets of the transient sample in Solano et al. (2022) and historical nuclear activity and aerial anomalies. This alone contradicts the idea that the entire sample consists of plate defects.

Finally, one of the most revealing tests involves Earth's shadow. No matter how asymmetric or irregular the distributions of plate defects may be, they have no plausible reason to avoid the Earth's shadow. In contrast, transients associated with solar reflections would. This shadow test provides a crucial empirical lever to distinguish between physical reflections and random defects—and remains an essential part of any validation framework moving forward.

In this paper, we rely on hypothesis testing across large samples—assessing statistical correlations, spatial alignments, and Earth-shadow sensitivity—offering a robust framework that remains valid even in the presence of substantial stellar-like contamination. In the future, we aim to use AI-driven methods to filter out transients that resemble plate defects or occur in problematic regions of the plates, and to establish an upper limit on the fraction of objects that may represent NTAs. For now, we will use the simplest methods to search for candidates that show signs of solar reflection.

[18] See e.g., Patrick Jackson's sphere network: https://www.amazon.com/Sphere-Network-Mr-Patrick-Jackson/dp/B0DXF1RGL6.

3. Predictions and Expectations

Natural transients occur at a rate several orders of magnitude lower than glints from artificial objects. Even detecting two natural transients within a few arcminutes of each other during a one-hour exposure is extremely unlikely.[19]

In contrast, glints caused by solar reflections from flat, highly reflective surfaces at high altitudes—such as GSOs—could result in multiple, simultaneous point-like transients during a single long-exposure image. If the glints originate from the same object, they may appear aligned along a narrow band or straight line. In simple geometries, the glints could be equidistant and of similar brightness. However, more complex surface structures may lead to irregular spacing and variable flux (e.g., Nir et al. 2021; Villarroel et al. 2022a). Also objects flying in formation or coordinated swarms, might be found along geometric patterns.

Multiple transients in a single image are frequently detected in modern automated surveys. Nearly all transients with durations shorter than 0.5 s are caused by this phenomenon, often originating from satellites or space debris (e.g., Corbett et al. 2020; Nir et al. 2021). These events typically have apparent magnitudes of $r \sim 9$–11. The rate of such artificial glints can reach $\sim$1800 events hr^{-1} sky^{-1} near the equator (Corbett et al. 2020), which would overwhelm any comparable phenomena in modern surveys unless specifically targeted. The red POSS-I plates, reaching $r \sim 20$ mag with $\sim$50 minutes exposures, are still capable of detecting glints as short as 0.5 s, although the flux is diluted by approximately 9 mag.

Plate defects, by contrast, are expected to be randomly shaped and distributed. The chance that several defects simultaneously mimic star-like point sources and align along a narrow band is small. The method proposed in Villarroel et al. (2022a) identifies "simultaneous transients" that appear within the same long-exposure photographic plate and are additionally aligned within a narrow tolerance. This alignment criterion helps distinguish potentially artificial signals from random celestial or instrumental sources.

For example, an image with nine transients inside a 10×10 arcmin^2 box may exhibit a 4-point or 5-point alignment, with a statistical significance between 2.5σ and 3.9σ depending on the geometry. For exact probabilities, we refer the reader to Section 5 in Villarroel et al. (2022a), which uses the statistical framework developed by Edmunds (1981), Edmunds & George (1985). Even 3-point alignments may be considered when the total number of transients in a region is low. Alignments with the lowest probability of occurring by chance should be prioritized for further examination, though not interpreted as conclusive evidence of geosynchronous reflections.

Taken together, these considerations show that the occurrence of aligned, simultaneous transients on photographic plates is an excellent candidate signature of reflective orbital objects, especially in the absence of natural or instrumental explanations.

While alignments of multiple transients provide a statistically robust signature, it is important to note that most glints caused by solar reflections are expected to appear as single, isolated transients on a photographic plate. This follows naturally from the geometry of specular reflection, where a glint is only visible when the orientation of a rotating object briefly aligns with the observer and the Sun. Assuming a large population of such objects in geosynchronous or higher orbits, the majority of events will not repeat and will appear on a single plate only. These point-like flashes may still exhibit perfect PSF shapes and are typically absent in Earth's shadow, further distinguishing them from both natural and instrumental phenomena. Although individual transients carry less statistical weight, the overall rate and behavior of such events can still be used to identify a non-natural origin. As shown in Villarroel et al. (2022a), statistical models incorporating both aligned and non-aligned transients offer complementary routes for detecting technosignatures in historical data.

4. Methods and Selection

We base our analysis on the catalog of 298,165 short-duration transients presented in Solano et al. (2022), detected in red POSS-I plates with typical exposure times of 45–50 minutes. These transients were identified using an automated pipeline developed as part of the VASCO project. For full details on the detection methodology, data characteristics, and vetting steps, we refer readers to Solano et al. (2022).

From this data set, we search for spatial groupings of transients within square boxes of varying sizes, typically ranging from a few arcminutes up to 20′–30′ per side (see typical sizes in Table 2). For each group, we evaluate whether the positions of the transients fall along a straight line (or more precisely a narrow band), within astrometric uncertainties.

We quantify the degree of alignment using the Pearson correlation coefficient α between right ascension and declination. We retain only those candidate alignments where $|\alpha| > 0.99$. We note that the correlation is computed without applying a $\cos(\delta)$ correction to right ascension. Given the small angular separations involved, this has a negligible effect on the ranking of candidate alignments.

Table 1 summarizes the number of aligned groups found with $r \geqslant 3$, $r \geqslant 4$, $r \geqslant 5$, and $r \geqslant 6$ transients, respectively. Because the search boxes vary in size, the number of transients per group is not directly comparable across cases.

[19] We consider the probability of detecting a transient within 1 hr in the POSS-I survey, based on Solano et al. (2022), who identified 298,000 transients over 780 hr of exposure. The chance of finding one transient in a 10 arcmin^2 box in one hour is approximately $\sim$0.0016. The probability of two such transients appearing in the same box is then $p \sim 10^{-6}$.

Table 1
Candidates

Region	$r \geqslant 3$	$r \geqslant 4$	$r \geqslant 5$	$r \geqslant 6$
$0 <$ R.A. $< 100,\ 0 <$ decl. < 90	22	5	⋯	⋯
$100 <$ R.A. $< 200,\ 0 <$ decl. < 90	18	7	⋯	⋯
$200 <$ R.A. $< 300,\ 0 <$ decl. < 90	32	6	1	⋯
$300 <$ R.A. $< 360,\ 0 <$ decl. < 90	11	2	1	⋯
Total	83	20	2	0

Note. Total number of aligned transient candidates identified in each sky region. r is the number of aligned points. Note that $r \geqslant 4$ and $r \geqslant 5$ are subsets of $r \geqslant 3$. R.A. and decl. are in degrees.

All 83 candidates are presented in the Appendix. Visual inspection reveals that duplets and triplets are relatively common. However, rather than evaluate every alignment with $N \geqslant 3$, we focus on higher-confidence candidates with at least four aligned transients.

Many POSS-I plates have been scanned by both DSS and the SuperCOSMOS Sky Survey (Hambly et al. 2001). Since SuperCOSMOS images generally offer higher spatial resolution, we used both sources to verify each alignment. We downloaded FITS images for all candidates with $N \geqslant 4$, selecting image boxes that encompass the full alignment.

In several cases, transients initially appearing as point sources in DSS were revealed—through SuperCOSMOS images—to be either scanning artifacts or round defects likely caused by emulsion flaws. Transients absent from the higher-resolution scan were excluded from further consideration. We thus retained only those candidates that:

1. Show at least four star-like transients in a roughly linear arrangement on the DSS scan;
2. Are confirmed by the corresponding SuperCOSMOS scan. The DSS and SuperCOSMOS scans are independent digitizations of the same physical photographic plate, obtained using different scanners, optics, and digitization procedures. This means that any object visible in both scans is almost certainly a real feature present on the plate emulsion. In contrast, an object visible in only one of the scans is most likely a scanning artifact caused by dust on the scanner glass, digitization noise, or compression effects—not a genuine plate defect. We therefore treat agreement between both scans as a strong indicator of authenticity. Furthermore, we note that some objects that initially appear point-like in DSS images may exhibit subtle asymmetries or deviate from a stellar PSF in the higher-resolution SuperCOSMOS images, leading us to reject them. This procedure helps ensure that the remaining candidates are not spurious artifacts introduced during digitization.

From this refined set, we identify five of the most promising candidates in the northern hemisphere, listed in Table 2.

There are two key ways the search procedure could be improved:

1. *Search area.* Objects in GSO move at $\sim 10''\ \mathrm{s}^{-1}$, or about 10° during a 50 minutes exposure. Our current box size (up to $30'$) is conservative and may miss longer alignments.
2. *Correlation threshold.* The criterion $|\alpha| > 0.99$ is unnecessarily strict and excludes mildly curved or non-ideal alignments.

However, relaxing either parameter would drastically increase the number of candidates—potentially into the tens of thousands—necessitating substantial manual vetting. To address this, we are developing an expansion of the VASCO citizen science platform (Villarroel et al. 2022b) tailored to this task.

5. The Shortlist

The shortlist in Table 2 shows the candidates. Each candidate is shown in Figures 1–5. Here we show only the transients themselves to assist the reader. The same images, but showing the actual alignments, can be found in Figures 6–10. The alignments differ in width; therefore, a dashed double line is shown in some particular cases where the width of the stripe is larger than $1''$.

In some cases—for example, the objects marked with crosses in Candidate 3 and Candidate 5—it is not certain that every transient is a point source, based on inspection of the images. Slight asymmetries in the light profiles are present in a few cases, manifesting as mild elongations (from e.g., movement) or qualitative irregularities in shape.[20] Therefore, the alignment is possibly a combination of transients and plate defects—or objects in the sky within our atmosphere. The reader can inspect the high-resolution images from SuperCosmos.[21] We improve the astrometry for the images using the Terapix *SWarp* procedure. We measure the improved coordinates and the FWHM for each transient; see Table 3. The dates are taken from the STScI DSS Plate Server.

In a few cases, it is possible to derive more than one variant of the alignment—for example, with either a 3-point or a 4-point alignment. In such cases, we show both options separately in the images in Figures 6–10. For the cases in the shortlist, we estimate the probability of a chance alignment; see Section 6.

[20] These asymmetries refer to deviations in morphology, not to the full width at half maximum (FWHM), which varies across the plates due to well-documented instrumental and photochemical effects. As discussed in Villarroel et al. (2025a), the nonlinear response of photographic emulsions causes brighter objects to naturally appear with broader profiles, contributing to the observed FWHM spread.

[21] http://www-wfau.roe.ac.uk/sss/pixel.html

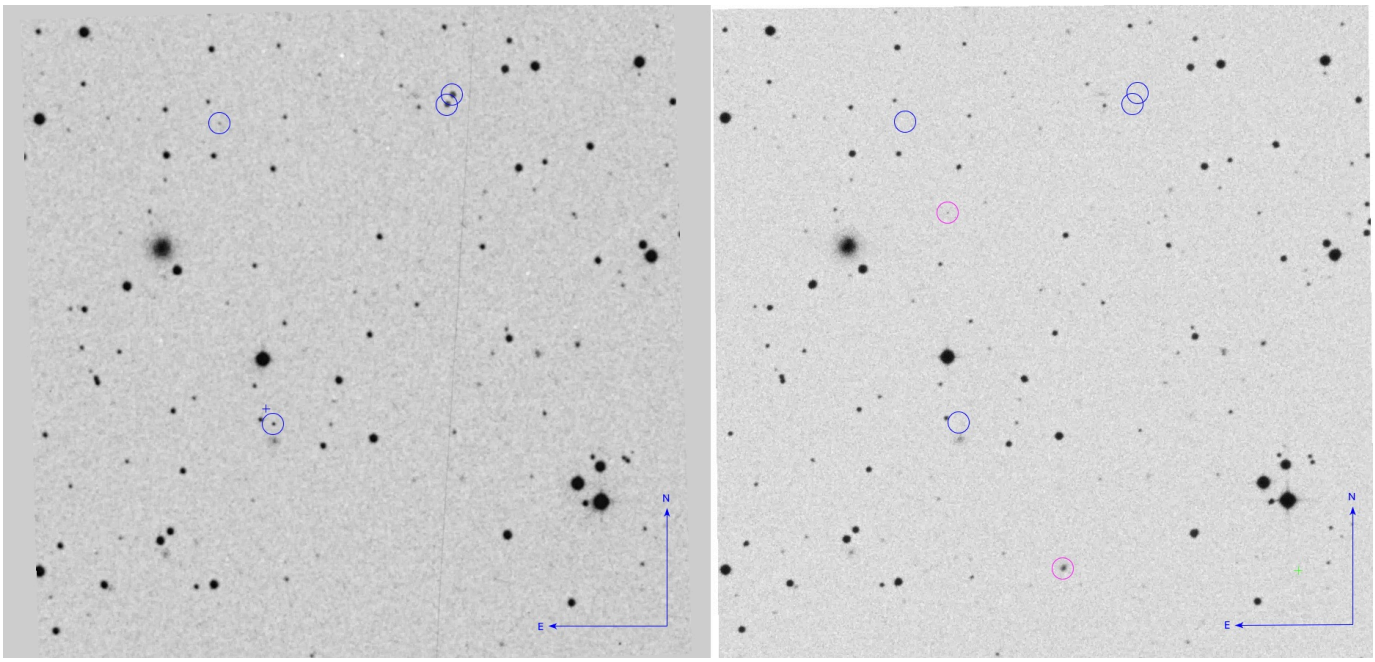

Figure 1. Candidate 1. We show the candidate in SuperCosmos scans of POSS-I red (left) and POSS-II red (right) images (inverted). Transients are marked with blue circles. The candidate with a measured coordinate is marked with a cross (+). Pink circles show defects. Also the gray line crossing the POSS-I field is a scanning defect. Four transients are visible in the POSS-I image, where three follow a straight line. Box size is 10×10 arcmin^2. See Figure 6 for a version with drawn lines that shows the possible alignment.

Table 2
Candidate Shortlist

Candidate Shortlist									
Candidate	Year	R.A. Decl. (sexag., J2000)	R.A. Decl. (deg, J2000)	r	N	A (arcmin^2)	$p_{\max}$ (arcsec)	$d_{\max}$ (arcmin)	μ_r
1	1954	02:29:33.71 +28:31:56.98	37.3904454 28.5324936	3	4	10×10	1.0	5.8	0.044
2	1955	03:05:42.48 +07:58:29.60	46.4269814 7.9748892	3	5	10×10	1.0	3.6	0.010
3	1954	03:08:27.13 +34:40:46.01	47.1130236 34.6794470	3	5	15×15–16	2.0	9.9	0.194
”	”	””	”	5*	5	”	15.0	”	0.002
4	1954	21:24:39.71 +68:31:30.04	321.1654740 68.5250111	3	6	12×12	1.0	5.15	0.049
”	…	”	”	4*	6	”	5.0	”	0.003
5	1952	19:16:45.76 +51:28:52.40	289.1906854 51.4812217	3	5	10×10	1.0	4.0	0.028
”	…	”	”	5*	5	10×10	10.0	4.0	0.0001

Note. We show the most interesting candidates emerging after the visual inspection. In some cases there could be different possibilities of r-point alignments, e.g., $r = 3$ or $r = 4$, and we show both possibilities marked by an asterisk (*). The given position coordinate corresponds to the transient marked with a cross (+) in each figure.

6. Statistics

The section below provides a brief recapture of the statistical framework developed in Section 5 of Villarroel et al. (2022a), where interested readers can explore the details of the framework. It builds on Edmunds (1981) and Edmunds & George (1985) which criticized Halton Arp's quasar alignments. The common critique was that with a large number density of objects, alignments will inevitably appear. These papers developed a statistical framework to investigate the actual probability of chance alignments.

For each of the interesting cases we consider the total number N of transient-like objects found in the image field, i.e., the area A of the image, and look for r objects aligned within a strip of width $p_{\max}$ and length $d_{\max}$. Such alignments will be referred to as r-point alignments.

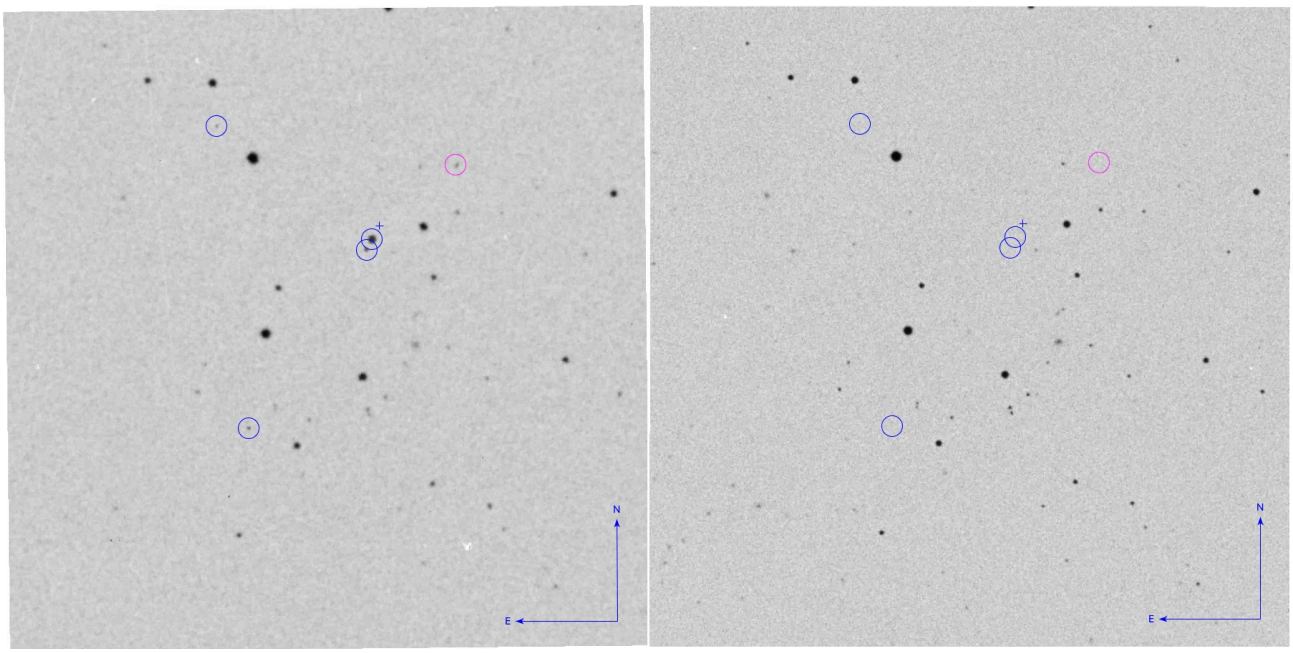

Figure 2. Candidate 2. We show the candidate in SuperCosmos scans of POSS-I red (left) and POSS-II red (right) images (inverted). Transients are marked with blue circles. The candidate with a measured coordinate is marked with a cross (+). Four transients are visible in the POSS-I image, where three follow a straight line. See Figure 7 for a version with drawn lines that shows the possible alignment. Box size is 10×10 arcmin^2.

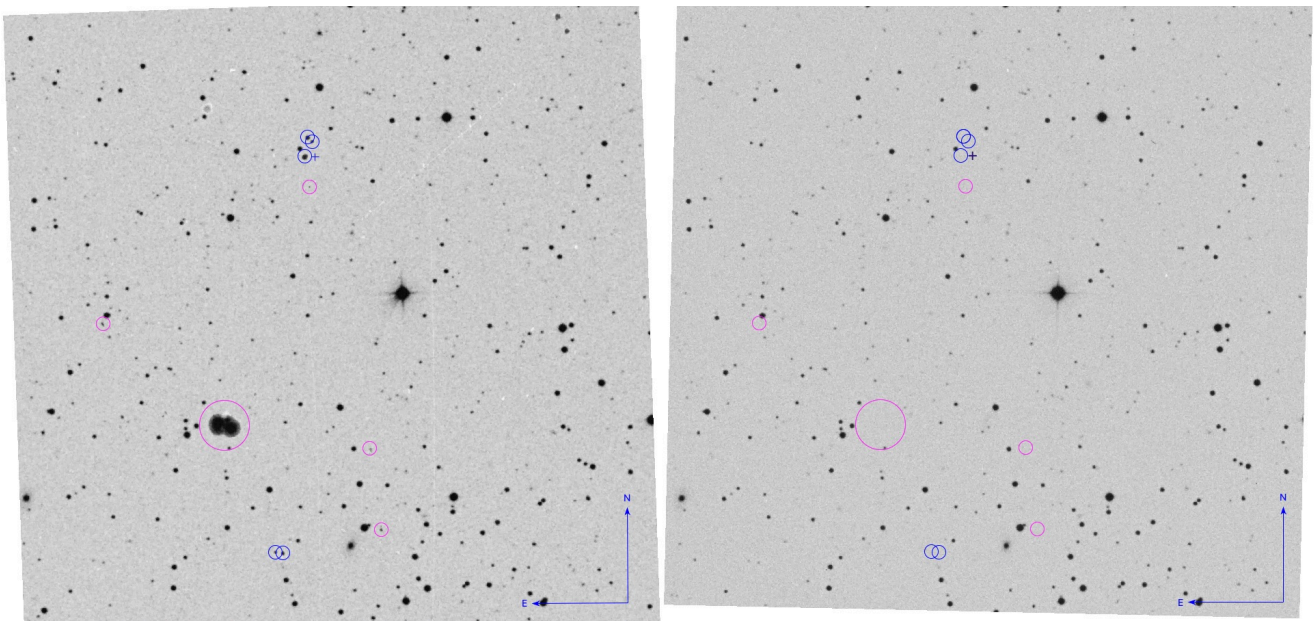

Figure 3. Candidate 3. We show the candidate in SuperCosmos scans of POSS-I red (left) and POSS-II red (right) images (inverted). Transients are marked with blue circles. The candidate with a measured coordinate is marked with a cross (+) and might be slightly dubious in shape. Pink circles show defects, both plate defects and scanning defects. See Figure 8 for a version with drawn lines that shows the possible alignment. Box size is roughly 15×15 arcmin^2.

As the area A is different for each case, we can only estimate the expected number of r-point alignments μ_r within a given field A. As suggested in Villarroel et al. (2022a), we use the generalized formula from Edmunds & George (1985),

$$\mu_r = \frac{\pi\, 2^{r-2}\, n^r\, p_{\max}^{r-2}\, A}{\Gamma(r-1)} \int_0^{d_{\max}} x^{r-1}\, e^{-2x\, n\, p_{\max}}\, dx, \qquad (1)$$

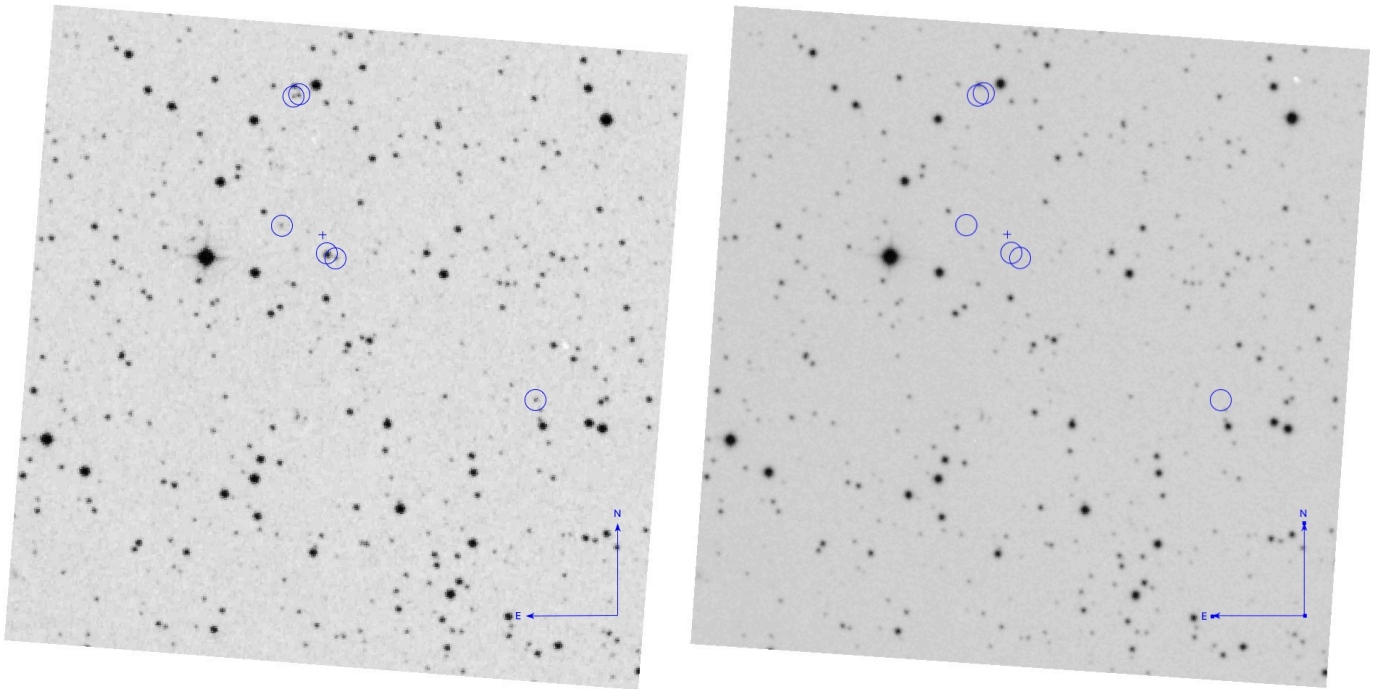

Figure 4. Candidate 4. We show the candidate in SuperCosmos scans of POSS-I red (left) and POSS-II red (right) images (inverted). Transients are marked with blue circles. The candidate with a measured coordinate is marked with a cross (+). See Figure 9 for a version with drawn lines that shows the possible alignment. Box size is 12×12 arcmin^2.

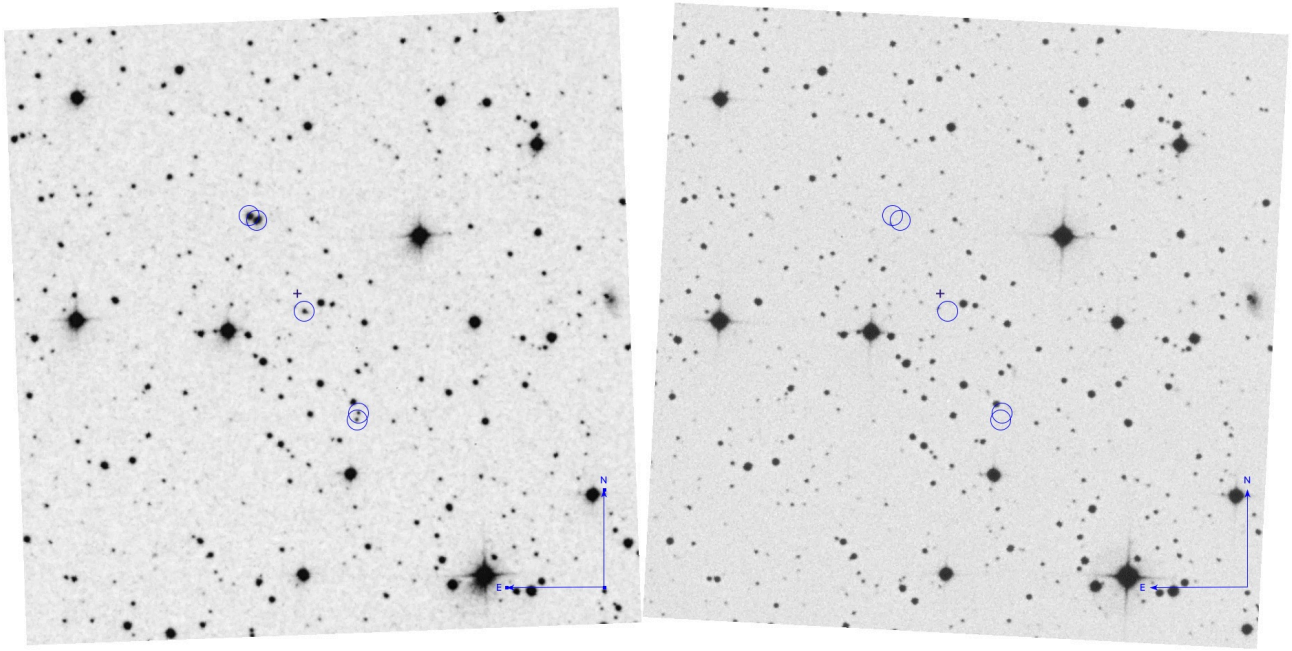

Figure 5. Candidate 5. We show the candidate in SuperCosmos scans of POSS-I red (left) and POSS-II red (right) images (inverted). Transients are marked with blue circles. The candidate with a measured coordinate is marked with a cross (+). See Figure 10 for a version with drawn lines that shows the possible alignment. Box size is 10×10 arcmin^2.

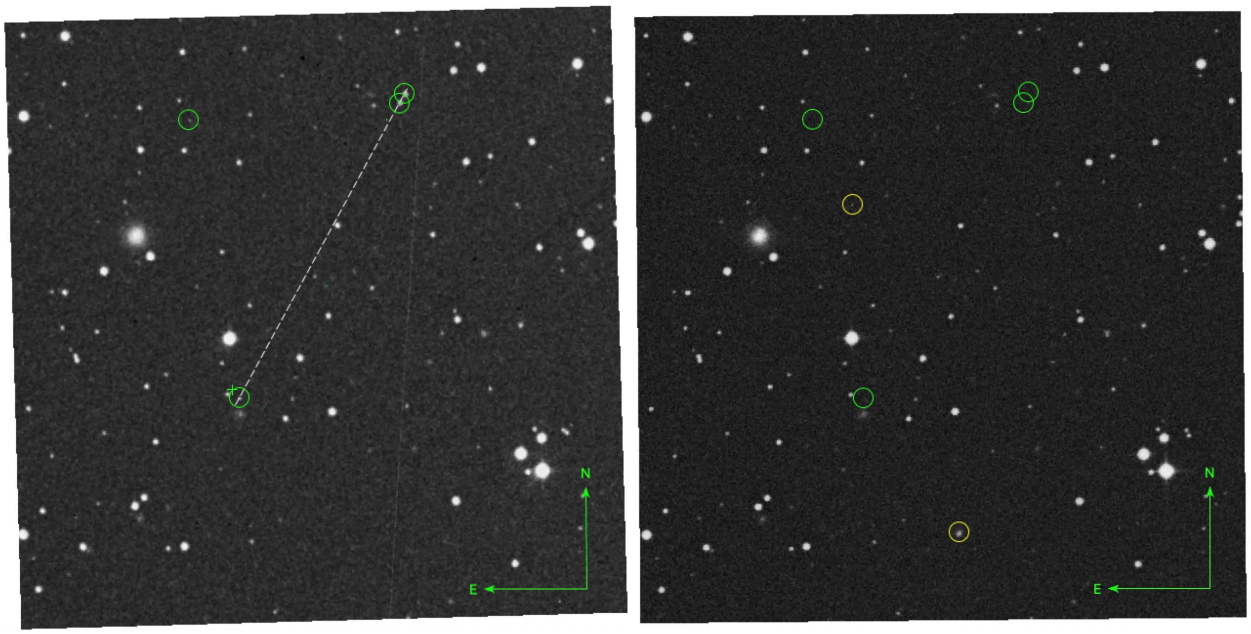

Figure 6. Candidate 1. We show the candidate in SuperCosmos scans of POSS-I red (left) and POSS-II red (right) images. Transients are marked with green circles. The candidate with a measured coordinate is marked with a cross (+). A dashed white line shows the alignment. Yellow circles show defects. Also the white line crossing the POSS-I field is a scanning defect. We see 4 transients in the POSS-I images where three follow a straight line.

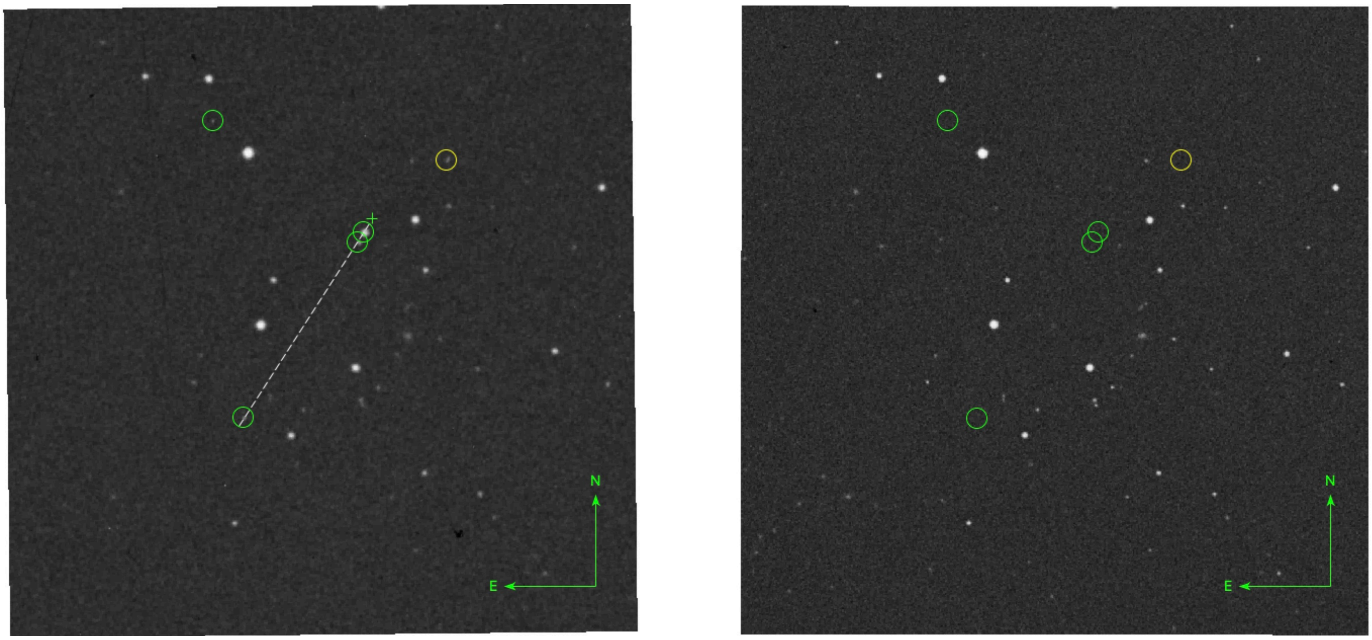

Figure 7. Candidate 2. We show the candidate in SuperCosmos scans of POSS-I red (left) and POSS-II red (right) images. Transients are marked with green circles. The candidate with a measured coordinate is marked with a cross (+). A dashed white line shows the alignment. Yellow circles show defects. Also the white line crossing the POSS-I field is a scanning defect. We see 4 transients in the POSS-I images where three follow a straight line.

where Γ is the gamma function, $n = N/A$, and all other quantities are as previously defined, with lengths given in arcmin and, consequently, the area A is in arcmin^2. As in Villarroel et al. (2022a) we use, for practical reasons, a limiting case of this generalization,

$$\mu_r \approx \frac{\pi\, 2^{r-2}\, n^r\, p_{\max}^{r-2}\, d_{\max}^r\, A}{r\,(r-2)!}, \quad r = 3, 4, 5, \cdots, \tag{2}$$

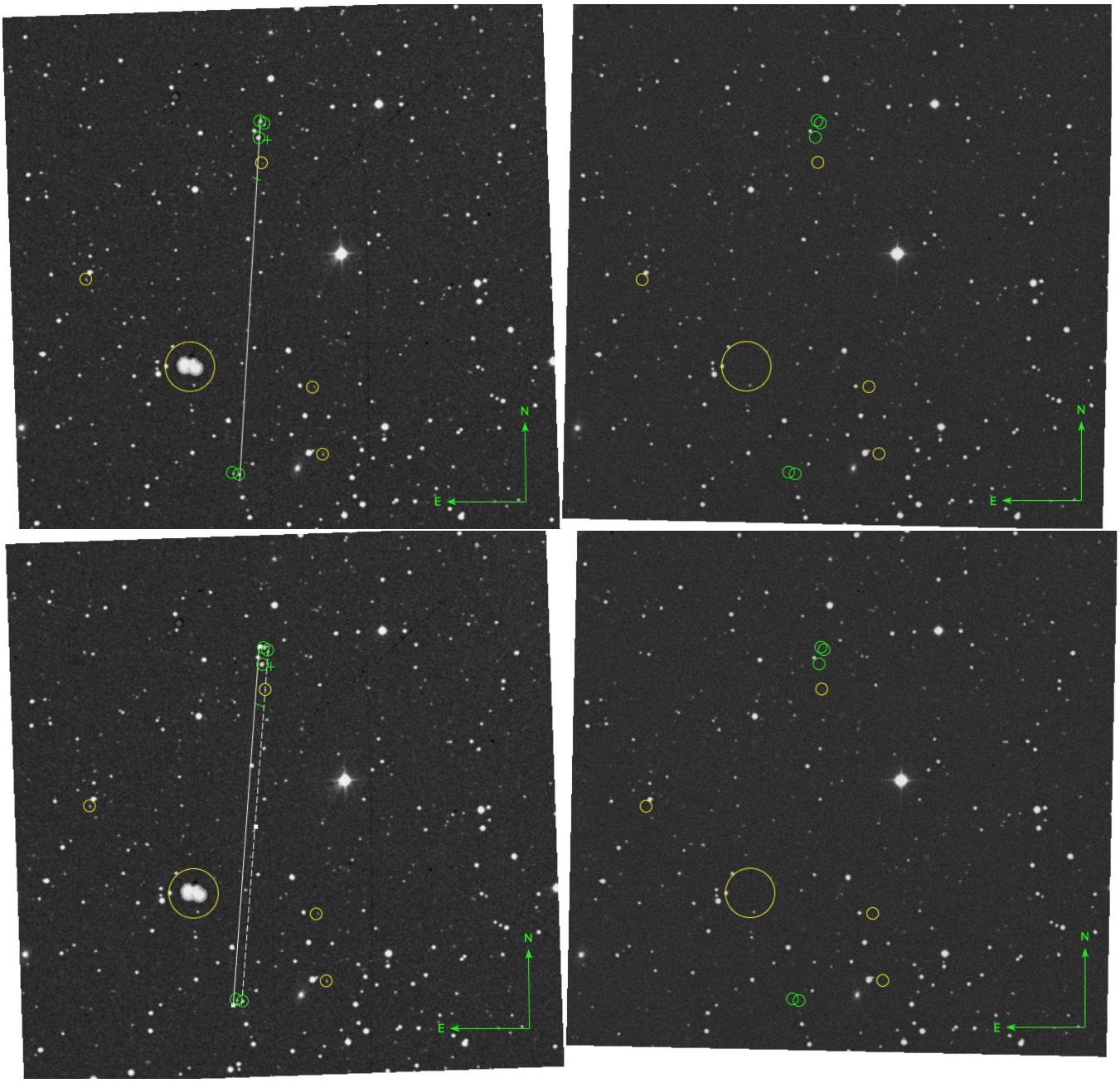

Figure 8. Candidate 3. We show the candidate in SuperCosmos scans of POSS-I red (left) and POSS-II red (right) images. The upper row shows a 3-point alignment within 1″–2″. The lower row shows a 5-point alignment of within 15″. Transients are marked with green circles. The candidate with a measured coordinate is marked with a cross (+) and might be slightly dubious in shape. The dashed lines shows the alignment (the white double line for the thicker alignment below). Yellow circles show defects, both plate defects and scanning defects.

which is a good approximation when $2\,d_{\max}\,p_{\max}\,n \ll 1$ and simplifies the calculations considerably. For the present study Equations (1) and (2) should yield very similar results, since $2\,d_{\max}\,p_{\max}\,n \lesssim 0.01$ for all cases considered.

We apply Equation (2) to calculate the expected number of r-point alignments μ_r for each case. We include all measurements in Table 2. The short list includes both 3-point alignments and 4-point alignments. Since each candidate case only has one alignment, the probability is given by the expectation value, $\mathcal{P} \sim \mu_r$. We can see that several of the cases are significantly statistically improbable (3σ–4σ) to happen in a single image.

The probability estimate is also very sensitive to the total number of transients (N) present. This number depends

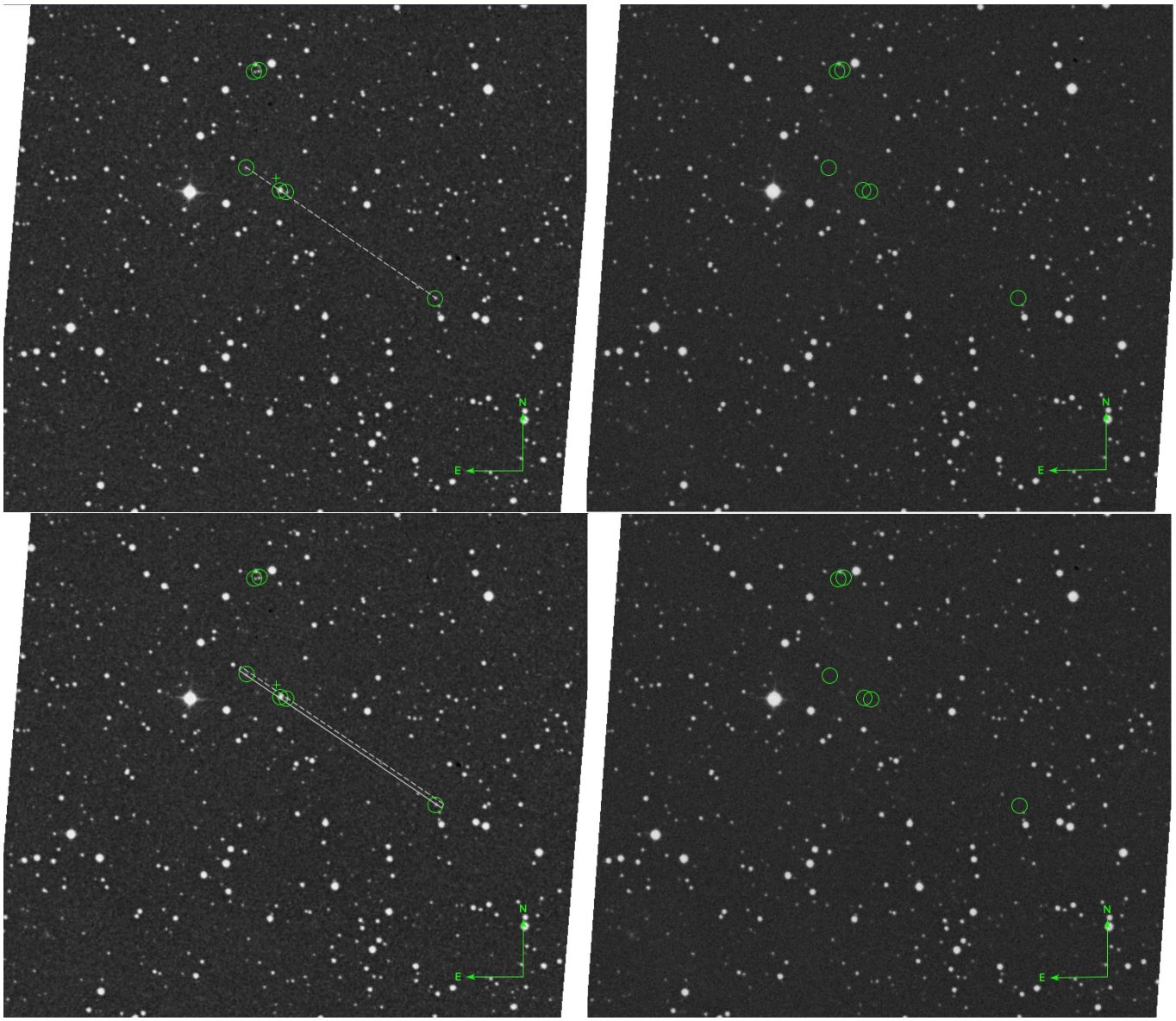

Figure 9. Candidate 4. We show the candidate in SuperCosmos scans of POSS-I red (left) and POSS-II red (right) images. The upper row shows a 3-point alignment within 1″. The lower row shows a 4-point alignment of within 5″. Transients are marked with green circles. The candidate with a measured coordinate is marked with a cross (+). The dashed lines shows the alignment (the white double line for the thicker alignment below).

strongly on the visual inspection that was made by blinking the POSS-I and POSS-II images in SAOImage DS9, taking into account the differences in depth. Any missed transients will change the value of N, and hence the estimated probability.

However, to estimate exactly the *total* probability $\mathcal{P}_{\rm tot}$ of each single event to happen during our searches, two more factors influence the total probability. The first is the probability for obtaining a perfectly 1, 2, … or N' star-like plate flaws within the same area of an image. Given the rarity of encountering a star-like plate defect, and even less so with a matching FWHM as the normal stars of the same magnitude range in the field, it may be even more unusual to encounter 2, or 3, or 4 plate flaws that all have the same coincidental features and this lowers dramatically the total probability of the event. The second factor is the total number of multiple transients in our data set: if there are sufficiently many star-like plate flaws causing "multiple transients," some of these will line up. With an infinite data set, any type of constellations will be found. This factor will, contrary to the first factor, increase the total probability for an event to occur.

Unfortunately, we have no grasp or means of estimating either of the two factors. Therefore, it is easier to examine the

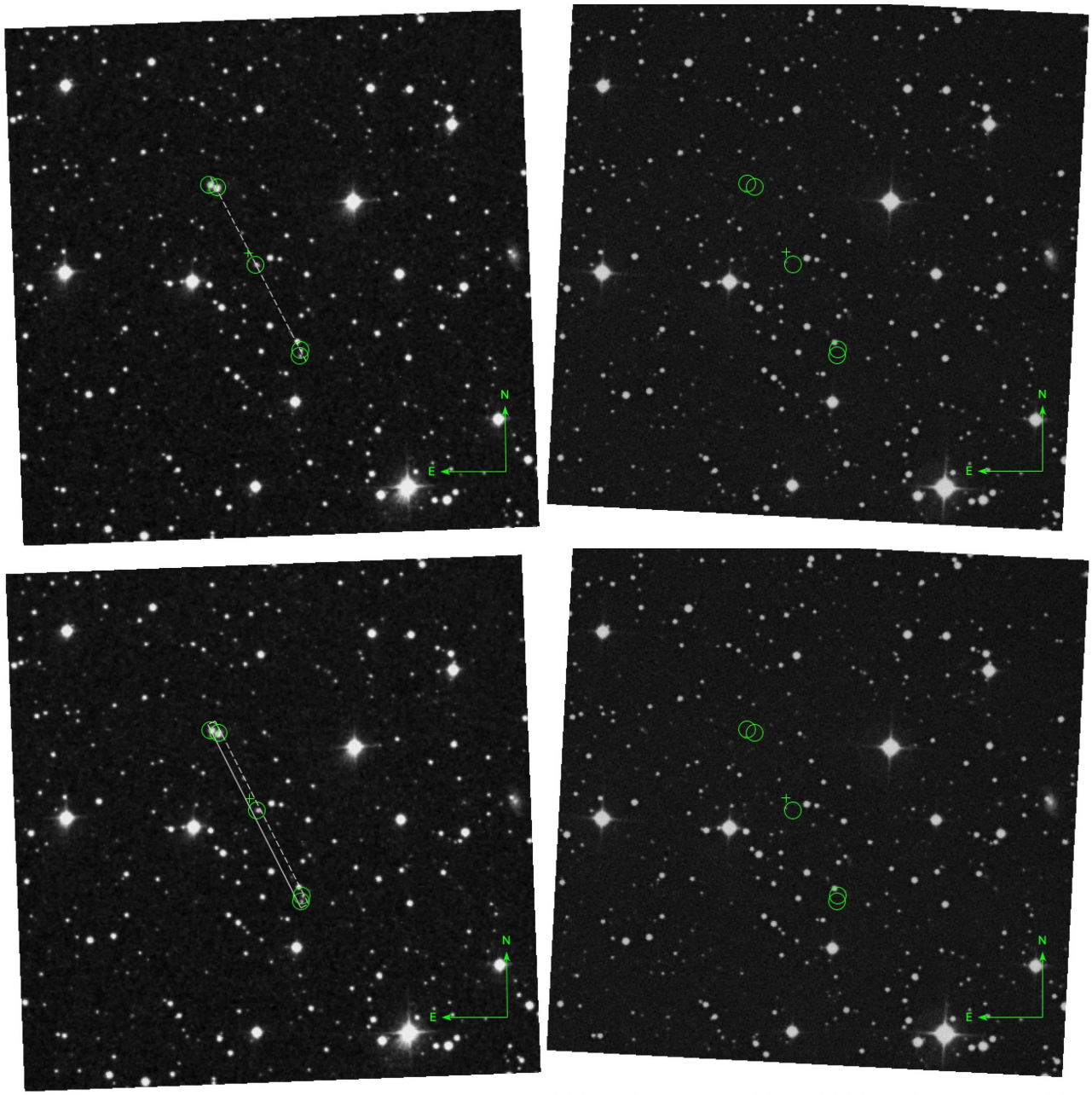

Figure 10. Candidate 5. We show the candidate in SuperCosmos scans of POSS-I red (left) and POSS-II red (right) images. The upper row shows a 3-point alignment within 1″. The lower row shows a 5-point alignment of within 10″. Transients are marked with green circles. The candidate with a measured coordinate is marked with a cross (+). The dashed lines shows the alignment (the white double line for the thicker alignment below).

effect of the choice of $p_{\max}$ on the probability estimates for single images. The choice of $p_{\max}$ depends on the science question of interest: are we interested whether the objects are truly aligned or whether they are just non-random? Showing non-randomness is all that is needed to argue for the authenticity of the points, but not necessarily enough to argue that they truly are aligned as in the case of GSO glints. We use Table 3 to adopt other values of $p_{\max}$, setting it equal to FWHM of the smallest star in an alignment (e.g., for Candidate 1, FWHM $= 2\farcs7$). Doing this, we see that all 3-point alignments are non-interesting events with $p > 0.05$ (less significant than 2σ), with an exception of the borderline case of Candidate 2. This shows that for POSS-I data where the seeing in general is rather large, 3-point alignments of simultaneous transients do not provide significant proof against randomness. The interesting cases are the 4-point and

Table 3
Measurements

Candidates 1–5					
Object	R.A.	Decl. (sexag., J2000)	FWHM (pixel)	FWHM (arcsec)	*R*
object1	2:29:37.57	+28:36:31.58	4.0	2.7	18.9
object2*	2:29:21.38	+28:36:57.89	7.2	4.8	16.6
object3*	2:29:21.76	+28:36:49.09	7.6	5.1	17.0
object4†*	2:29:33.80	+28:31:56.83	4.1	2.7	18.3
Date of observation = 1954-10-04					
Object	R.A.	Decl. (sexag., J2000)	FWHM (pixel)	FWHM (arcsec)	*R*
object1	3:05:52.34	+8:00:16.97	3.8	2.5	19.2
object2†*	3:05:42.46	+7:58:30.22	10.0	5.7	15.2
object3*	3:05:42.81	+7:58:20.56	5.9	4.0	17.9
object4*	3:05:50.24	+7:55:33.86	4.4	2.9	18.3
Date of observation = 1955-01-14					
Object	R.A.	Decl. (sexag., J2000)	FWHM (pixel)	FWHM (arcsec)	*R*
object1*	3:08:29.90	+34:31:25.73	6.2	4.2	17.1
object2*	3:08:30.72	+34:31:27.44	5.2	3.5	18.1
object3†*	3:08:27.42	+34:40:46.00	9.9	6.6	15.4
object4*	3:08:27.05	+34:41:13.49	8.1	5.4	16.1
object5*	3:08:26.56	+34:41:07.89	6.0	4.0	17.1
Date of observation = 1954-12-21					
Object	R.A.	Decl. (sexag., J2000)	FWHM (pixel)	FWHM (arcsec)	*R*
object1	21:24:45.51	+68:34:00.29	4.4	2.9	N.A.
object2	21:24:44.59	+68:34:01.20	4.6	3.1	16.6
object3*	21:24:47.62	+68:31:58.92	4.4	2.9	17.9
object4†*	21:24:39.72	+68:31:31.22	8.9	6.0	15.2
object5*	21:24:38.18	+68:31:27.97	5.0	3.4	17.2
object6*	21:24:03.94	+68:29:14.36	4.6	3.1	17.8
Date of observation = 1954-08-05					
Object	R.A.	Decl. (sexag., J2000)	FWHM (pixel)	FWHM (arcsec)	*R*
object1*	19:16:51.46	+51:30:24.51	11.0	7.4	13.2
object2*	19:16:50.64	+51:30:20.86	12.0	8.0	12.7
object3†*	19:16:45.73	+51:28:52.04	7.2	4.8	16.0
object4*	19:16:40.13	+51:27:12.85	5.0	3.4	16.3
object5*	19:16:40.27	+51:27:06.29	5.5	3.7	16.0
Date of observation = 1952-07-27					

Note. We list the astrometry-improved measurements for the objects inside the green circles in Figures 1–5. Objects that are placed inside an alignment are marked with an asteriskm ∗. The central objects presented in Table 2 are marked with a dagger (†). We show the FWHM in pixel and arcsec, based on SuperCosmos POSS-I images. The SuperCosmos resolution is $0\farcs67$ pixel^{-1}. The object have an improved astrometry with help of Terapix swarp procedure, using zero-point calculations with SDSS as a reference field. The *r* magnitudes are obtained via the photometric procedure described by B. Villarroel et al. (2025 in preparation) for DSS scanned POSS-I red plates, building on methods by Andruk et al. (1995, 2017, 2019). When an object either is too faint or two objects are too close to each other, the photometry code (that measures *R* Johnson magnitudes) fails to detect them, meaning we have no photometric information. For these cases, we mark the magnitudes as Non Available (N.A.).

5-point cases, namely Candidates 3, 4 and 5. Yet, one could argue that without an inspection with a microscope one still cannot exclude plate defects.

However, what makes the events even more interesting is that Candidate 5 occurs on the same date as one of the most famous UFO mass sightings in history—namely, the 1952 Washington UFO flap (Villarroel 2024). This could be a coincidence. We also note that Candidate 1 occurs within a day of the peak of the 1954 UFO wave. We shall discuss this further in Section 10. These additional two coincidences further motivate scrutiny of the plate defect hypothesis, especially in light of the combined statistical and contextual factors presented in this study.

7. Assessment of Conventional Explanations

The central challenge of this work lies in determining whether the transients represent authentic observations. A previous analysis of the multiple transient event in Villarroel et al. (2021) ruled out all known astrophysical origins, and most instrumental causes as well. What remains is the possibility of unknown plate contamination or emulsion defects that coincidentally resemble star-like shapes, despite their variation in brightness. While gravitational lensing by a short-lived transient passing behind an undetected supermassive black hole (SMBH) was proposed in Solano et al. (2023), such a model would require an implausibly large population of undetected SMBHs in the Milky Way to explain the broader set of events found by VASCO. The phenomenon remains unresolved—now made even more intriguing by the discovery that several events are aligned along a narrow band.

A potential concern is optical ghosts. Ghosts typically exhibit extended or clumpy morphologies and do not match stellar point spread functions (PSFs). In contrast, the transients identified in both Villarroel et al. (2021) and the current study were preselected based on their PSF-like properties (Solano et al. 2022), making classical ghosting an unlikely explanation. While most optical ghosts on POSS-I plates appear extended or irregular, one might ask whether more unusual ghosting patterns—such as point-like reflections—could in principle occur. Modern CCD-based surveys using the same telescope (e.g., ZTF, PTF) have documented rare ghost patterns that, under specific optical conditions, can mimic point sources at significant angular separations from their parent stars (Waszczak et al. 2017; Irureta-Goyena et al. 2025). A dedicated optical modeling effort would be required to fully evaluate such hypothetical scenarios, taking into account the different detector areas (CCDs versus photographic plate field sizes) and pixel scales. However, such an analysis lies beyond the scope of the present study. Instead, we compare two images of the same field taken with the same configuration, separated by only 30 minutes: the red and the blue plates for the five

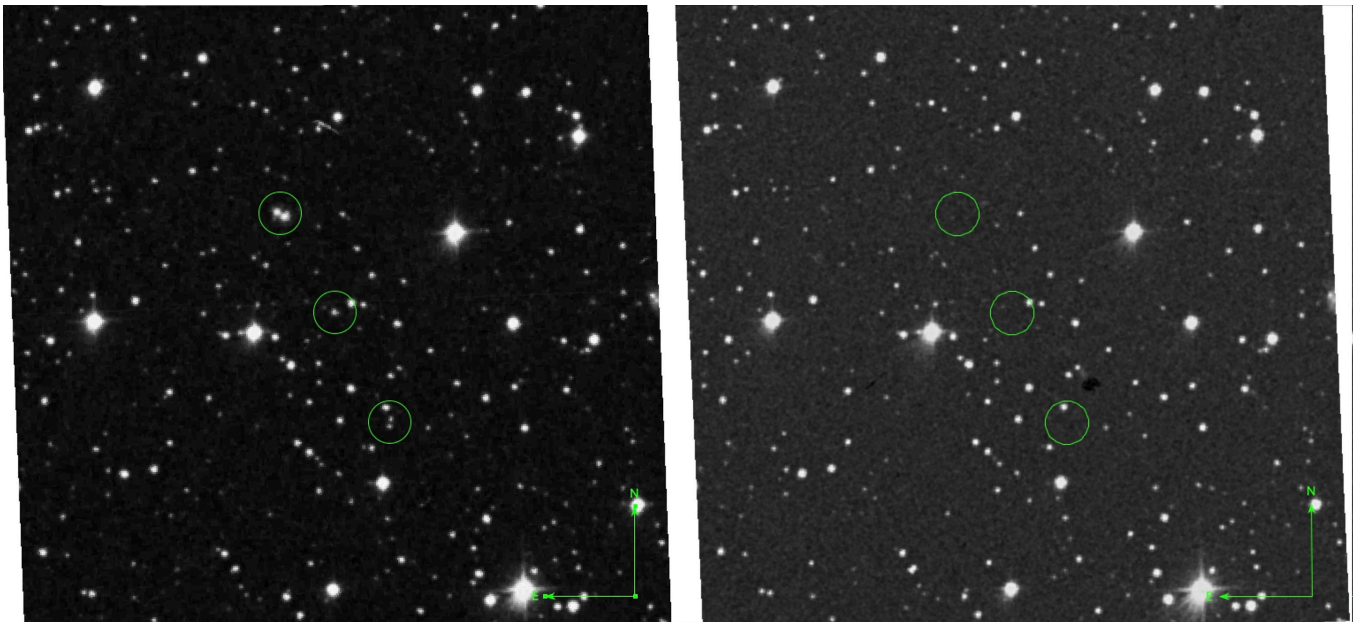

Figure 11. Red vs. blue image of Candidate 5. Comparison between the red (left) and blue (right) DSS images for Candidate 5. No coincident sources are found in the blue image.

candidates. This is similar to the case of the triple transient, where stars of about 16th magnitude appear and vanish within half an hour, yet are not seen on the corresponding blue plate with similar configuration. The blue exposures are significantly shorter, yet we do not see any similar stars or repeating patterns in them, see for example Figure 11. This further reduces the likelihood that optical ghosting can explain the alignments, though differences in exposure time and in the reflectivities of optical coatings (causing different ghosting levels in different color bands) prevents us from fully excluding it.

Another concern is photographic plate defects. Historically, astronomers have excluded single-epoch point sources to avoid false positives—an approach that also inadvertently eliminate many genuine, short-lived astronomical events. For example, Hambly & Blair (2024) argued that the transients reported in Villarroel et al. (2021), despite their point-like morphology, are likely emulsion artifacts. This conclusion was primarily based on the finding that the transients exhibit slightly narrower full width at half maximum (FWHM) values, on average, compared to normal stars. However, the analysis did not account for the known nonlinearity of photographic emulsions, which causes fainter sources to naturally exhibit narrower profiles. In addition, the "artifact" sample in their study was selected using criteria that mirror the VASCO project's transient selection pipeline, which may introduce circular reasoning. Crucially, the study did not consider that sub-second optical flashes are predicted—on physical grounds—to appear sharper and more circular than stars in long-exposure plates, due to the absence of atmospheric seeing, wind shake, and tracking-induced smearing. These effects are discussed in detail in a dedicated technical commentary (Villarroel et al. 2025a). To date, no study has systematically quantified the fraction of single-plate detections that are authentic transient phenomena versus coincidentally star-like emulsion defects.

A summary of excluded astrophysical, observational, and instrumental causes is provided in Villarroel et al. (2021). Assuming the observed transients are genuine and not artifacts, we turn to alternative physical explanations beyond the GSO glint hypothesis.

Point-like events could result from either reflected sunlight or intrinsic emission. As shown in Villarroel et al. (2021), such objects must be located within the solar system. We consider four broad possibilities: (i) the objects are inside Earth's atmosphere, (ii) they are in low Earth orbit (LEO), (iii) they are in GSO, or (iv) they are located at significantly greater distances.

If the transients originated from luminous or reflective atmospheric objects, they should leave visible trails over the 45–50 minutes POSS-I exposures, given that the telescope tracked stars during imaging. Stationary objects would also appear streaked. Objects very close to the observer would appear significantly out of focus due to proximity to the focal plane. For instance, an object at 50 km altitude would suffer a defocus of several hundred microns on the Palomar 48 inch system, resulting in an extended PSF incompatible with a stellar appearance. Only at altitudes above several hundred kilometers would point-like morphology be achievable. This effectively rules out phenomena such as red sprites or rare

luminous atmospheric events like the Hessdalen phenomenon (Teodorani 2004). The only plausible scenario in which multiple objects within Earth's atmosphere could produce point-like transients without visible trails is if they were light-emitting and appeared simultaneously for a split second—brief enough to avoid leaving motion blur—before vanishing. However, such objects within the atmosphere would be subject to focal blur. Alternatively, they would need to mimic the appearance of stars as seen from Earth. While speculative, such a scenario cannot be ruled out a priori and would fall under the category of unidentified aerial phenomena. Some asymmetries observed in, for instance, Candidate 5, might still be marginally consistent with high-altitude sources near the upper atmosphere. All plausible scenarios would fit with the observations of UAP, see Knuth et al. (2025).

LEO-based explanations are not impossible, but they are much less likely. PSF-like glints due to short millisecond flashes can be produced at any orbit altitude by rapidly spinning objects. Nevertheless, objects in LEO typically leave continuous trails, and explanations involving glints from experimental rockets or missiles at altitudes of 100–200 km are improbable due to their rapid motion and constrained illumination geometry. Further, empirical studies based on short-exposure CCD surveys (e.g., Corbett et al. 2020; Nir et al. 2021) have shown that most PSF-like glints are associated with GSO. However, if an object were capable of actively controlling both its motion and its optical signature as perceived from Earth-based observatories, then altitude constraints would no longer apply. Such a scenario would imply an engineered system of extraordinary sophistication.

We also considered more distant origins. As discussed in Villarroel et al. (2021), fast-moving Solar System objects such as asteroids will produce trails, while slow-moving ones should appear in multiple images taken close in time. Objects like tumbling interstellar bodies (e.g., *'Oumuamua*) would also produce visible trails across long exposures. Hence, no known population of solar system or interstellar objects can explain point-like transients that appear only in one long exposure and are entirely absent shortly before and after.

While we cannot exhaustively rule out all possible explanations, including those not yet imagined, the absence of known natural or instrumental causes—combined with the spatial alignment of certain events along a narrow band—calls for further investigation. And maybe the simplest way of testing the mechanism behind these flashes, is by performing a test that can reveal whether they originate from solar reflections—or if not.

8. Testing the Solar Reflection Hypothesis

The VASCO project has identified thousands of short-lived, point-like transients in pre-Sputnik photographic plates (Villarroel et al. 2020; Solano et al. 2022). The multiple transient candidates were found among this general population, with several events sharing similar timescales, morphologies, and apparent magnitudes. It is therefore reasonable to treat the multiple transients as a statistically identifiable subpopulation within this broader distribution.

One possible interpretation for transients is that they are caused by sunlight reflecting off objects with flat surfaces in GSOs, such as small rotating objects briefly glinting as they pass through a favorable viewing geometry (Villarroel et al. 2022a). If this interpretation holds, we would expect a significant deficit of such events within Earth's shadow (umbra), where sunlight cannot reach the object to produce a glint. If the transients, on the other hand, are caused by their own emission or are due to plate defects, we would expect no deficit in the number of transients within the shadow. The method of using Earth's shadow to filter out reflections is further discussed in Villarroel et al. (2025b).

While it is possible to compute the fraction of each photographic plate that lies in Earth's shadow for any given orbital altitude, not all heights are equally meaningful for our analysis. At low altitudes (e.g., below $\sim$10,000 km), Earth's shadow may cover large fractions of the plates, making any deficit or surplus hard to interpret. While plate defects do not respond to the position of Earth's shadow, the diagnostic power of this test depends on the assumption that the shadow is randomly placed with respect to plate geometry and artifact distribution. When the shadow covers a large portion of the plate (e.g., $>$50%), this assumption breaks down, and even a random distribution of artifacts will naturally yield an overdensity in the shadowed region. In such cases, the test becomes less sensitive to systematic avoidance, making small shadow coverages (e.g., $<$5%–10%) more reliable.

Moreover, reflective objects in low orbits tend to move rapidly and would often appear as streaks rather than point-spread-function (PSF)-like transients. Since our sample only includes PSF-like detections, it is physically unlikely that many of them originate from low Earth orbits, where glints would need to be extremely short-lived (on the order of milliseconds). Nir et al. (2021) show that most sub-second flares are glints of sunlight reflected from satellites in geosynchronous and graveyard orbits. For these reasons, we focus our main analysis on altitudes where less than 5% of the field is typically shadowed—regions where the shadow behaves approximately randomly, and where reflective glints, if present, would be both detectable and physically plausible.

We use the transient candidates from Solano et al. (2022), but with the additional requirement that they have no counterparts within 5″ in Gaia, Pan-STARRS and NeoWise. Furthermore, we restrict our analysis to objects in the northern hemisphere (decl. $>$ 0°). This yields a sample of 106,339 transients, which we use for our study.

An important note about the sample is that, contrary to the other transient candidates discussed throughout the paper, this

Table 4
Comparison of Earth's Umbral Shadow Coverage with Observed Transient Fractions in the Northern Celestial Hemisphere (20,626.5 square degrees)

Alt. (km)	θ (deg)	N	$A_{\rm sph}$	$A_{\rm pl}$	$f_{\rm sph}$	$f_{\rm pl}$	$f_{\rm obs}$	$f_{\rm sph}/f_{\rm obs}$
42,164	8.69	349	237.4	237.2	0.0115	0.0115	0.00328	3.50
80,000	4.57	79	66.0	65.6	0.0032	0.0032	0.00074	4.32

Note. We show the altitude (km), the shadow radius in degrees (θ), the number N of VASCO transients detected inside the shadow, the shadow area $A_{\rm sph}$ assuming spherical sky geometry (sq. deg), shadow area $A_{\rm pl}$ assuming planar approximation (sq. deg), expected fraction $f_{\rm sph}$ of transients in shadow using spherical area, expected fraction $f_{\rm pl}$ using planar area, the observed fraction $f_{\rm obs}$ of VASCO transients in shadow, and the ratio $f_{\rm sph}/f_{\rm obs}$.

sample has not been visually inspected. As such, it is expected to contain a substantial number of false positives, including clustered artifacts such as edge fingerprints or other plate defects that contaminate our sample. In addition, the spatial distribution of the sample is not isotropic due to inhomogeneous sky coverage in the original POSS-1 survey. Some regions of the sky are more densely sampled than others, leading to variation in the overall detection density.

However, these effects do not bias the results of our shadow analysis. The reason is that we are comparing a small, well-defined subset of this population—those that fall within the Earth's shadow cone at the time of observation—with the rest of the same population. Since the selection effects and potential false positives affect both the shadowed and unshadowed regions similarly, any large and statistically significant difference in detection rates between these regions must reflect an intrinsic property of the detections themselves, not an observational bias. Or to express it simply: plate defects do not know where the Earth's shadow is, and have no reason to avoid that region more than any other.

The fraction of transients expected within the umbra depends on the angular radius of Earth's shadow at different altitudes. We use the software library `earthshadow` published by Guy Nir published (Guy Nir's code 2024) to estimate the size of the Earth's Shadow at 40,000 km ($8.^{\circ}69$) and 80,000 km ($4.^{\circ}57$). The code determines whether a given point at a specified altitude and geographic position lies inside Earth's shadow, based on the solar angle and the geometric configuration of the Sun, Earth, and the object. We apply it to each transient using their J2000 coordinates and Julian Dates. We compare the expected and observed rates for two different altitudes capable of producing PSF-like transients, namely 42,164 km and 80,000 km. We can calculate the expectations based on how large fraction of the northern hemisphere is covered by the shadow, and compare with the observed fractions. We calculate the area in two different ways, both based on based on spherical geometry: $2\pi(1-\cos\theta)$) as well as planar sky coverage, as an approximation. Table 4 shows the results. We note that multiple plates ($\sim$10) fall within Earth's shadow, so the observed deficit is not driven by a single outlier plate.

To estimate the statistical significance of the difference in transient detection rates within Earth's umbra at different altitudes, we compute Poisson uncertainties for the observed and expected fractions. At 42,164 km altitude, we expect $N = 1223$ transients in shadow out of 106,339 total, corresponding to an expected fraction of $f_{\rm exp}$=0.0115 $\pm$ 0.00033. However, we observe only $N = 349$ transients in shadow, yielding $f_{\rm obs} = 0.00328 \pm 0.00018$. The difference between these fractions is highly significant, with a significance level of 21.9σ, computed by combining the Poisson uncertainties in quadrature:

$$\sigma = \frac{|f_{\rm exp} - f_{\rm obs}|}{\sqrt{\sigma_{\rm exp}^2 + \sigma_{\rm obs}^2}} = \frac{|0.0115 - 0.00328|}{\sqrt{(0.00033)^2 + (0.00018)^2}} \approx 21.9.$$

At 80,000 km altitude, we expect $N = 339$ transients in shadow out of 106,339 total, corresponding to a fraction of $f_{\rm exp}$=0.00319 $\pm$ 0.00017. However, we find only $N = 79$ transients in shadow, yielding $f_{\rm obs} = 0.00074 \pm 0.000084$. The difference in these observed fractions is also highly significant, with a significance level of 12.7σ, computed by combining the Poisson uncertainties in quadrature:

$$\sigma = \frac{|f_{\rm exp} - f_{\rm obs}|}{\sqrt{\sigma_{\rm exp}^2 + \sigma_{\rm obs}^2}} = \frac{|0.00319 - 0.00074|}{\sqrt{(0.00017)^2 + (0.000084)^2}} \approx 12.7.$$

This result further strengthens the conclusion that sunlight is necessary for producing the transient events. The strong deficit of transients within the Earth's umbra suggests that the majority of these events depend on sunlight illumination, consistent with the glint hypothesis. This strongly defies the plate defect hypothesis and many of the alternative hypotheses presented in Section 7.

We performed an additional test to estimate the actual fraction of the survey sky that was covered by Earth's shadow during the actual POSS-I observations, and to compare it to the

actual observed fraction of transients falling within the shadow. The transient sample is based on 635 unique photographic plates, each with a designated central coordinate (R.A., decl.) in J2000 and a corresponding observation time. Each plate spans $6^\circ \times 6^\circ$ on the sky, as listed by STScI. We simulated 180 random points per plate, for a total of 114,300 points. For each simulated point, we tested whether it would fall within Earth's shadow at a geosynchronous altitude (42,164 km) during a 50 minutes exposure starting from the recorded observation.

Out of the 114,300 simulated points (180 points per plate), 610 were found to lie within Earth's shadow, implying that approximately 0.53% of the survey area should be shadowed at GSO. However, in our actual transient data set, only 349/107,875, 0.32% of the events occur within the shadow, corresponding to a $\sim$39% deficit, significant at the 7.6σ level. We repeated the same procedure at a higher altitude of 80,000 km. In this case, the actual shadow coverage drops to (109/114,300) 0.1%, while the observed fraction of transients (76/107,875) within the shadow is only 0.07%—a $\sim$26% deficit, significant at the 2σ level. The simulated points within each plate are used solely to estimate the expected geometric coverage of the Earth's shadow during the exposure time, and are not meant to represent the spatial distribution of actual transients. This also suggests that a larger fraction of objects may be located near GSO than at 80,000 km, although the limited number of events at 80,000 km makes the comparison statistically uncertain.

We perform an additional, conservative test on the transients, this time assuming a total exposure time of 50 minutes. While our main shadow test assumes that the transient event occurs at a single moment (which is reasonable given their short duration), we now test whether the Earth's shadow passes through the transient's position at *any time* during a 50 minutes window. This increases the chance that the transient would fall within the shadow. We find that 387 (0.3587%) are in the Earth Shadow at 42,168 km, and 80 (0.072%) at 80,000 km. Even under this generous upper limit assumption, where a transient is considered shadowed if the Earth's shadow passes through its position at *any* during a 50 minutes exposure, the deficit remains strong. This result provides robust evidence that the VASCO transients systematically avoid Earth's shadow, consistent with a population of reflective objects that are only visible while sunlit.

The normalization technique presented here is grounded in a direct simulation of shadow coverage based on the actual photographic plates used in the survey. Each plate's position and observation were used to simulate uniformly distributed test points across the plate area, allowing us to empirically estimate the expected fraction of the survey sky that falls within Earth's shadow. This approach minimizes assumptions and avoids potential systematic biases that may arise from analytical solid angle approximations. To avoid introducing spatial selection bias, we include all observed transients in the analysis, including those clustered near the edges of the plates, since plate defects do not know where is the Earth's shadow. As a quick check, nevertheless, we also test by masking edge transients ($>2^\circ$ from plate center) to remove all artifacts close to the plate edge. Removing the edge of the plate in the analysis, yields a similar $\sim$30% deficit in Earth's shadow, though with borderline significance (2.6σ) due to the decrease in sample sizes.

As a note, at low altitudes—where the shadow covers a large fraction of the plate—it is also possible to observe a significant overdensity of transients in the shadowed region. This is a natural consequence of the geometric coverage: when most of the field lies in shadow, any transient—regardless of origin—is statistically more likely to fall there. Such overdensities are therefore not physically meaningful and cannot be used to infer the nature or altitude of the objects. We therefore recommend restricting the analysis to altitudes where the Earth's shadow covers no more than 5% of the plate area, in order to preserve the assumption that its placement is effectively random with respect to plate geometry and defect distribution.

An important implication of this analysis is that the total number of glinting objects near GSO may be significantly underestimated if one only considers the aligned transient candidates, since they represent only a minor subset (albeit visually vetted) of the full transient population. Our results suggest that a much larger population of objects capable of producing sunlight reflections exists, as inferred from the full VASCO transient sample. This systematic deficit of transients in Earth's shadow—especially at altitudes where sunlight reflections dominate—supports the interpretation that a significant fraction, roughly $\sim$1/3rd of all VASCO transients, are caused by highly reflective objects in GSO. However, in order to determine the absolute number of such objects, we would need to quantify the true fraction of false positives in the sample—such as artifacts and plate defects—a major undertaking that will be addressed in a forthcoming study.

9. The GSO Hypothesis

9.1. Object Properties

In this section, we discuss the conditions under which reflections from objects in GSO could produce the observed glints.

An important question is what types of object shapes and reflective geometries are capable of creating the transient signatures observed in the POSS-I plates. A rapidly spinning object may produce multiple glints during a 50 minutes exposure, whereas a more slowly rotating object might generate only one or two.

If we assume a fast spin rated interpret the observed stripe length $d_{\max}$ as corresponding to the path traversed by the

object during the exposure, we can estimate a projected velocity of approximately $0\farcs5\ s^{-1}$. This is significantly slower than the nominal angular velocity of an object at GSO ($\sim 15''\ s^{-1}$). Under these circumstances, we might expect additional transients to be visible along the same narrow band, particularly if the image were extended. Conversely, if the object spins slowly and has only a few small, highly reflective surfaces distributed across a predominantly non-reflective structure, glints may occur only briefly during the exposure, and only at specific orientations.

To explore this further, we use the open-source graphics engine *Blender*[22] to simulate how various 3D shapes could produce glinting patterns similar to those observed. We model five distinct geometries: a sphere, a multi-faceted polyhedron, a cone, a double pyramid, and a structure with two reflective panels. Each shape is composed primarily of non-reflective material, with limited flat surfaces capable of producing strong specular reflections when oriented precisely between the observer and the Sun. In addition to rotation, we allow for precession in some models, which modulates the visibility and timing of glints. The five test geometries are shown in Figure 12.

As expected, a purely spherical object does not generate short, distinct glints; flat, mirror-like surfaces are required. In the cone model, we assume that that the top and bottom surfaces are reflective, yielding double glints per rotation cycle. Adding precession further restricts glint visibility, producing only a few observable flashes per exposure.

The double pyramid model illustrates another plausible case: a reflective structure that becomes partially degraded over time, leaving only small reflective regions. With rotation and precession, such objects may produce intermittent glints, consistent with what we observe in the data.

Overall, we find that each of the five test shapes—under specific assumptions regarding spin, precession, and reflective surface coverage—can, in principle, reproduce a glinting pattern compatible with the transients observed in POSS-I images.

The geometric models presented in this section are intended to demonstrate the plausibility of producing aligned glint patterns from tumbling or precessing objects in high-altitude orbits. We emphasize that these models are illustrative rather than predictive, and no attempt is made to fit the specific time separations or angular offsets of the individual candidates.

While no clear periodicity has been identified in the current POSS-I data, it is well known from modern short-exposure surveys that some Earth-orbiting objects, including those in GSO, can produce isolated, PSF-like glints without clear repetition patterns (e.g., Nir et al. 2021). This lack of periodicity may result from slow rotation, irregular shapes, or specific phase-angle constraints that produce only a few observable flashes per orbital cycle.

Additionally, the observed sky distribution of aligned transients does not always follow a simple great-circle geometry, which could reflect the possibility of complex trajectories, attitude drift, or even the presence of multiple independent objects. Powered objects could even change their altitudes or trajectories. We acknowledge these uncertainties and note that more detailed modeling would be required to establish stronger constraints on orbital parameters or glint periodicity.

9.2. The Background Density

We use the 106,339 transients with decl. $> 0°$ to estimate a rough detection rate. We also count the transients within 2° from the center to avoid potential defects on the edge of the plate (22,314 transients). About 635 plates with 50 minutes exposures on average, correspond to 529 hr and an average transient rate of 36.3 transients per plate circle of 2° radius. Based on the deficit in the Earth Shadow test in Section 8, roughly 1/3rd of the transients appear to be due to solar reflections, so roughly 12.1 transients per plate. We can simply normalize 12.1 over the exposure time and plate coverage (12.57 sq.deg), which gives us $\sim$1.1 transients hr^{-1} deg^{-2} of flux-diluted flashes, visible down to $r \sim 20$ mag. This transient rate is the sum of transients on all altitudes and distances from Earth.

Nevertheless, this comparison should be viewed as an approximate, order-of-magnitude contrast as the the number of transients per plate is very approximate. Also, modern short-exposure surveys such as ZTF operate under vastly different conditions—using CCDs, automated pipelines, and millisecond-level time resolution—whereas the POSS-I transients were recorded on photographic plates with long integration times and are subject to different detection biases and false positive rates. A rigorous comparison would require modeling of completeness, instrument sensitivity, and event classification criteria, which is beyond the scope of this study.

We can also calculate the actual number density of objects. If we assume that the population of objects has a uniform number per surface unit (n), then the number of objects (N) detectable at any given time is given by:

$$N = n \times S, \tag{3}$$

where S is the spherical survey surface containing the observed reflective objects:

$$n = \frac{N}{S}, \tag{4}$$

[22] www.blender.org

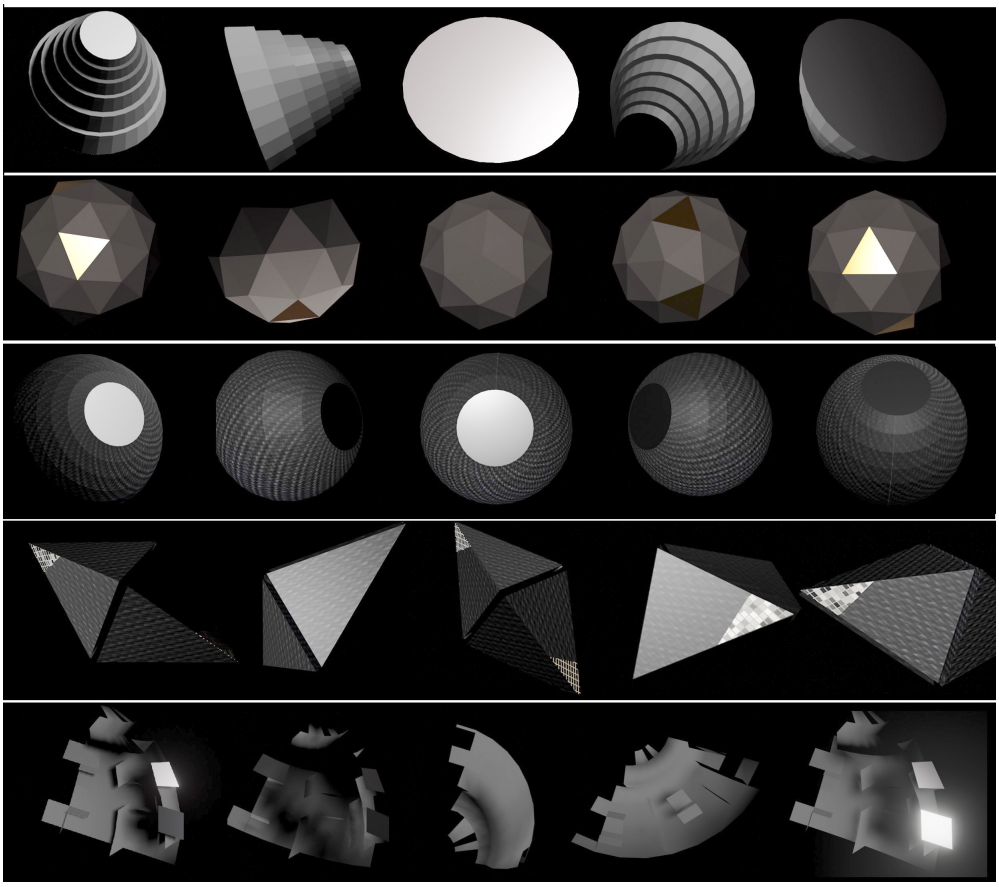

Figure 12. Simulated shapes. We show five different shapes that under slow spinning could produce a handful of glints and in particular double glints. Each shape has two highly reflective surfaces. From top to bottom: (a) cone-like shape, (b) multifaces shape, (c) sphere, (d) 3D hexagone, (e) piece of debris. Each object has both dull and reflective materials on its surface, painted in gray respective light tones. Each object spins around an axis that also has precession, causing the reflective surface not to be visible at all times.

and the surface area $S = 2\pi d^2$ is calculated for the sunlit hemisphere at the radius of a GSO d. Thus:

$$n = \frac{N}{2\pi d^2}. \tag{5}$$

We set $d = 42{,}164$ km as the radius of the GSO.

Using the glint detection rate of approximately $\sim$1.1 transients per hour per square degree (assuming one detectable glint per object per hour):

$$n_{\rm all} \approx 2.0 \times 10^{-6}\,{\rm km}^{-2}. \tag{6}$$

These estimates provide a guide to the surface number density of objects. However, not every object will produce several glints. Since some objects might produce more than one glint (see Section 3.4 in Nir et al. 2021), we can assume that one object might produce from 5 to 20 glints. The shape and the reflectivity of an object will determine the likelihood for one or more glints. This uncertainty also leads to an underestimation of the number density of objects, which could actually be even one order of magnitude higher. The surface density constraint quoted here is a first-order estimate based on our event detection rate and assumed sky coverage. These estimates do not include a full treatment of incompleteness, observational bias, or formal statistical confidence levels, and should therefore be interpreted as an indicative upper bound rather than a rigorous limit. Moreover, the true fraction of false positives in the larger sample from Solano et al. (2022), due to plate defects or other instrumental artifacts, remains unknown. While the overall statistical test in Section 8 is robust to this uncertainty, the absolute number density $n_{\rm all}$ inferred here should be interpreted with caution until a full validation of the sample has been performed.

10. Discussion

Are there signatures of artificial objects in Earth's orbit in pre-Sputnik images? This is the central question explored in the present study. We adopt a straightforward strategy: searching for multiple transients aligned along a narrow band within long-exposure photographic plates from a period prior

to known artificial satellite activity. This approach follows the principle of seeking NTAs via distinctive, low-probability observational signatures, or "smoking gun indicators" (Villarroel et al. 2021). Using the published catalog of VASCO transients in the northern hemisphere (Solano et al. 2022), we identify ∼83 initial candidate *r*-point alignments, along with a larger number of double and triple transient groupings. Triplets are of particular interest, as they are consistent with reflections from flat, rotating surfaces (Deil et al. 2009). One such example was previously reported in Solano et al. (2023).

We manually inspect all 22 candidate alignments containing four or more transients (noting that some reduce to three after closer analysis), and highlight the five most statistically significant cases in Section 6. Although the uncertainties do not allow us to compute a total occurrence probability for such alignments across the entire survey, we do estimate the chance probability of each event within a single image field. These estimates—dependent on assumptions about point-spread function widths—yield significance levels ranging from 2.5σ to 4σ for the most promising cases. Notably, three candidates with four or more aligned points emerge as especially strong, although two of them show minor morphological irregularities. These are not related to FWHM differences, which are addressed separately in the literature (Villarroel et al. 2025a). While we cannot fully exclude the possibility of rare PSF-like optical ghosts producing the alignments, we note that no similar features appear on the blue plates taken with similar configurations.

Among the remaining 3-point alignments (61 in total), some may also merit follow-up if confirmed as genuine transients. Traditionally, this would require microscopic examination of the original plates. However, our discovery of a statistically significant ($>3\sigma$) temporal correlation between VASCO transients and independent historical reports of UAPs (Bruehl & Villarroel 2025) offers additional support for the authenticity of the transients. Plate defects or scanning artifacts are expected to occur randomly in time; the fact that these transient alignments appear preferentially within a day of reported UAP events strongly disfavors instrumental or spurious origins. In this light, the correlation itself provides indirect but meaningful validation of the transients' reality—thus reducing the necessity of microscopic inspection as the only path to confirmation.

But most importantly, Section 8 presents a critical test of the glint interpretation: we find a strong deficit of transient detections, at the $\sim 22\sigma$ statistical significance level, within the Earth's umbral shadow. This is consistent with the idea that sunlight is required to produce the observed flashes. If these events are sunlight reflections off orbiting objects, they should vanish in the shadow cone of the Earth—exactly what we observe. This lends substantial support to the interpretation that the transients are real astrophysical or near-Earth events, and not plate defects or optical ghosts. The disappearance of the population in Earth's shadow would not be expected for emulsion flaws or chemical irregularities. The same holds true for optical ghosts.

Of particular interest is Candidate 5, which occurred on 1952 July 27—the second weekend of the widely documented Washington D.C. "UFO flap." This wave of sightings involved numerous radar detections and pilot observations over two consecutive weekends, July 18–19 and 26–27. Coincidentally, Candidate 1 also occurred within one day of the peak of the 1954 UFO wave. The triple transient reported in Solano et al. (2023) falls on the first weekend of the Washington event. Importantly, these candidates were analyzed before the authors became aware of their proximity to UAP reports, helping to minimize cognitive bias.

Additionally, a correlation has been found between VASCO transients and historical nuclear test dates (Bruehl & Villarroel 2025), echoing past statistical studies linking nuclear activity to increased UAP reports, see e.g., review by Knuth et al. (2025). While causality remains undetermined, the convergence of these independent correlations suggests that the VASCO transients are not random artifacts, but potentially linked to physical phenomena worthy of further investigation.

Using the theoretical framework outlined earlier, we simulate glinting patterns from plausible object shapes in GSO. These include multifaceted and partially reflective objects with slow spins and precessing axes. The inferred surface density of detectable objects is 2.0×10^{-6} km^{-2}, though this estimate is subject to uncertainty both from unknown shape and reflectivity factors (which may cause underestimation), and from the unknown fraction of false positives in the sample (which may cause overestimation). It is worth considering whether such a population could be associated with the so-called uncorrelated targets (UCTs), which have been consistently reported in substantial numbers by military optical sensors and radars since the early 1960s.[23]

Although the GSO hypothesis is consistent with the data, no clear evidence for periodic or quasi-periodic glinting has yet been identified. Objects spinning slowly or possessing complex reflective geometries may produce only a few flashes, complicating efforts to establish a repeating signature. Moreover, it remains possible that some events extend beyond the field of view of a single plate. An object moving at $\sim 10''$ per second could traverse up to 10° during a 50 minutes exposure, suggesting the possibility of longer alignment chains than those captured here.

Conversely, if all transients were to be confirmed as false positives—e.g., due to rare but star-like photographic plate artifacts—our search still constitutes a meaningful upper limit

[23] For example, see declassified U.S. Department of Defense documents released under FOIA, available via The Black Vault: https://documents2.theblackvault.com/documents/dtic/FOIA2014-128-GC8000301.pdf.

on the density of NTAs in the near-Earth environment. In this scenario, we derive a rough surface density constraint of $<10^{-6}$ objects km^{-2} for high-altitude orbits in the Earth's vicinity (thousands to hundreds of thousands of kilometers), even if this limit must be carefully approached due to the lack of modeling for bias and incompleteness. Thus, regardless of interpretation, our findings provide new constraints on possible technosignatures near Earth.

Future work should consider searching for "dashed-line" alignments over larger plate regions, and investigating subtle elongation effects in high-resolution digitizations. Such elongations could indicate motion across the sky or large object size, especially if consistent with the alignment direction.

In summary, we have presented a small but compelling set of aligned transient candidates from a pre-satellite era sky survey. While the ultimate explanation remains uncertain, the convergence of spatial alignment, statistical significance, and temporal correlation with independent aerial anomaly reports supports the view that these events are likely real—and may represent a class of astronomical phenomena not yet understood. Alternative explanations are discussed in Section 7.

11. Conclusions

This paper presents a first systematic search for multiple, simultaneously appearing and vanishing optical point sources on long-exposure photographic plates that also exhibit spatial alignment. We focus on the red POSS-I plates, and present five top candidate events with three or more transients aligned along a narrow band. The most statistically significant case (Candidate 5) coincides in time with the well-documented Washington D.C. 1952 UFO flap—one of the most prominent mass sightings of UAPs in recorded history. A separate study (Bruehl & Villarroel 2025) confirms a statistically significant ($>3\sigma$) temporal correlation between VASCO transients and independent historical UAP reports.

The origin of the transients remains unknown. One plausible explanation is that they are caused by brief light emissions from artificial objects in orbit or by objects with anomalous movements in Earth's atmosphere—emissions so brief that they appear as point sources rather than streaks, despite the telescope tracking the stars. Alternatively, they could arise from solar reflections off flat, highly reflective surfaces at geosynchronous altitudes. The latter interpretation is further supported by our shadow test in Section 8, which reveals a significant deficit of such events within the Earth's umbra, consistent with a solar reflection origin and difficult to reconcile with many explanations, including photographic plate defects.

Our results motivate continued investigation of historical sky surveys and the application of similar alignment-based detection methods to modern deep-sky imaging. Whether or not these events ultimately point to the existence of NTAs, the identification of statistically improbable, spatially aligned transients in pre-satellite data represents a novel observational anomaly deserving of further scientific attention. Future work may help clarify whether these transients constitute a new class of astronomical phenomena—or represent the first hints of artificial activity near our planet.

Acknowledgments

B.V. wishes to thank the anonymous referee, that gave challenges and suggestions that great improved this work. B.V. wishes to thank Dennis Åsberg for his support and for inspiring discussions about the work. She also wishes to thank Dave Altman for teaching her about the Washington 1952 UFO flap. B.V. also wishes to thank Geoff Marcy, Avi Loeb (Galileo project), Robert Powell (SCU/Galileo), Sarah Little (SCU/Galileo) for helpful and constructive comments.

The Digitized Sky Surveys were produced at the Space Telescope Science Institute under U.S. Government grant No. NAG W-2166. The images of these surveys are based on photographic data obtained using the Oschin Schmidt Telescope on Palomar Mountain and the UK Schmidt Telescope. The plates were processed into the present compressed digital form with the permission of these institutions. The National Geographic Society—Palomar Observatory Sky Atlas (POSS-I) was made by the California Institute of Technology with grants from the National Geographic Society. The Second Palomar Observatory Sky Survey (POSS-II) was made by the California Institute of Technology with funds from the National Science Foundation, the National Geographic Society, the Sloan Foundation, the Samuel Oschin Foundation, and the Eastman Kodak Corporation. The Oschin Schmidt Telescope is operated by the California Institute of Technology and Palomar Observatory. The UK Schmidt Telescope was operated by the Royal Observatory Edinburgh, with funding from the UK Science and Engineering Research Council (later the UK Particle Physics and Astronomy Research Council), until 1988 June, and thereafter by the Anglo-Australian Observatory. The blue plates of the southern Sky Atlas and its Equatorial Extension (together known as the SERC-J), as well as the Equatorial Red (ER), and the Second Epoch [red] Survey (SES) were all taken with the UK Schmidt. All data are subject to the copyright given in the copyright summary. Copyright information specific to individual plates is provided in the downloaded FITS headers. Supplemental funding for sky-survey work at the STScI is provided by the European Southern Observatory.

This research has made use of the Spanish Virtual Observatory (http://svo.cab.inta-csic.es) supported from Ministerio de Ciencia e Innovación through grant PID2020-112949GB-I00. B.V. is funded by the Swedish Research Council (Vetenskapsrådet, grant No. 2024-04708) and is also

supported by an anonymous donor to whom she is deeply grateful. M.E.S. acknowledges financial support from the Annie Jump Cannon Fellowship, supported by the University of Delaware and endowed by the Mount Cuba Astronomical Observatory.

Data Availability

Data will be shared on reasonable request to the corresponding author.

ORCID iDs

Alina Streblyanska https://orcid.org/0000-0001-8876-9102

References

Andruk, V., Eglitis, I., Protsyuk, Y., et al. 2019, OAP, 32, 181
Andruk, V., Kharchenko, N., Schilbach, E., & Scholz, R.-D. 1995, AN, 316, 225
Andruk, V. M., Pakuliak, L. K., Golovnia, V. V., et al. 2017, SciIn, 13, 17
Bracewell, R. N. 1960, Natur, 186, 670
Bruehl, S., & Villarroel, B. 2025, Scientific Reports, in press, https://www.researchsquare.com/article/rs-6347224/v1
Corbett, H., Law, N. M., Soto, A. V., et al. 2020, ApJL, 903, L27
Deil, C., Domainko, W., Hermann, G., et al. 2009, APh, 31, 156
Edmunds, M. G. 1981, Natur, 290, 481
Edmunds, M. G., & George, G. H. 1985, MNRAS, 213, 905
Freitas, R. A., Jr., & Valdes, F. 1980, Icar, 42, 442
Freitas, R. A., Jr., & Valdes, F. 1985, AcAau, 12, 1027
Greiner, J., Wenzel, W., & Degel, J. 1990, A&A, 234, 251
Grindlay, J., Tang, S., Los, E., & Servillat, M. 2012, in IAU Symp. 285, New Horizons in Time-Domain Astronomy, Proc. Int. Astronomical Union (Cambridge: Cambridge Univ. Press), 29
Guy Nir's code 2024, https://github.com/guynir42/earthshadow
Hambly, N. C., & Blair, A. 2024, RASTI, 3, 73
Hambly, N. C., MacGillivray, H. T., Read, M. A., et al. 2001, MNRAS, 326, 1279
Haqq-Misra, J., & Kopparapu, R. 2012, AcAau, 72, 15
Irureta-Goyena, B. Y., et al. 2025, PASP, 137, 054503
Knuth, K. H., Ailleris, P., Agrama, H. A., et al. 2025, Progress in Aerospace Sciences, 156, 101097, https://www.sciencedirect.com/science/article/abs/pii/S0376042125000235
Nir, G., Ofek, E. O., Ben-Ami, S., et al. 2021, MNRAS, 505, 2477
Solano, E., Villarroel, B., Rodrigo, C., et al. 2022, MNRAS, 515, 1380
Solano, E., Marcy, G., Villarroel, B., et al. 2023, MNRAS, 527, 6312
Teodorani, M. 2004, Journal of Scientific Exploration, 18, 217
Tokovinin, A. 2002, PASP, 114, 1156
Valdes, R. A., & Freitas, F., Jr. 1983, Icar, 53, 453
Vavilova, I. B., Pakulyak, L. K., Shlyapnikov, A. A., et al. 2012, KPCB, 28, 85
Vavilova, I. B., Yatskiv, Y. S., & Pakuliak, L. K. 2017, in IAU Symp. 325, Astroinformatics, Proc. Int. Astronomical Union (Cambridge: Cambridge Univ. Press), 361
Villarroel, B. 2024, The Vanishing Star Enigma and the 1952 Washington D. C. UFO Wave (Popular Science)
Villarroel, B., Imaz, I., & Bergstedt, J. 2016, AJ, 152, 76
Villarroel, B., Marcy, G. W., Geier, S., et al. 2021, NatSR, 11, 12794
Villarroel, B., Mattsson, L., Guergouri, H., et al. 2022a, AcAau, 194, 106
Villarroel, B., Pelckmans, K., Solano, E., et al. 2022b, Univ., 8, 561
Villarroel, B., Solano, E., & Marcy, G. W. 2025a, arXiv:2507.15896
Villarroel, B., Soodla, J., Comerón, S., et al. 2020, AJ, 159, 8
Villarroel, B., Watters, W. A., Streblyanska, A., Solano, E., & Geier, S. 2025b, MNRAS, in press
Waszczak, A., Prince, T. A., Laher, R., et al. 2017, PASP, 129, 034402

scientific reports

Check for updates

OPEN

Transients in the Palomar Observatory Sky Survey (POSS-I) may be associated with nuclear testing and reports of unidentified anomalous phenomena

Stephen Bruehl[1]✉ & Beatriz Villarroel[2]

Transient star-like objects of unknown origin have been identified in the first Palomar Observatory Sky Survey (POSS-I) conducted prior to the first artificial satellite. We tested speculative hypotheses that some transients are related to nuclear weapons testing or unidentified anomalous phenomena (UAP) reports. A dataset comprising daily data (11/19/49—4/28/57) regarding identified transients, nuclear testing, and UAP reports was created (n = 2,718 days). Results revealed significant ($p = .008$) associations between nuclear testing and observed transients, with transients 45% more likely on dates within +/- 1 day of nuclear testing. For days on which at least one transient was identified, significant associations were noted between total number of transients and total number of independent UAP reports per date ($p = 0.015$). For every additional UAP reported on a given date, there was an 8.5% increase in number of transients identified. Small but significant ($p = .008$) associations between nuclear testing and number of UAP reports were also noted. Findings suggest associations beyond chance between occurrence of transients and both nuclear testing and UAP reports. These findings may help elucidate the nature of POSS-I transients and strengthen empirical support for the UAP phenomenon.

Keywords Transient, Unidentified anomalous phenomena, UAP, UFO, Nuclear testing

Transient star-like objects have been identified in sky surveys conducted prior to the launch of the first artificial satellite on October 4, 1957[1,2]. These short-lived transients (lasting less than one exposure time of 50 min) have point spread functions and are absent in images taken shortly before the transients appear and in all images from subsequent surveys[3]. As reported previously in this journal[3], in some cases multiple transients appear in a single image, exhibiting characteristics not easily accounted for by prosaic explanations (e.g., gravitational lensing, gamma ray bursts, fragmenting asteroids, plate defects)[3,4]. We have identified numerous transients in the Palomar Observatory Sky Survey (POSS-I) as well as in other sky surveys as part of the Vanishing and Appearing Sources during a Century of Observations (VASCO) project[1–3].

The source of the transients identified remains unknown and cannot be directly tested due to their historical nature. Nonetheless, examination of contemporaneous correlates of these transients may provide information useful for elucidating their possible origin. Systematic research of this type has not previously been conducted. However, anecdotal reports suggest speculative hypotheses regarding possible correlates of transients for which sufficient data are available to enable empirical testing.

Possible associations of transients with nuclear weapons testing might be considered for two reasons. From 1951 until the launch of Sputnik in 1957, at least 124 above-ground nuclear tests were conducted by the United States (U.S.), Soviet Union, and Great Britain. In some circumstances, nuclear radiation is known to cause a visible glow (i.e., Cherenkov radiation)[5]. This phenomenon can be observed in the atmosphere in response to high energy particles (e.g., gamma rays), although it is influenced by both particle energies and atmospheric density[6]. Consistent with this concept, glowing "fireballs" in the sky were reported in multiple instances to occur shortly after nuclear tests in locations where significant nuclear fallout was expected[7,8].

[1]Department of Anesthesiology, Vanderbilt University Medical Center, 701 Medical Arts Building, 1211 Twenty-First Avenue South, Nashville, TN 37212, USA. [2]Nordita, KTH Royal Institute of Technology and Stockholm University, Hannes Alfvéns Väg 12, 106 91, Stockholm, Sweden. ✉email: Stephen.Bruehl@vumc.org

Based on such observations, we hypothesize that some transients might represent an unrecognized atmospheric effect of nuclear testing. Alternatively, it is also possible that fallout from nuclear testing may itself cause direct contamination of astronomical photographic plates, with a characteristic appearance of fogged spots noted on X-Ray sensitive photographic film[9]. We also considered a very different potential reason for links between nuclear testing and transients. Contemporaneous newspaper accounts and records from the Air Force's Project Blue Book investigation of what are now called Unidentified Anomalous Phenomena (UAP) indicate that unusual, apparently metallic objects of unknown origin were reported in the sky on multiple occasions on dates immediately before, during, and after nuclear weapons tests[7]. UAP have often been reported at nuclear power plants and sites involved in nuclear weapons production as well[7,10]. We hypothesized that if UAP seen during nuclear tests were metallic, they might reflect sunlight (or possibly emit light directly) and thus appear as transients if they were in geosynchronous orbits immediately before or after their appearance during nuclear testing.

In an extension of this latter hypothesis, transients might also be associated with witness reports of UAP more broadly, outside of the nuclear testing context. Consistent with this, we note POSS-I images from July 19, 1952 and July 27, 1952, each of which exhibit multiple bright transients (see Fig. 1)[4,11]. These dates coincide with two consecutive weekends during which multiple UAP were observed for several hours both visually and on radar over Washington, D.C.[11,12]. We speculate that some transients could potentially be UAP in Earth orbit that, if descending into the atmosphere, might provide the stimulus for some UAP sightings.

In the current study, we conducted a preliminary test of the speculative hypotheses above using a database we have created of > 100,000 transients identified in POSS-I survey images (see Methods). Each of these transients does not appear in a POSS-I image taken shortly before or in images from subsequent surveys. We examined associations of both the presence of any transient (Yes/No) and the number of transients (across the entire sky) identified on each date with: 1) dates of above-ground nuclear testing (from publicly available sources) and 2) reports of at least one UAP on that date (Yes/No) and the total number of independent UAP reported on that date in a comprehensive database of UAP witness reports (UFOCAT; see Methods). While we anticipated significant noise in the UAP sighting data (e.g., due to witness error) and potentially in the transient data as well (e.g., misidentifications related to dust, cosmic radiation, etc.), we believed it was important to subject these novel hypotheses to direct empirical test to provide a preliminary evaluation of possible associations between observed transients and both nuclear testing and UAP sightings.

Results

Descriptive characteristics

Transient data were available for the period November 19, 1949 – April 28, 1957, inclusive, with the latter date more than 5 months prior to the launch of the first artificial satellite (Sputnik). Of the 2,718 days in this period, transients were observed on 310 days (11.4%). In the overall sample, the number of transients per date ranged from 0 to 4,528 (across multiple locations on multiple plates), with 5% trimmed mean = 10.09 and median = 0.0. The distribution of number of transients per date was highly right-skewed (skewness = 10.35) and over-dispersed (variance = 28,938.64).

Above-ground nuclear weapons tests (U.S., Soviet, and British) were conducted on 124 days (4.6%) during the study period. UAP reports were recorded in the UFOCAT database on 2,428 days during the study period (89.3%). For days on which at least one UAP sighting was reported, the 5% trimmed mean number of independent sightings (i.e., in different states or countries) was 3.77, with a median of 3.0 sighting reports. The number of UAP reports was significantly higher within a nuclear testing window (5% trimmed mean = 3.68) than outside of a nuclear testing window (5% trimmed mean = 3.31; Mann–Whitney U = 447,057, p = 0.008), suggesting some degree of association between these two outcomes.

Association of transients with nuclear weapons testing

We first tested for possible associations between occurrence of transients and nuclear weapons tests. The primary nuclear testing outcome reflected a window comprising the test date + /- 1 day (see Methods). Potential associations with transients were tested in two ways. Table 1 displays a 2 X 2 crosstabulation portraying whether each date was within a nuclear testing window (Yes/No) by whether any transient was observed on that date (Yes/No). Transients occurred significantly more often within a nuclear testing window than outside of a nuclear testing window, Chi-Square (1) = 6.94, $p = 0.008$. We note that 15.6% of nuclear test dates were associated with at least one transient whereas only 10.8% of dates outside of a nuclear testing window were associated with a transient. Our findings indicated that the relative risk ratio for a transient to occur when within a nuclear test window (relative to being outside of a nuclear test window) was 1.45 (95% Confidence Interval: 1.10 – 1.90). Thus, a transient was 45% more likely to be observed on dates within a nuclear test window (day of test + /- 1 day) compared to dates outside of a nuclear test window.

Follow-up secondary analyses were then conducted to examine in more granular fashion the timing of the association between nuclear testing and occurrence of transients. Table 2 summarizes the association between occurrence of transients and different time windows relative to nuclear testing, ranging from 2 days before a test until 2 days after a test. The only association that reached statistical significance was for the association in which transients occur 1 day *after* nuclear testing. Transients were observed on 18.5% of days that were 1 day following a nuclear test, whereas transients were noted on only 11.0% of days not meeting this criterion. These findings indicate that the chances of observing a transient were 68% higher on the day following a nuclear test compared to days unassociated with nuclear testing.

Beyond dichotomous occurrence of transients, we also tested for differences in the total number of transients observed on a given date as a function of whether that date fell within a nuclear testing window. Significantly

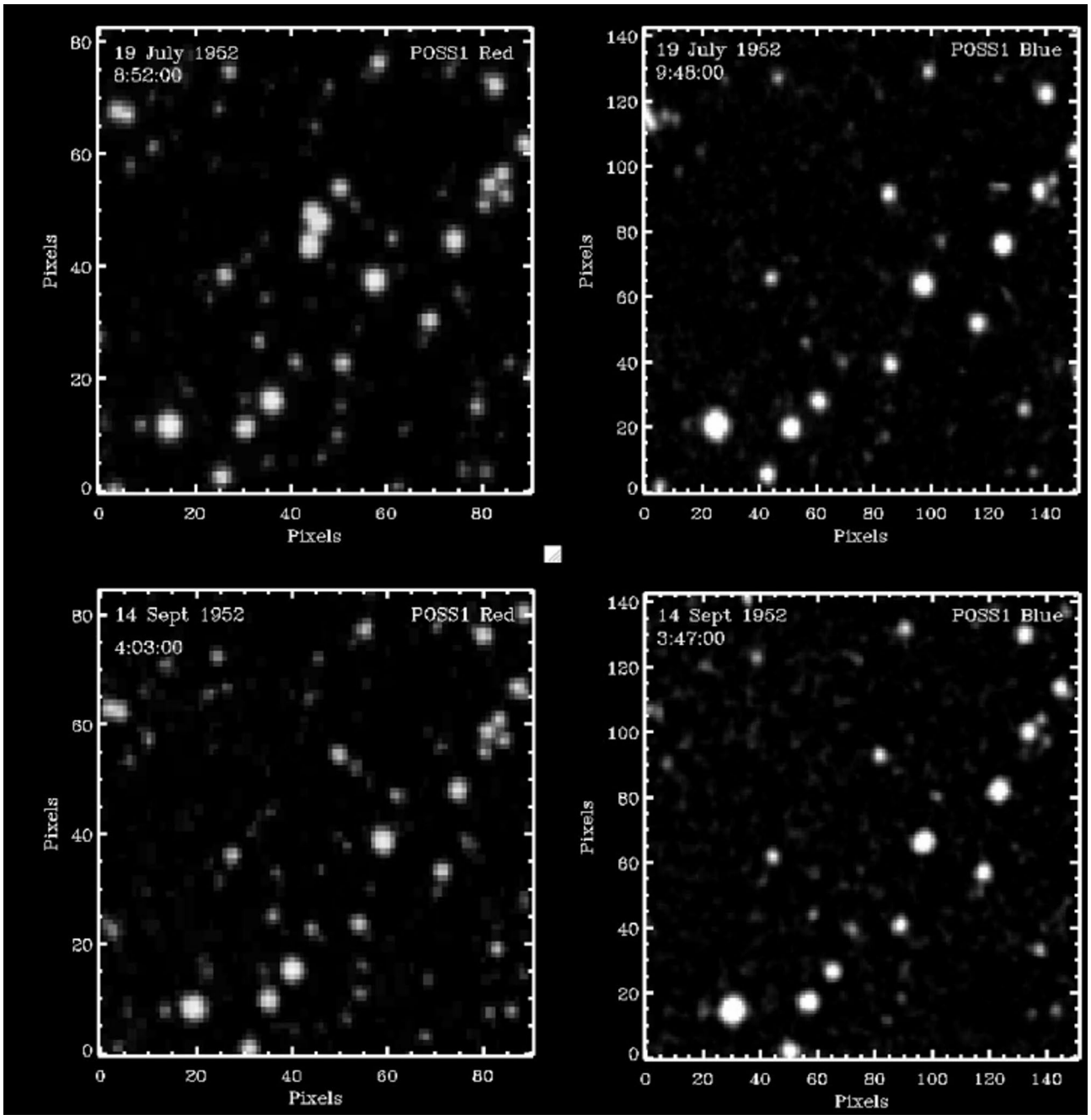

Fig. 1. Four exposures of the 3 × 3 arcmin region of sky centered on the triple transient identified in July 1952. Upper left: The POSS I red image on July 19, 1952 at 8:52 (UT) containing the triple transient just above center. Upper right: A 10 m exposure POSS I blue image of the same region taken immediately afterward with no evidence of the triple transient. Lower left and right: POSS I red (left) and blue (right) images taken two months later (September 14, 1952) showing the transient still gone. Adapted from Solano et al. (2024)[4].

more transients were observed on dates within a nuclear testing window (5% trimmed mean = 23.40) than outside of a nuclear testing window (5% trimmed mean = 8.55; Mann–Whitney U = 431,649.5, $p = 0.007$).

Association of transients with UAP sightings

Because UAP reports were so common (at least one report on 89.3% of study dates), examination of possible links between transients and UAP sightings as dichotomous measures was of limited value (this test was not significant; Chi-Square = 2.43, $p = 0.12$). Instead, statistically more powerful analyses based on continuous measures were used to test associations between the *number* of UAP reports and *number* of transients observed on a given date. These analyses employed two approaches. The first approach simply examined the correlation between number of transients and number of UAP sighting reports on a given night. This analysis was restricted

	Transient observed?	
Within a nuclear testing window?	**No**	**Yes**
No	2,116 (89.2%)	255 (10.8%)
Yes	293 (84.4%)	54 (15.6%)

Table 1. 2 X 2 crosstabulation of transient status on a given date by whether that date fell within a nuclear testing window (test date + /- 1 day). Frequency (and percentage across nuclear testing window categories) are presented. Differences across cells are significant ($p = .008$).

Time window relative to nuclear test	Percentage of transient positive days within nuclear window	Percentage of transient positive days outside of nuclear window	Chi square value	*P* value	Relative risk (95% CI) of transient occurring within nuclear window
2 days before test	13.7	11.2	0.726	0.394	1.22 (0.775, 1.924)
1 day before test	14.5	11.2	1.307	0.253	1.30 (0.835, 2.017)
Day of test	15.3	11.2	2.016	0.156	1.37 (0.894, 2.102)
1 day after test	18.5	11.0	6.647	0.010	1.68 (1.145, 2.472)
2 days after test	12.9	11.3	0.290	0.590	1.14 (0.712, 1.822)

Table 2. Associations of transients with nuclear testing within different time windows. CI = Confidence Interval.

to dates on which at least one transient occurred (n = 310), an analysis that eliminates the substantial bias due to the large number of zero values in the transient data (there were no transients observed on 88.5% of the days in the dataset). This simple analysis revealed a very small but statistically significant association (i.e., beyond chance) between the total number of transients and total UAP reports on a given date (Spearman's rho = 0.138, $p = 0.015$). A scatterplot of this association is presented in Fig. 2.

To address limitations of the simple correlation analysis approach above, we employed a second and statistically more powerful analytic approach to test our transient-UAP hypothesis in a manner that utilized all of the information available in the data. That is, we observed that the total number of transients per date was highly right-skewed and over-dispersed, approximating a negative binomial distribution. We therefore used Generalized Linear Model (GLM) analyses specifying a negative binomial distribution to test associations between number of UAP reports and number of transients each day in the overall sample. Model fit was good (Chi Square = 18.50). Results revealed a significant positive association between number of UAP reported and number of transients observed (Beta = 0.081, Standard Error = 0.006, $p < 0.001$). The exponentiated parameter estimate [Exp(B)] = 1.085] indicated that for every additional UAP reported on a given date, there was an 8.5% increase in the number of transients observed.

Finally, because both nuclear testing and UAP reports were individually associated with transients, we also explored whether their linear combination was associated with total number of transients (i.e., are the observed associations additive?). We created a new categorical variable coded as follows: 0 = No UAP on that date and the date was not within a nuclear testing window, 1 = At least one UAP report that date or the date was within a nuclear testing window, and 2 = At least one UAP report that date and the date was within a nuclear testing window. The dependent variable was total number of transients for each date, so for reasons described above we again used a GLM analysis specifying a negative binomial distribution. Results were statistically significant, Beta = 1.073, Standard Error = 0.0834, $p < 0.001$. Estimated marginal means (with 95% confidence intervals) for each group are presented in Table 3. Dates with no UAP reports that were not within a nuclear testing window were associated with the fewest total transients whereas dates with at least one UAP report and that *were* within a nuclear testing window displayed the highest total number of transients. All pairwise differences between these individual groups were significant (p's < 0.001) and the 95% confidence intervals for each did not overlap. The overall pattern of results suggests that associations of UAP reports and nuclear testing with number of observed transients may be additive.

Discussion

This study provided a preliminary test of hypothesized associations between short-lived star-like transients identified in POSS-I sky survey images from 1949 and 1957 and both nuclear weapons testing and reports of UAP sightings. The study premise was that identifying contemporaneous correlates of transients might help elucidate their nature and origin, which currently is unknown. Our results revealed several intriguing statistical associations.

First, although not the primary study focus, we observed a small but statistically-significant association between nuclear weapons testing and increased UAP sightings. Significantly more UAP sightings were reported within nuclear weapons testing windows (test date + /- 1 day) than outside of testing windows. To our knowledge, this statistical association has not previously been reported in the peer-reviewed literature, although it is consistent with anecdotal reports of such associations[7].

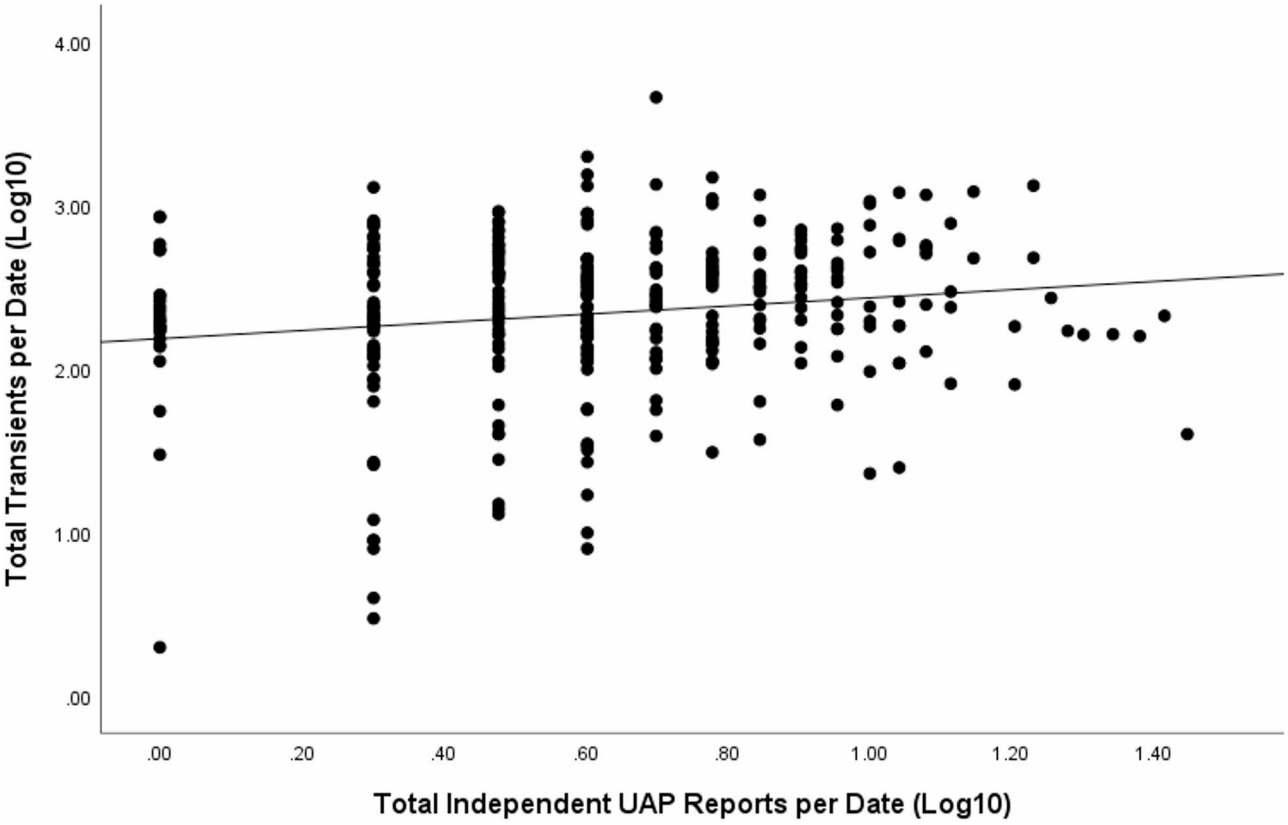

Fig. 2. Scatterplot of total number of transients identified by total number of independent UAP reports for dates on which at least one transient occurred (n = 310). Both variables have been log10 transformed to enhance scaling for clarity.

Combined predictor group	Mean total transients	Standard error	95% confidence interval
No UAP reports and not in nuclear window	20.0	1.24	17.69, 22.57
≥ 1 UAP report or within nuclear window	40.6	0.89	38.88, 42.38
≥ 1 UAP report and within nuclear window	58.4	3.25	52.39, 65.15

Table 3. Estimated marginal means for total number of transients identified per date across the three combined predictor groups (+/- UAP reports combined with +/- nuclear testing window). All pairwise comparisons are significant at $p < .001$.

Next, in tests of our primary hypotheses, we found that both dichotomous occurrence of transients and the total number of transients observed on a given date were associated with nuclear testing beyond chance. Transients were 45% more likely to be observed on dates that were within a nuclear test window than on dates not in a nuclear test window. More granular examination of the temporal sequencing of these associations revealed that the strongest (and only significant) association was between nuclear testing and increased likelihood of a transient occurring one day after that test.

We also note an intriguing incidental finding regarding possible nuclear testing-transient links. The last date on which a transient was observed within a nuclear testing window in this dataset was March 17, 1956, despite there being an additional 38 above-ground nuclear tests in the subsequent 13 months of the study period. A prior study of associations between UAP reports and nuclear weapons-related production and assembly sites (excluding nuclear weapons tests) concluded that elevated UAP activity at such sites began in 1948, increased dramatically and continued through 1952, but then precipitously decreased in 1953 and remained low through 1975 (end of their study period)[10]. This sudden and sustained decrease in UAP reports at nuclear production facilities in 1953 occurred despite major new nuclear weapons production and assembly facilities coming online during that time (e.g., the Savannah River and Pantex sites)[10]. Taken together, the period between 1953 and 1956 seems to mark a shift in a multiyear pattern of apparent UAP-nuclear associations. While the meaning of these parallel decreases in UAP activity at both nuclear weapons production and testing locations in the mid-1950s is unclear, they may represent convergent evidence for the validity of associations between UAP and nuclear weapons-related activity.

Finally, our hypothesis of associations between transients and UAP reports was also supported. We detected a very small positive correlation, which was well beyond chance, between the number of transients observed and the number of UAP reported on a given date (Spearman's rho = 0.14). This association was observed when analyses were restricted to dates on which at least one transient occurred, an analysis mitigating the potentially significant bias resulting from the large proportion of dates (88.5%) on which no transients were observed. This finding supports our hypothesis of potentially meaningful associations between transients and UAP reports. Other analyses examining the full sample indicated that for every additional UAP reported on a given date, there was an 8.5% increase in number of transients observed on that date. Overall, findings of this study support our speculative hypotheses that transients exhibit some degree of association with both nuclear testing and reports of UAP. Our results further suggest these associations are additive, with the largest number of transients seen for dates within a nuclear testing window on which at least one UAP was reported.

Our findings do not definitively indicate what transients are nor do they necessarily imply causal associations. However, our results do argue against several prosaic explanations for transients. Our overall pattern of results is clearly not consistent with the proposition that most transients are due to contamination or defects in photographic plates or scanned images, or to any other local confounds at the observatory itself. Contamination of photographic plates by nuclear fallout produces diffuse fogged spots quite different in appearance than the discrete star-like brightness profiles with point spread functions characteristic of transients[3,9]. These explanations would also not account for the association of transients with UAP reports from multiple locations distant from the observatory. Associations between transients and both UAP and nuclear testing reported in this study also cannot be plausibly attributed to any form of observer bias, as the existence of transients was unknown at the time they occurred and the dates/times of nuclear tests were generally unknown to the individuals who were reporting the UAP. Finally, the fact that transients were most likely to occur one day after a nuclear test (rather than the day of the test) argues against bomb debris ejected into the atmosphere as a plausible explanation.

Regarding what transients might be, our findings point toward two hypotheses that could account for associations of transients with both nuclear testing and UAP reports. The first involves an unexpected and previously undocumented atmospheric phenomenon triggered by nuclear detonations or related to nuclear fallout that may serve as a stimulus for some UAP reports and appear as transients on astronomical images. While the latter is potentially plausible, effects in the atmosphere (rather than geosynchronous orbit) would be likely to result in a streak on the image over the 50 min exposure, yet all transients appear as distinct point sources rather than streaks. Moreover, this hypothesis is made even more unlikely given that transients were most often observed one day after a nuclear test; such atmospheric phenomena would have to be sustained and remain localized in one location for approximately 24 h to account for the visual appearance of transients. The second hypothesis is more speculative, drawing on a well-known strand of UAP lore suggesting that nuclear weapons may attract UAP[7,8]. While this alleged connection has been claimed for decades based on anecdotal evidence, it has until now lacked any systematic supporting data. Within this latter hypothesis, our results could be viewed as indicating that transients are artificial, reflective objects either in high-altitude orbits around Earth[13] or at high altitudes within the atmosphere. Whether and how this hypothesis might be further tested remains to be determined. Regardless of what transients are ultimately determined to be, our results add to growing evidence supporting the interpretation of transients as real observations[1,3,13] rather than as emulsion defects.

The small magnitude of the significant associations reported must be addressed. Detection of these small effects was enabled by the high statistical power resulting from the large sample size available. Several factors may have contributed to the small magnitude of the associations observed. These associations may have been limited in part by noise in the transient data. Automated methods were applied to identification of the > 100,000 transients comprising the data examined in this study. While a small subset of these have been subjected to manual confirmation, application of more sophisticated systematic validation methods employing artificial intelligence might reduce any misidentifications of transients and result in a higher signal to noise ratio, thereby increasing the magnitude of associations like those reported here. There is also undoubtedly substantial noise in the UAP data examined that could have minimized the size of observed associations. Witness reports are affected by various types of errors[14–16] and reports in the UFOCAT database that provided UAP data for the current work have not been evaluated for validity in any systematic way. Additionally, the magnitude of the associations between transients and both nuclear tests and UAP might have been limited by the fact that the Palomar Observatory from which transients were observed only provides observations from a single geographic point, whereas nuclear weapons tests and UAP reports can occur worldwide. Finally, transients may be heterogeneous in nature and derived from multiple causes, limiting the magnitude of their association with any single correlate.

In conclusion, data obtained prior to launch of the first artificial satellite in 1957 reveal small but statistically-significant associations between short-lived star-like transients and both above-ground nuclear weapons testing and UAP sightings. Our findings provide additional empirical support for the validity of the UAP phenomenon and its potential connection to nuclear weapons activity, contributing data beyond eyewitness reports. The possibility that some transients may represent UAP events in orbit captured on photographic plates prior to the launch of the first artificial satellite cannot be ruled out. This study adds to the small peer-reviewed literature seeking to apply systematic scientific methods to the study of UAP-related data[8,10,17–20]. The ultimate importance of the associations reported in the current work for enhancing understanding of transients and UAP remains to be determined.

Methods

Data sources

Transient data

The initial transient dataset consisted of a list of 107,875 transients identified that occurred between 11/19/49 and 4/28/57. These transients were identified in publicly-available scanned images from the POSS-I survey

available on the DSS Plate Finder website (https://archive.stsci.edu/cgi-bin/dss_plate_finder). The process used to identify transients and eliminate misidentifications was conducted via an automated workflow detailed fully in Solano et al.[1]. In brief, transients were defined as distinct star-like point sources present in POSS-I E Red images that were absent both in images taken immediately prior to the POSS-I Red image and in all subsequent images. A final criterion for classifying an object as a transient was that there were no counterparts either in PanStarrs DR1 or Gaia DR3 at less than 5 arcsec.

This transient dataset contained the dates, times, and coordinates of each transient identified. For many dates, transients were noted in multiple images reflecting observations of different locations in the sky. The transient dataset (ASCII format) was converted to an SPSS for Windows data file that included a single line for each date on which at least one transient occurred, with a count variable created to summarize the total number of transients observed on each date.

Nuclear weapons testing data

An SPSS dataset was created from public sources which included the dates of all above-ground nuclear weapons tests during the study period. Tests conducted by the United States were identified from:

https://nnss.gov/wp-content/uploads/2023/08/DOE_NV-209_Rev16.pdf

Tests conducted by the Soviet Union were identified from: https://en.wikipedia.org/wiki/List_of_nuclear_weapons_tests_of_the_Soviet_Union.

Tests conducted by Great Britain were identified from: https://chrc4veterans.uk/knowledge-hub/british-nuclear-weapons-testing/.

Anecdotal reports from individuals present during nuclear tests in the 1950's have variously reported UAP to be present at nuclear test sites before, during, and after nuclear tests[7]. Therefore, our primary outcome was a nuclear testing window variable (coded 1/0 for Yes/No) that indicated whether a given date fell within a 3-day window surrounding any nuclear test (test date + /- 1 day). This decision to use a 3-day window as the primary nuclear testing outcome was made while the authors were still blinded to the transient data. To permit subsequent examination of the temporal sequencing of transient associations with nuclear testing at a more granular level, we also created (post-hoc) several variables indicating whether a given date occurred at specific intervals relative to nuclear testing: 2 days before, 1 day before, day of testing, 1 day after, and 2 days after.

UAP witness report data

UAP witness report data were derived from the publicly-available comprehensive UFOCAT database maintained by the Center for UFO Studies (https://cufos.org/cufos-publications-databases/ufocat/). This database originated with the U.S. Air Force funded-University of Colorado UFO Study led by Dr. Edward Condon (1966–1968). It has been updated periodically since that time. It represents the most comprehensive publicly-available UAP sighting database covering the 1949–1957 period that was the focus of the current work. The original UFOCAT Microsoft Access database was imported into SPSS. This database contained many identical, duplicate entries (same date and location) obtained from different sources; only a single entry for each discrete report was retained. Next, to reduce the chances of duplicate reports of the same UAP described by separate witnesses on the same date and the same location (i.e., same state), only a single entry was retained in these cases. Finally, a variable reflecting the total count of UAP sightings reported from independent locations on each date was created.

Procedure

The final analyzed dataset began with creation of an SPSS master file with a separate record for every date within the study period, 11/19/49 to 4/28/57 (n = 2,718 days). Then, the transient database, nuclear test database, and the UAP database were merged by date with this master file. Next, dichotomous variables (coded 1/0 for Yes/No) were created to indicate whether each date in the master file was associated with at least one transient and/or with at least one UAP report. Both dichotomous and continuous variables were available for the transient data (any transient Yes/No and total number of transients identified on each date) and for the UAP data (any UAP Yes/No and total number of independent UAP reports on each date). The nuclear testing variable was only available as a dichotomous index, that is, whether each date fell within a nuclear testing window (coded 1/0 for Yes/No).

Statistical analysis

All analyses were carried out using the SPSS for Windows Version 29 statistical package (IBM Corp., Armonk, NY). For testing associations between dichotomous variables [Nuclear Testing Window (Yes/No) versus Transient Observed (Yes/No)], chi-square tests were used. To aid in interpretation of the magnitude of the association between nuclear testing and transients, we adopted a relative risk approach like that commonly used in medical research. That is, we calculated the likelihood of a transient being observed (the "outcome") based on whether its date was within a nuclear weapons testing window (the "exposure"). This relative risk ratio was calculated using an online calculator: https://www.medcalc.org/calc/relative_risk.php. Due to significantly non-normal distributions of the variables reflecting total number of transients and total number of UAP per night, differences in these variables as a function of nuclear testing were examined using the nonparametric Mann–Whitney U test. For characterizing the nature of group differences in these nonparametric tests, we present 5% trimmed means given the highly skewed distributions of these variables and that median values were generally uninformative (e.g., median total transients = 0). Also for distributional reasons, associations between these two continuous measures were tested using the nonparametric Spearman's rho correlation. To provide an interpretive context for the magnitude of the association between total number of transients and UAP reported per night, we conducted generalized linear model (GLM) analyses, specifying a negative binomial distribution given the highly right-skewed and over-dispersed nature of the transient data. The resulting exponentiated

parameter estimate was then used to derive an estimate of the effect's magnitude (i.e., impact of number of UAP sightings on total transients observed that date) in terms of incidence rate ratio. For display purposes in Fig. 2, total transients and total UAP reports have both been log10 transformed (after adding a constant [+1] to avoid zero values) in order to optimize scaling in the figure.

Data availability

The final analyzed SPSS dataset will be made available by the authors upon reasonable request to Dr. Stephen Bruehl (stephen.bruehl@vumc.org).

Received: 31 March 2025; Accepted: 22 September 2025
Published online: 20 October 2025

References

1. Solano, E., Villarroel, B. & Rodrigo, C. Discovering vanishing objects in POSS I red images using the virtual observatory. *Mon. Not. R. Astron. Soc.* **515**, 1380–1391 (2022).
2. Villarroel, B. et al. The vanishing and appearing sources during a century of observations project I USNO objects missing in modern sky surveys and follow-up observations of a "Missing Star". *Astronom. J.* **159**, 8 (2020).
3. Villarroel, B. et al. Exploring nine simultaneously occurring transients on April 12th 1950. *Sci Rep* **11**, 12794 (2021).
4. Solano, E. et al. A bright triple transient that vanished within 50 min. *Mon. Not. R. Astron. Soc.* **527**, 6312–6320 (2024).
5. Neamtan, S. M. The Čerenkov effect and the dielectric constant. *Phys. Rev.* **92**, 1362–1367 (1953).
6. Belz, J. et al. Comparison of air fluorescence and ionization measurements of EM shower depth profiles: Test of a UHECR detector technique. *Astropart. Phys.* **25**, 57–63 (2006).
7. Hastings, R. *UFOs & nukes: extraordinary encounters at nuclear weapons sites* (2nd Edition). (Self-Published, 2017).
8. Knuth, K.H. et al. The new science of unidentified aerospace-undersea phenomena (UAP). Preprint at: https://www.arxiv.org/abs/2502.06794. (2025).
9. Webb, J. H. The fogging of photographic film by radioactive contaminants in cardboard packaging materials. *Phys. Rev.* **76**, 375 (1949).
10. Grosvenor, S., Hancock, L. & Porritt, I. UAP indications analysis 1945–1975 United States atomic warfare complex". *Limina—J. UAP Stud.* **2**(1), 109–128. https://doi.org/10.59661/001c.131854 (2025).
11. Villarroel, B. (2024) The vanishing star enigma and the 1952 Washington DC UFO wave. The Debrief. https://thedebrief.org/the-vanishing-star-enigma-and-the-1952-washington-d-c-ufo-wave/.
12. Ruppelt, E. The Washington merry-go-round in *The report on unidentified flying objects*. -172 (Doubleday & Company, 1956).
13. Villarroel, B. et al. A glint in the eye: Photographic plate archive searches for non-terrestrial artefacts. *Acta Astronaut.* **194**, 106–113 (2022).
14. Frenda, S. J., Nichols, R. M. & Loftus, E. F. Current issues and advances in misinformation research. *Curr. Dir. Psychol. Sci.* **20**, 20–23 (2011).
15. Loftus, E. F. & Palmer, J. C. Reconstruction of automobile destruction: An example of the Interaction between language and memory. *J. Verbal Learn Verbal Behav.* **13**, 585–589 (1974).
16. Norman, J. F. et al. The visual perception of long outdoor distances. *Sci. Rep.* **14**, 3207 (2024).
17. Medina, R. M., Brewer, S. C. & Kirkpatrick, S. M. An environmental analysis of public UAP sightings and sky view potential. *Sci. Rep.* **13**, 22213 (2023).
18. Watters, W. A. et al. The scientific investigation of unidentified aerial phenomena (UAP) using multimodal ground-based observatories. *J. Astronom. Instrum.* **12**, 2340006 (2023).
19. Nolan, G. P., Vallee, J. F., Jiang, S. & Lemke, L. G. Improved instrumental techniques, including isotopic analysis, applicable to the characterization of unusual materials with potential relevance to aerospace forensics. *Prog. Aerosp. Sci.* **128**, 100788 (2022).
20. Bruehl S, Little S, Powell R.M. Cluster analysis of features associated with unidentified anomalous phenomena described in 216 select reports from 1947- 2016. *World Futures* (in press).

Acknowledgements

B.V is supported by a generous donor and is also funded by the Swedish Research Council (Vetenskapsrådet, grant 2024-04708).

Author contributions

S.B. and B.V. designed the study. B.V. prepared and interpreted the transient data. S.B. compiled the multiple datasets that were merged into the final analyzed dataset and conducted and interpreted the statistical analyses. S.B. prepared the initial draft of the manuscript, and both S.B. and B.V. edited the draft manuscript and wrote the final version. B.V. prepared Fig. 1 and S.B. prepared Fig. 2 and Tables 1, 2 and 3. All authors have reviewed the final manuscript.

Funding

Vetenskapsrådet, 2024-04708

Declarations

Competing interests

The authors declare no competing interests.

Additional information

Correspondence and requests for materials should be addressed to S.B.

Reprints and permissions information is available at www.nature.com/reprints.

A Cost-Effective Search for Extraterrestrial Probes in the Solar System

Beatriz Villarroel,[1]★ Wesley A. Watters,[2] Alina Streblyanska,[3] Enrique Solano,[4] Stefan Geier,[3,5] Lars Mattsson[1]

[1] *Nordita, KTH Royal Institute of Technology and Stockholm University, Hannes AlfvÃl'ns vÃd'g 12, SE-106 91 Stockholm, Sweden*
[2] *Whitin Observatory, Dept. Physics & Astronomy, Wellesley College, 106 Central Street Wellesley, MA 02481, USA*
[3] *Instituto de Astrofísica de Canarias, Vía Láctea, 38205 La Laguna, Tenerife, Spain*
[4] *Departamento de Astrofísica, Centro de Astrobiología (CSIC/INTA), P.O. Box 78, E-28691 Villanueva de la Cañada, Spain; esm@cab.inta-csic.es*
[5] *GRANTECAN: Cuesta de San José s/n, 38712 Breña Baja, La Palma, Spain*

Accepted XXX. Received YYY; in original form ZZZ

ABSTRACT

For centuries, astronomers have discussed the possibility of inhabited worlds âĂŤ from HerschelâĂŹs 18th-century observations suggesting Mars may host life, to the systematic search for technosignatures that began in the 1960s using radio telescopes. Searching for artifacts in the solar system has received relatively little formal scientific interest and has faced significant technical and social challenges. Automated surveys and new observational techniques developed over the past decade now enable astronomers to survey parts of the sky for anomalous objects. We briefly describe four methods for detecting extraterrestrial artifacts and probes within the Solar System and then focus on demonstrating one of these. The first makes use of pre-Sputnik images to search for flashes from glinting objects. The second method makes use of space-borne telescopes to search for artificial objects. A third approach involves examining the reflectance spectra of objects in Earth orbit, in search of the characteristic reddening that may imply long-term exposure of metallic surfaces to space weathering. We focus here on a fourth approach, which involves using Earth's shadow as a filter when searching for optically luminous objects in near-Earth space. We demonstrate a proof-of-concept of this method by conducting two searches for transients in images acquired by the Zwicky Transient Facility (ZTF), which has generated many repeated 30-second exposures of the same fields. In this way, we identified previously uncatalogued events at short angular separations from the center of the shadow, motivating more extensive searches using this technique. We conclude that the Earth's shadow presents a new and exciting search domain for near-Earth SETI.

Key words: extraterrestrial intelligence – transients – surveys – minor planets, asteroids, general

1 INTRODUCTION

Searches for Extraterrestrial Intelligence (SETI) using optical and radio telescopes have been going on for sixty years. This work has demonstrated remarkable technical advances alongside the development of creative search strategies and frameworks for discovery and rigorous evidential standards. Ever since astronomers understood that our own radio transmissions could be received by extraterrestrial astronomers (Cocconi & Morrison 1959), radio observations have been running episodically, such as at the Green Bank telescope and Allen Telescope Array in California (United States). Despite this progress, no confirmed signal of extraterrestrial (ET) origin has been detected. Several research groups have made major contributions to radio searches: the SETI institute (e.g., Tarter 2001) have been engaged for decades. The Five-hundred-meter Aperture Spherical radio Telescope (FAST) in China has recently joined the search (Li et al.

★ E-mail: beatriz.villarroel@su.se

2020). In 2015, the Breakthrough Listen program launched their effort to perform the most systematic and comprehensive radio search to date, observing 1 million stars, the galactic plane, and over 100 galaxies for radio signals. Their work has led to firm upper limits on radio emitters. For example, Enriquez et al. (2017) conducted searches for artificial signals in the 1.1–1.9 GHz range, operating at powers higher than $\sim 10^{13}$ W, concluding that less than $< 0.1\%$ of all systems within 50 pc have radio transmitters this powerful. It should be noted that these limits apply to continuously transmitting and omnidirectional or Earth-directed transmitters. Garrett & Siemion (2022) identified 143,000 galaxies that apparently also show no artificial radio signals, placing limits on the luminous end of the SETI luminosity function. Subsequent work by Price et al. (2020) searched for radio transmitters in the 1.10–3.45 GHz range, finding no transmitters stronger than $\sim 10^{12}$ W. Again, these limits apply under the assumption of continuous and omnidirectional or Earth-directed transmission. Other notable efforts include SETI Italia (Montebugnoli et al. 2001) and searches conducted using the Russian RATAN-600 telescope (Bursov et al. 2016). Sixty years of radio searches have so far not yielded a candidate signal that satisfies agreed criteria for a detection of interest.

The lack of a clear discovery from radio searches has motivated searches for optical lasers, as they provide more privacy and higher bit rate than radio communication. Lasers used by extraterrestrial civilizations could have long-lived (continuous over minutes or hours or even longer) beams or emit short pulses, where the latter are much more energy efficient. These may also rotate or stay fixed with respect to the observer. One method to detect such a laser is to search for repeated, short pulses (PANOSETI; Wright et al. 2018; Maire et al. 2020). An all-sky all-the-time search has been conducted by LaserSETI for the past 10 years[1] (Gillum 2023), where a network of small cameras survey the sky from different positions in search of a laser flash. Another tested method relies on examining the spectra of stars. A powerful laser source that transits its host star is expected to leave a monochromatic emission line in stellar spectra (Tellis & Marcy 2017). For example, a 60 Megawatt laser with a 10 meter aperture laser beam at a distance of ~30 pc, is detectable in the spectra of a host star above the continuum level—even when the laser pulse is as short as a second (e.g., Marcy et al. 2022b). Only limited parts of the entire parameter space have been sampled so far, and no candidate laser source has been identified up to now (Stone et al. 2005; Howard et al. 2007; Reines & Marcy 2002; Marcy 2021; Marcy et al. 2022b,c,a).

In contrast, there have been few searches for extraterrestrial artifacts and probes in our Solar System. But this possibility was well understood since the early 1960s after interstellar spaceflight became realistic, raising the idea that ET civilizations might intentionally send probes (or unintentionally send other artifacts) to our immediate neighborhood (Bracewell 1973). Carl Sagan suggested that an advanced extraterrestrial civilisation might send relativistic probes to our Solar System (Sagan 1963) and that the Earth might have been visited as many as $\sim 10^4$ times. Indeed, while relativistic probes are extremely energy-demanding, it is not unimaginable that other civilisations have attempted sending probes similar to Voyager or Pioneer to other star systems, or even a simpler "message-in-a-bottle" style of artifact. In 2011, Voyager left the Solar System, and even with its non-relativistic, humble velocity, it is estimated to reach the distance of the closest star in about 77,000 years. These types of probes are far cheaper and more energy efficient for transmitting information to another civilisation (Rose & Wright 2004), although they are arguably far more difficult to discover (Haqq-Misra & Kopparapu 2012). In California, the 100 million dollar Breakthrough Starshot project was investigating new propulsion technologies to launch a probe with relativistic speed to the closest star (see e.g. Lubin (2016)). Had they succeeded, the probe could reach the closest star in as little as twenty years. Sadly, the project was canceled.

An ET civilization may configure interstellar probes to land on the surfaces of planets (Carlotto & Stein 1990; Arkhipov & Graham 1996; Davies & Wagner 2013), or asteroids (Papagiannis 1978; Benford 2019), or else to park in a stable orbit around planets like Earth for millions of years (Villarroel et al. 2022c). Some probes may be intact, while others could have been around for hundreds of thousands of years and disintegrated over time. It has been speculated that thousands, millions, or even more probes might be spread throughout the galaxy, as part of a network of robotic spacecraft (Schwartz & Townes 1961; Freitas 1980, 1981; Zuckerman 1985; Hippke 2018, 2020; Gertz & Marcy 2022), some of which may communicate using lasers. In the early 1980s, searches for ET probes nearby the Earth were conducted with optical telescopes (Freitas & Valdes 1980; Valdes & Freitas 1983), without yielding positive results. One study has been carried out using photographic plate material from the 1950s (Villarroel et al. 2022a), yielding two statistically significant preliminary candidates. The search for nearby probes and artifacts turned out to be the least-traveled path in SETI research, due to the heavy requirements of such searches, often based on astronomically expensive space missions.

There is an evident need for new, rigorous, and verifiable observations in the search for ET artefacts (Shostak 2020). The recent efforts within academic institutions to investigate Unidentified Aerial Phenomena (UAP), although not necessarily related to ET technology, have brought the search closer to home (in Earth's atmosphere) through efforts like the *Galileo* project (Loeb & Laukien 2023; Watters et al. 2023; Domine et al. 2025), UAPx (Szydagis et al. 2025), and IFEX (Interdisziplinären Forschungszentrum für Extraterrestrik; Kayal (2022); Kayal et al. (2023)).

The search for ET probes exclusively *outside* the Earth at geosynchronous orbits and beyond is motivated by a desire to avoid detecting national security assets and minimize false positives. As mentioned above, the possibility that ET probes or artifacts are present in the Solar System is based on reasonable extrapolation from conservative estimates of spacefaring capabilities of advanced civilizations (Sagan 1963; Knuth 2024), and indeed from the examples of our own Voyager and Pioneer probes. Moreover, a handful of curious astronomical observations are at least somewhat suggestive that we should search closer to home, such as observation of the asteroid VG 1991 (Steel 1995), the elongated

[1] http://www.laserseti.net

object 'Oumuamua (Bialy & Loeb 2018), and the finding of multiple transients in small regions of the sky (Villarroel et al. 2021, 2022a; Solano et al. 2024). The most impressive case to date is arguably that of three bright "stars" appearing and vanishing within 50 minutes (Solano et al. 2024). The goal of finding ET artifacts and probes can be achieved through dedicated searches for specular reflections from the surfaces of artificial objects (Lacki 2019; Villarroel et al. 2022b) as well as intrinsic optical emissions.

In this paper, we present search methods that permit us to filter out human-made satellites and other background noise, together with preliminary, proof-of-concept searches using telescopic images acquired in the past 8 years, using the Earth's shadow as a filter.

2 FILTERING OUT THE NOISE

The greatest challenge when searching for ET probes and artifacts in interplanetary space using modern instruments is that our skies are polluted with thousands of satellites and millions of reflective pieces of space debris, even as more and more satellites are being launched into orbit. This contamination is an especially challenging problem for anyone wishing to search for non-anthropogenic objects. Below we present several solutions to separate the many glints and emissions caused by human-made objects from potential ET artifacts and potential ET probes and artifacts, and then we describe a demonstration of one of these.

2.1 Going back in time: using pre-Sputnik images

A promising avenue is to examine digitized pre-Sputnik astronomical images captured by Palomar, Carte du Ciel, Harvard, and Lick observatories. These images, many of which date back to the early 1950s and earlier, can be analyzed for both anomalous events in the sky that occurred prior to the proliferation of satellites and space debris, and to search for typical signs of artificial satellites and space debris (Villarroel et al. 2022c). Discoveries made through this process might be usefully compared to the records of anomalous celestial observations made by astronomers before 1850, including those by Cassini and Messier as documented by Vallee & Aubeck (2010), adding to their interest and value.

Previously, Villarroel et al. (2022c) discussed a straightforward search method for specular reflections from artificial objects in geosynchronous orbits: multiple transients that are aligned as the object moves and rotates. The paper proposed that any alignments with more than four transients are particularly noteworthy and warrant further investigation to distinguish them from plate defects with atypical shapes (i.e., not point-like or extended due to movement). Although a few preliminary candidates have been identified (Villarroel et al. 2022a), the origin of these transients remains unknown. The events might be caused by an entirely different and unanticipated phenomenon than what the given paper tested (solar reflections from artificial objects in geosynchronous orbits), e.g. atmospheric or exoatmospheric, in which multiple stationary light sources appear and disappear from the field. A recent discovery of a bright triple transient event in Palomar plates on the 19th of July 1952 is particularly puzzling and convincing (Solano et al. 2024).

The Vanishing & Appearing Sources during a Century of Observations (VASCO) project is currently planning a new generation of its citizen science project, which will search for glinting satellites instead of "vanishing stars" (Villarroel et al. 2022b).

2.2 Observations with Space-Borne Telescopes

An additional uncontaminated search approach involves examining a search volume that resides beyond the orbits of satellites and therefore beyond geosynchronous orbit. This approach can be achieved by using existing space telescopes, such as Kepler, or the Transiting Exoplanet Survey Satellite (TESS), and analyzing their existing datasets in search of anomalous objects.

TESS, for example, uses four wide-field cameras all pointed at the same field, making it an ideal tool for searching for rare events involving multiple or "simultaneous" transients, as reported in studies by Villarroel et al. (2021, 2022b) and Solano et al. (2024). However, it is worth noting that events fainter than approximately 12 magnitudes may not be detectable by the telescope, which utilizes small mirrors.

While this experiment may not be able to detect any ET technological objects in orbit around the Earth, it does permit the search for objects farther out in the solar system.

2.3 Color-coded Clues of Ancient Space Debris

Those who wish to examine Earth orbits in modern-day data for dead artifacts without intrinsic emission will face a significant challenge: the view is spoiled by millions of human objects. Other projects, such as the Galileo project, tackle this challenge by searching for signs of interstellar meteors similar to 'Oumuamua in image data – and even by exploring the ocean depths for potential artifacts following fireball events with potential hyperbolic atmospheric entry velocities (Loeb et al. 2024).

An object that has resided in Earth's orbit for a long period of time will have been exposed to dust particles, cosmic rays, and micrometeorites, leading to a reduction in its reflectivity and causing a reddening of the object (e.g., Hapke 2001; Pearce et al. 2020). We can leverage this phenomenon to obtain the reflection spectra of the top 5% most reddened artificial objects in Earth's orbit without a known "owner", meaning objects that are not listed by the USSTRATCOM. Of course, military satellites will not be in USSTRATCOM, which comprise a significant fraction. Nevertheless, solar reflectance spectra from an object will contain both the solar spectrum and a pattern of absorption features that are characteristic of the surface materials (Vasile et al. 2024). Therefore, spectra from the most reddened population, showing unusual absorption or emission lines that suggest an unknown material, could indicate strong candidates for ET artifacts.

2.4 Using Earth's Shadow as a Filter

The Earth's shadow is an ideal uncontaminated search space. Every night, the Earth casts a shadow cone where direct sunlight cannot reflect from satellites or space debris (although there is still a possibility of reflection from the much fainter Moonlight). The size of this shadow varies throughout the year, but the base has an average radius of around 8 – 9 degrees for objects at geosynchronous orbits (GSO; approximately 35,700 km) (Nir 2024). With typical velocities of artificial objects at GSO, which move at approximately 15 arcsec per second, a brief flash caused by intrinsic emission lasting only 0.2 – 0.5 seconds can produce a point source, with its magnitude depending on the strength of its intrinsic emission.

The Earth's shadow is much larger at Low Earth Orbit (LEO), and objects emitting flashes move so quickly that they are likely to create long streaks as they rotate in most long-exposure imagery, rather than short flashes. Also, objects with continuous, longer-lasting emission further out than LEO might produce long streaks. It is therefore interesting to search for elongated streaks that occur within the shadow of the Earth and yet are well outside the atmosphere, in this way excluding aircraft and meteors. Such streaks are unlikely to be human satellites, which typically do not carry intrinsic optical light sources. The rare exceptions are largely confined to LEO and include (i) lasers used for communication (usually NIR) or laser ranging and atmospheric LIDAR; (ii) LEDs for optical self-identification; (iii) short-range LEDs used for optical tracking and formation flying; and (iv) spacecraft propulsion (e.g., rocket burns). At the distance of the Moon, an orbiting object will move at angular velocities of roughly ~ 0.5 arcsec sec^{-1}. At a few times the distance of the Moon, we might search instead for streaks inside the shadow (which narrows down further as one moves away from Earth) indicating angular velocities < 0.1 arcsec sec^{-1}. Determining the distance to streaking objects will require triangulation, as envisaged for the Ex-Probe experiment[2] (Villarroel & Marcy 2023).

The shadow of the Earth consists of the penumbra and umbra or "full shadow"; the latter is depicted in Figure 1. The full shadow consists of a dark core (the "dark full shadow" or DFS) and an outer fringe of light refracted by the Earth's atmosphere, which can produce satellite glints and which measures $\gamma \sim 2^\circ$. Assuming $r_{\rm orb} = 35{,}786$ km for geosynchronous orbit, the largest fractional change in observer position with respect to this altitude is $\Delta R/R \sim R_\oplus/r_{\rm orb} \approx 0.18$, which is hence also the largest fractional change in apparent angular size of the refraction fringe (γ') and DFS radius (ϱ) as a function of position on the Earth's night side. At the geocenter, the total umbra radius is $\varrho + \gamma = \sim 8$ to 9° from Earth's surface below the antisolar point (Figure 1a), $\varrho + \gamma \approx 10^\circ$. A "safe" shadow radius (for avoiding satellite glints) is therefore below $8^\circ - 2^\circ = 6^\circ$. Alternatively, this could be calculated as a function of position φ to maximize the search radius. In this initial study, in most cases we applied a cutoff of $\rho < 6^\circ < \varrho$ for the radial angular separation (ρ) from the shadow center when we filtered detections.

[2] https://thedebrief.org/a-new-era-of-optical-seti-the-search-for-artificial-objects-of-non-human-origin/

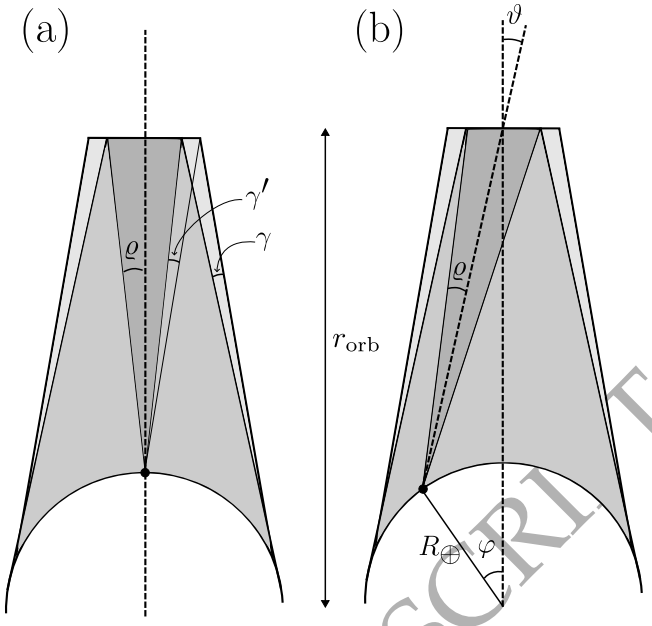

Figure 1. Earth's umbra out to an orbit radius $r_{\rm orb}$ (not to scale). The Sun is in the direction of the bottom of the page. The lightest shading marks the "refraction fringe" into which sunlight is refracted by the atmosphere (angular size γ). Intermediate shading is used to mark the "dark full shadow" (DFS). The darkest shading highlights the shadow volume visible to an observer on the Earth's surface (this shading implies nothing about darkness in this volume, which is the same as the DFS). DFS radius is given by ϱ; parallax of the shadow center with respect to the antisolar point is ϑ; angular separation of the observer from the geocenter-antisolar axis is φ. (a) Shows the shadow geometry for an observer on the Earth's surface beneath the antisolar point (the "subantisolar point" or SAP), and (b) shows the shadow geometry for an observer at an arbitrary position on Earth's surface, with angular separation φ from the SAP.

At distances far enough from Earth, such as those greater than or equal to 0.01 astronomical units (au), any detectable flashes will occur from beyond the Earth's shadow cone. Since very few human-made objects are located at these distances and their positions are well documented, there is a negligible risk of mistakenly identifying them as extraterrestrial artifacts or probes.

Previous work has used the Earth's shadow to search for real astrophysical transients lasting only a few seconds (Richmond et al. 2020; Arimatsu et al. 2021; Nir et al. 2021a), but no significant findings have been reported thus far. Our objective, however, is to identify extraterrestrial artifacts moving in Earth's orbits and beyond.

Conducting searches in the Earth's shadow with a ground-based telescope permits the identification of *candidates* for active (self-luminous) extraterrestrial technological objects that are moving outside of the Earth's atmosphere, while a definitive identification will require follow-up triangulation and spectroscopic analysis for repeating or new events. We note that this approach may not be effective for detecting old or defunct ET artifacts in orbit around the Earth. This means that objects similar to those posited in Villarroel et al. (2022a) might not be detected; only objects with an intrinsic emission could be detected in this way. We note that the only intrinsic emission from known

human objects are **mainly** from lasers designed for communications and from spacecraft propulsion systems (e.g., rocket thrusters); no other type of intrinsic emission from satellites is **widely** known.

3 SEARCHES FOR ZTF TRANSIENTS IN EARTH'S SHADOW

The Zwicky Transient Facility (ZTF; Bellm et al. 2019; Graham et al. 2019) is an untargeted wide-field transient survey observing transient events ranging from Solar System objects to powerful extragalactic events with the help of its systematic data acquisition system. The ZTF uses the 1.2m Samuel Oschin telescope at Palomar Observatory in California and reaches a limiting magnitude of $r \sim 20.5$.

The analyses in this section concern three sample sets of ZTF images. These are labeled as samples A, B, and C. Sample set A is defined and discussed in Section 3.1. The much larger sample sets B and C are described in Section 3.2. See Table 1 for the definitions of each sample.

3.1 Examination of transient alerts (Sample A)

For sample A, we selected transient alerts from a public ZTF transient survey (courtesy of Igor Andreoni). The data set we searched spans from July 1, 2019, when real / bogus deep learning classification became available (Duev et al. 2019), until August 1, 2022. The data set excluded from the search those ZTF fields close to the Galactic plane to reduce contamination from M-dwarf stellar flares and other types of fast transients from astrophysical sources within the Milky Way. To achieve this, we ignored those fields with a Galactic extinction higher than E(B - V) = 0.3 mag at the central coordinates of the fields (using the Planck Collaboration (2014) dust maps) following Andreoni et al. (2020).

One-off transients are, in principle, only visible in a single image before vanishing. This limits us to transients that, when bright and detectable (brighter than ~ 20.5 mag), persist for a shorter time than the sum of the exposure time and the time difference with subsequent or previous images (this adds up to ~ 30 seconds, since the subsequent image is captured in immediate succession).

Each alert included in the sample has at least 5 other alerts in the same image (i.e., same field, same JD) which were also detected only once during the ZTF survey, to focus on multiple transients. All sources within 1.5 arcseconds from a catalogued object were discarded. Also, all sources within 10 arcseconds from catalogued asteroids were removed. We obtained 11,029 transient alerts to examine closer.

3.1.1 *Exploiting the Earth's Shadow*

We use the Julian Date and the J2000 coordinates of each transient, as well as the software library `earthshadow` published by Guy Nir published (Nir 2024), in order to select only events that were observed in the shadow of the Earth at the altitude of geosynchronous orbits ($\rho < 8.5°$ for Sample A; we use the stricter bounds of the DFS when filtering sets B and C: i.e., $\rho < 6°$).

Out of the sample of 11029 candidates, 262 (2.4%) of the examples are in the Earth's shadow, which excludes any specular reflections for these particular cases. We show the distributions of the candidate "shadow transients" over the sky in Figure 2.

3.1.2 *Classifying detections*

This exercise permitted us to quickly identify a set of classes of note: (1) images affected by a difference in depth (different magnitude limit) or other observational issues; (2) two images showing how a short transient is first visible in one image, and then another transient is seen in a second, later image (in nearly all cases of this kind, the transient is first seen in the eastern part of the image, and later in the western, which suggests a moving object); (3) images showing the synchronized movement of multiple objects moving from the east to west; (4) events that have been, in a preliminary sense, identified as candidate multiple transients. Category 1 objects are irrelevant to us. Category 2 objects are assigned a low priority as they are unlikely to be multiple transients, as indicated by their east-to-west movement. For Category 3, We find 29 cases of multiple objects moving throughout the field (from east to west), that we assume to be asteroids. Finally, in Category 4, we find 39 candidates of preliminary interest. However, examining them against the JPL Small-body Identification tool and a generous crossmatch radius of 30 arcseconds, identifies the majority of these as catalogued asteroids.

Two interesting candidates remain from Category 4. The first is the case of a possible transient appearing next to a moving asteroid, creating the impression of a "triple transient," shown in Figure 3. The detections in the two left-most circles correspond to 2001 VC136, a ~19.6 mag asteroid. The detections in the two right-most circles appear only once, although the lower turns out to be a spurious detection (two bright pixels, non-psf).

The second candidate is a good example of an uncatalogued object that could be interesting if more information were available. Figure 4 shows a ~17 magnitude object or objects that have no match when queried using the JPL Horizons database in April 2025. The astrometric measurements are tabulated in Table 3. This object (or set of objects) occurs within ~0.07 arcseconds s^{-1} of the ecliptic, suggesting that it may be an asteroid. On the other hand, if this sequence represents multiple images of the same object, then its apparent motion in right ascension is about 6× times greater than of typical main belt asteroids, suggesting it is closer to the Earth. The entire track spans 430 arcseconds during 100 minutes. The second set of images and positions ((b) and (c) in Table 3) were both acquired in the g band, and differ in maximum raw intensity above background by only 5%. Using these two positions, we predicted the expected location 71 minutes after the position in (c), assuming a linear path and constant angular speed (R.A. (J2000) = 145.163329°, Dec. (J2000) = 15.608823°) in the same field (570), filter (g), sensor (c02), and and quadrant (q3) with timestamp `20210211359132`: no object was visible because it was projected to reside in the seam gap between CCDs. We also searched the neighboring sensor+quadrant in r band images 136 minutes after (c), although the object was still projected to reside in the gap between quadrants and was not visible. The image for (b) also appears some-

Table 1. Definitions of ZTF image samples.

Sample	Definition	N (images)	Purpose
A	Based on transient survey (courtesy of Igor Andreoni) and culled to include only images residing within 8° of the center of Earth's shadow ($\rho < 8°$)	678	Demonstrating manual inspection method
B	$(b > 20°) \wedge (\rho < 6.5°)$	224,168	Demonstrating automated method in largely uncrowded fields (avoiding low galactic latitudes (β)); located confidently within shadow ($\rho < 6$)
C	$\beta > 84°$	326,823	Control sample (ecliptic pole; ecliptic latitude (β) exceeds 84°; all fields well outside the shadow)

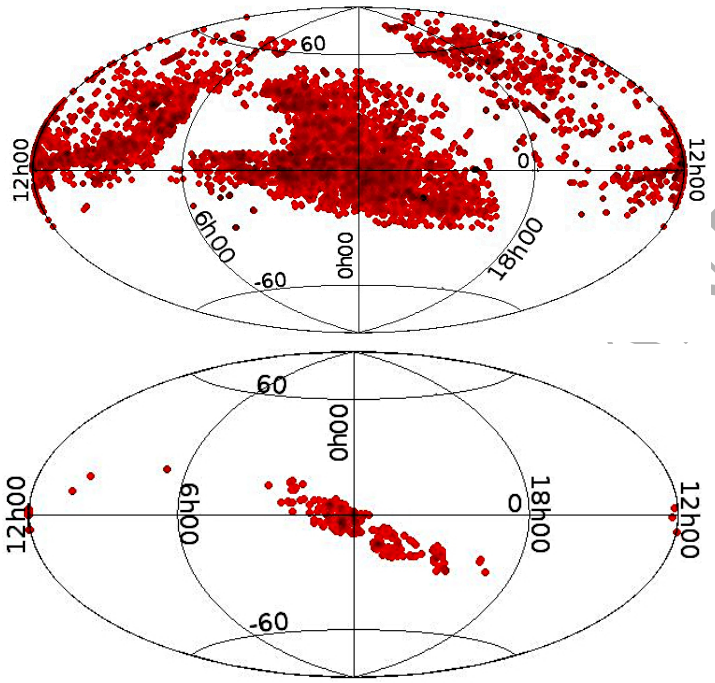

Figure 2. Distribution on the sky. The distribution of the Sample A transient candidates on the sky in Galactic coordinates. Upper panel (a) all one-off transient candidates, (b) one-off transient candidates in the shadow.

what streaked in the approximate direction of motion (East-West), although other objects in the scene (including stars) also appear to exhibit an elongation (if less pronounced) in the same orientation, suggesting an effect of inaccuracies in tracking.

3.1.3 Analysis of candidate clustered transients

We performed an additional analysis by examining candidates that, in addition to appearing in images with > 5 transients in the same field, two of these are within 10 arcminutes of each other. We found 85 cases of such clustered candidate transients. We then retrieved the images from the same day from the IRSA Gator's image survey for ZTF.[3] We found that 23 of these cases have no transients at all visible in the image and 44 cases appear to be just an asteroid moving between two images. (Note this is hard to distinguish from the case of two transients happening close to each other (a double transient), which would look similar.) Two images have single transient candidates, and 7 show several probable asteroids moving in the same field.

Finally, we also conducted an investigation of the closest 10 arcminute field near each of the 262 transient candidates in the shadow. In this way, we found interesting cases of multiple asteroids moving together and one possible solitary transient.

We note that, with only 2 or 3 exposures of 30 seconds on each field every day, it is difficult or unlikely to find multiple transients if they happen over half an hour. We also note that the hypothetical case of a double transient might be indistinguishable from an asteroid if they appear in only two images, and might only be distinguished by the fact that asteroids move always from east to west.

[3] https://irsa.ipac.caltech.edu/applications/Gator/

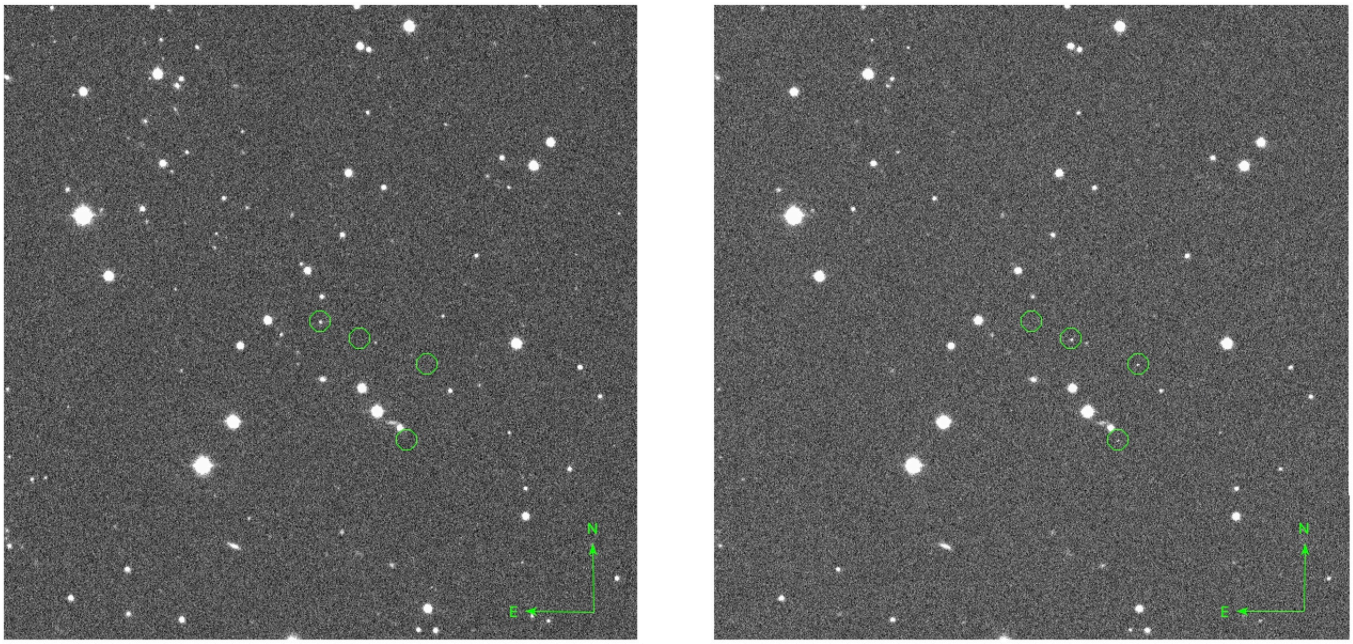

Figure 3. Asteroid 2001 VC136. A complex candidate, including asteroid 2001 VC136 and a transient was found inside a box measuring 10×10 arcmin and centered at R.A. (J2000)=6.3634206 deg. and Dec.(J2000)= 2.4341476, J.D.=2458760.7977431. See Table 2 for astrometric measurements and Table 9 for data product filenames. The lower-most object (right), not visible on the left, is a spurious detection (non-psf).

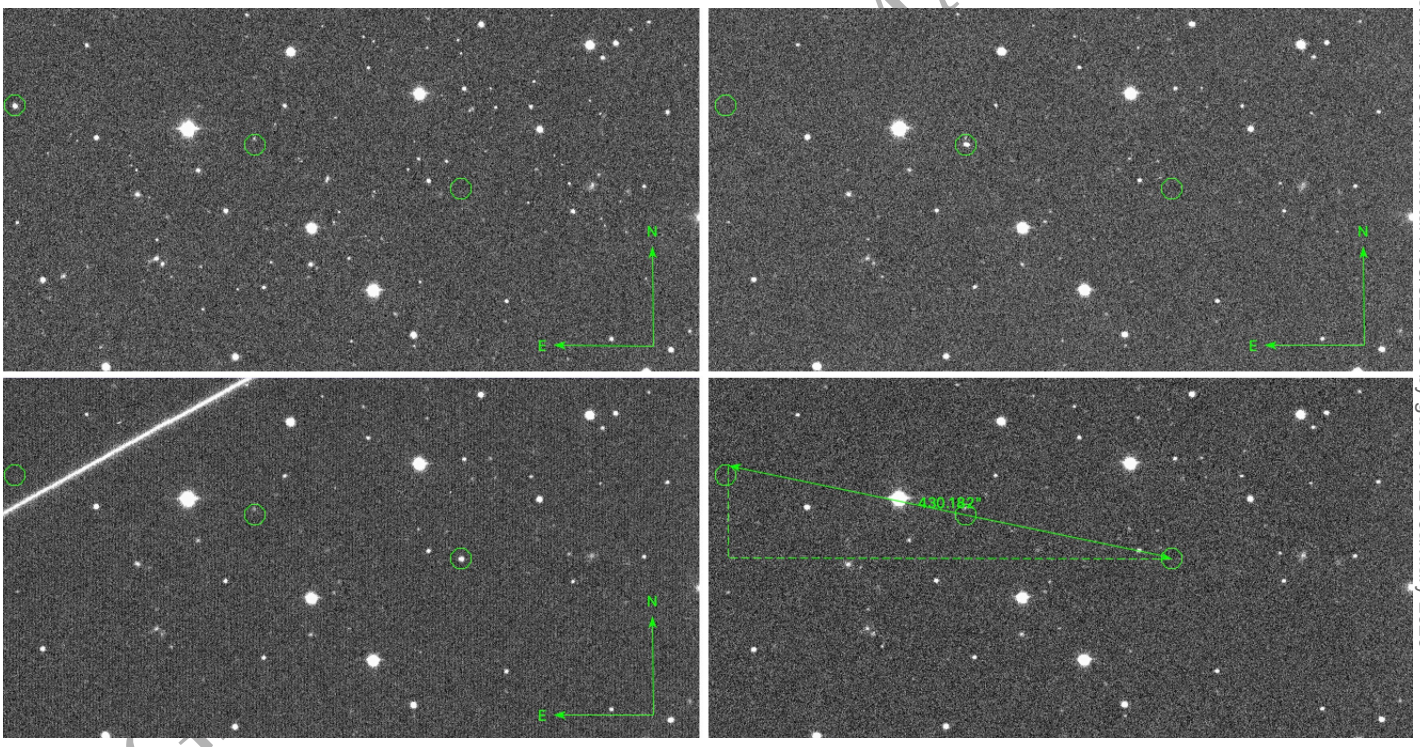

Figure 4. Near-Earth object or triple transient? The object(s) of interest can be found within a 1000 arcsecond box centered at R.A. (J2000)= 145.2448564 and Dec.(J2000)= 15.6224391, J.D.= 2459256.8096296; see Table 2 for astrometric coordinates. A luminous object is seen streaking through the upper-left corner of the third image (lower left), possibly a meteor or aircraft. A fourth image in the *g* band with no object detected is added to the sequence (lower right), to show the deviation from a straight path. See Table 3 for astrometric measurements and Table 9 for data product filenames.

Table 2. Astrometric measurements of the three transient candidates shown in Figure 3. Objects 1 and 2 were determined to be asteroid 2001 VC136. Coordinates (R.A., Dec.) are given in J2000 for each detection, along with the Julian Date (J.D.) and UTC observation time. All observations were taken in the ZTF r-band. Missing coordinate values are indicated as N.A. ZTF data product filenames are listed in Table 9.

Asteroid 2001 VC136; see Figure 3					
Object 1	Band	R.A. (J2000)	Dec. (J2000)	J.D.	Observation time
(a) left	r	6.3636953	2.4339307	2458760.7977431	2019-10-04 at 07:56:45.26
(b) right	r	6.3529988	2.4294331	2458760.8510417	2019-10-04 at 08:25:30.89
Object 2	Band	R.A. (J2000)	Dec. (J2000)	J.D.	Observation time
(a) left	r	N.A.	N.A.	2458760.7977431	2019-10-04 at 07:56:45.26
(b) right	r	6.3355465	2.4229677	2458760.8510417	2019-10-04 at 08:25:30.89
Object 3	Band	R.A. (J2000)	Dec. (J2000)	J.D.	Observation time
(a) left	r	N.A.	N.A.	2458760.7977431	2019-10-04 at 07:56:45.26
(b) right	r	6.3406132	2.4030027-	2458760.8510417	2019-10-04 at 08:25:30.90

Table 3. Astrometric measurements of the uncatalogued object(s) shown in Figure 4. Coordinates (R.A., Dec.) are given in J2000 for each detection, along with the Julian Date (J.D.) and UTC observation time. Observations were taken on 2021 February 11 in the ZTF r and g-bands. ZTF data product filenames are listed in Table 9.

Uncatalogued object(s) (Figure 4)					
Object	Band	R.A. (J2000)	Dec. (J2000)	J.D.	Observation time
(a) upper left	r	145.3668218	15.6441562	2459256.7390625	2021-02-11 at 05:44:16.26
(b) upper right	g	145.3011827	15.6335293	2459256.7789352	2021-02-11 at 06:41:40.693
(c) lower left	g	145.2448868	15.6220271	2459256.8096296	2021-02-11 at 07:25:52.616

Groups or clusters of objects moving in similar ways through a scene are unusual and potentially of interest for a study like the one proposed here. The greatest likelihood is that these represent (1) clusters of asteroids or (2) clusters of terrestrial spacecraft or spacecraft components in heliocentric orbit. Alternatively, such detections could represent (3) clusters of artificial objects of extraterrestrial origin in heliocentric orbit or moving in formation. Reflectance spectra are likely essential for distinguishing these cases if the inferred kinematics are prosaic.

The first two clusters were observed crossing a region 10 by 10 arcminutes in size, at angular velocities of ~1 arcsecond per minute. We show two examples of fields with multiple asteroids moving from east to west (see Figures 5 and 6). Figure 5 shows four objects moving in two frames, each with a normal 30s ZTF exposure, while Figure 6 shows two objects moving across four frames. The individual coordinates for the two examples can be found in Tables 4 and 5. The five other cases (of the 7 earlier mentioned) were observed on 2019-07-29, 2019-09-23, 2019-10-04, 2020-10-08, and 2021-09-02. All told, each of the seven cases were found to involve multiple asteroids moving in tandem (similar angular speeds) from east to west. In some cases, the displacements are of comparable size during the same time interval, but the direction of the motion is not exactly the same for each object in a given image, suggesting that the observation records a crossing of orbits of comparable radius.

We investigated whether any of these objects are found in the JPL Horizon databases. Indeed, both cases illustrated in Figures 5 and 6 are catalogued asteroids. Every single case of multiple asteroids that we have found in Sample A are of previously identified asteroids.

The searches described in this section for ZTF transients with durations shorter than 30 seconds in the Earth's shadow resulted in only one detection of significant interest, which may represent an uncatalogued asteroid (see Table 3 and Figure 4). This work illustrates a manual approach to evaluating in-shadow candidate transients (in this case identified by a 3rd party automated search) as candidate exotic objects, including artifacts of ET origin. In the next section, we demonstrate a relatively exhaustive and automated search using image processing techniques to search for non-catalogue ("unmatched") objects in the Earth's shadow.

3.2 Automated transient survey (sets B–C)

Sample sets B and C, which are derived from the set of all publicly-accessible ZTF images predating 2024-04-15, are defined in Table 1. Sample B was confined to the Earth's shadow and designed to avoid glinting satellites. In particu-

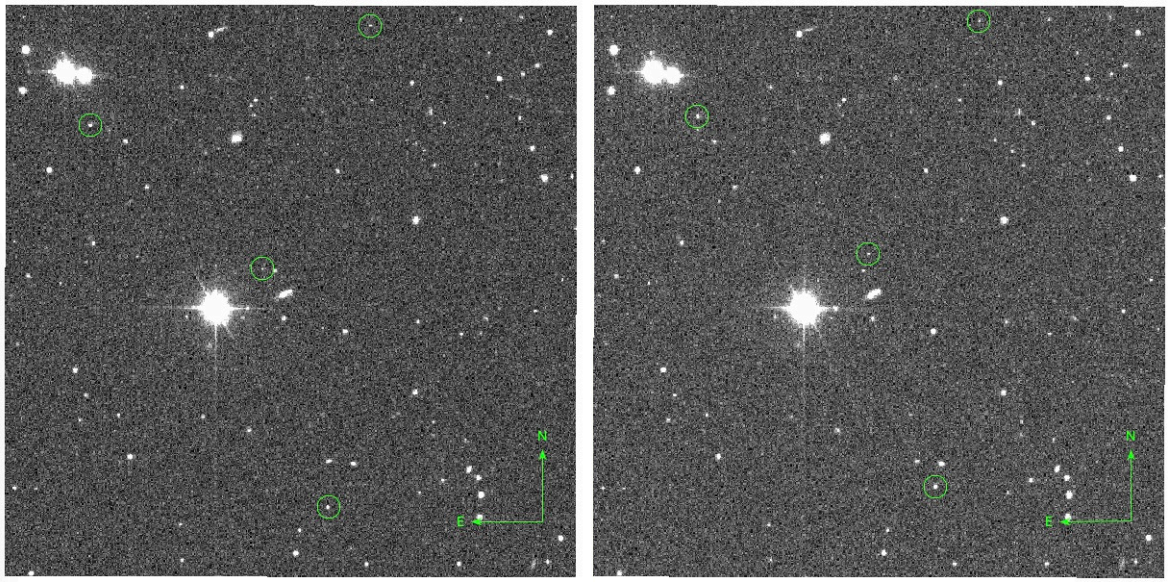

Figure 5. Example with multiple asteroids. From uppermost to lowermost in each image, these objects are the catalogued asteroids 237629 (2001 RZ128), 34921 (4801 P-L), 468722 (2010 GF35), and 408570 (2013 LO5), respectively; they are shown here moving between these image, captured 34 min apart. Both images are *r* band images and were observed on 2021-03-19. See Table 4 for astrometric parameters, and Table 9 for ZTF data product filenames.

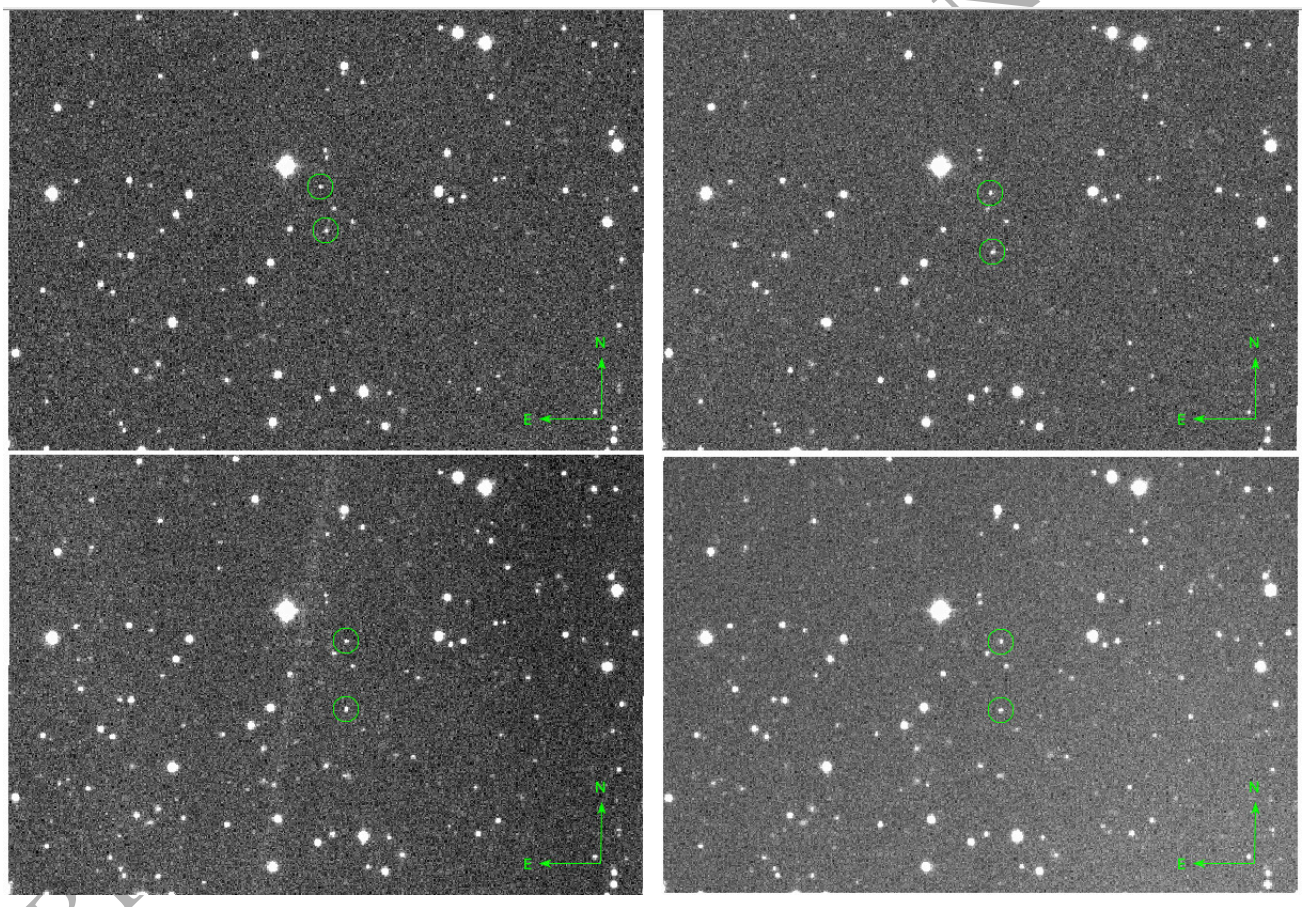

Figure 6. Example with multiple asteroids. These objects were captured within 3° of the Earth shadow center. The two upper images are *g* band and the two lower images are *r* band. The uppermost and lowermost objects within each image have been identified as the asteroids 239154 (2006 KX9) and 728206 (2010 LF127), respectively. See Table 5 for astrometric measurements. ZTF data product filenames are listed in Table 9.

Table 4. Astrometric measurements of three moving objects identified in Figure 5. Coordinates (R.A., Dec.) are given in J2000 for each detection, along with the Julian Date (J.D.) and UTC observation time. All observations were made on 2021 March 19 in the SDSS r-band. ZTF data product filenames are listed in Table 9. Objects 1 to 4 have been identified as asteroids 237629 (2001 RZ128), 34921 (4801 P-L), 468722 (2010 GF35), and 408570 (2013 LO5), respectively.

Example case 1					
Object 1	Band	R.A. (J2000)	Dec. (J2000)	J.D.	Observation time
(a) left	r	182.2828716	2.3212253	2459292.8540046	2021-03-19 at 08:29:46.685
(b) right	r	182.2779462	2.3223948	2459292.8789236	2021-03-19 at 09:05:40.534
Object 2					
(a) left	r	182.3511210	2.2971117	2459292.8540046	2021-03-19 at 08:29:46.685
(b) right	r	182.3466646	2.2992191	2459292.8789236	2021-03-19 at 09:05:40.534
Object 3					
(a) left	r	182.3091393	2.2621854	2459292.8540046	2021-03-19 at 08:29:46.685
(b) right	r	182.3049176	2.2656986	2459292.8789236	2021-03-19 at 09:05:40.534
Object 4					
(a) left	r	182.2933499	2.204017	2459292.8540046	2021-03-19 at 08:29:46.685
(b) right	r	182.2885649	2.209137	2459292.8789236	2021-03-19 at 09:05:40.534

Table 5. Astrometric measurements of two moving objects shown in Figure 6. Coordinates (R.A., Dec.) are given in J2000 for each detection, along with the Julian Date (J.D.) and UTC observation time. All observations were made on 2019 July 29 in the SDSS g- and r-bands. ZTF data product filenames are listed in Table 9. Objects 1 and 2 have been identified as the asteroids 239154 (2006 KX9) and 728206 (2010 LF127), respectively.

Example case 2					
Object 1	Band	R.A. (J2000)	Dec. (J2000)	J.D.	Observation time
(a) upper left	g	309.9298057	-26.9091492	2458693.8131481	2019-07-29 at 07:30:56.985
(b) upper right	g	309.9258638	-26.9105563	2458693.8291319	2019-07-29 at 07:53:57.595
(c) lower left	r	309.9234980	-26.9112611	2458693.8384954	2019-07-29 at 08:07:27.393
(d) lower right	r	309.9232354	-26.9114958	2458693.8393981	2019-07-29 at 08:08:45.309
Object 2					
(a) upper left	g	309.9284917	-26.9187663	2458693.8131481	2019-07-29 at 07:30:56.985
(b) upper right	g	309.9253378	-26.9234575	2458693.8291319	2019-07-29 at 07:53:57.595
(c) lower left	r	309.9234978	-26.9262724	2458693.8384954	2019-07-29 at 08:07:27.393
(d) lower right	r	309.9232349	-26.9265072	2458693.8393981	2019-07-29 at 08:08:45.309

lar, sample B is confined to an area within 6.5° of the center of Earth's shadow (i.e., $\rho < 6.5°$, for search radius ρ from the shadow center), avoiding the most crowded fields at low galactic latitudes ($b > 20°$). Sample C is a control sample, residing completely outside of the Earth's shadow, encompassing a 6° radius from the north ecliptic pole, where few to no minor bodies are expected ($\beta > 84°$).

The goal of our search was to identify nonastrophysical transients unrelated to satellite glints. Of special interest were luminous objects that are (i) markedly streaking; (ii) point sources that cannot be identified as planetesimals in heliocentric orbit, (iii) clustered transients, and especially (iv) trains of point sources, as of flashing, luminous objects or of metallic glinting objects from beyond geosynchronous altitudes. The prospect of detecting objects that meet one of these descriptions can be used to motivate triangulation for estimating range, in order to determine whether an object of interest resides within Earth's atmosphere and, if not, in order to estimate its orbital parameters. This could permit detailed follow-up observations and further characterization.

We detected transient candidates using the segmentation method in the `photutils` library(Bradley et al. 2024). For each ZTF FITS image in the sample, the following pro-

cedure was carried out using a software package called *NEOrion* that was developed in-house.[4]

(i) **Detection:** A detection threshold of 3σ was applied above an adaptive (spatially varying) estimate of the background, essential for nonflat fields. The minimum area for segment detection was 9 connected pixels.

(ii) **Characterization:** We calculated and stored parameters related to intensity and morphology, to identify artifacts (e.g., cosmic ray tracks) and to identify objects exhibiting specific features (e.g., elongation/streaking).

- S/N (q): $\mathcal{F}/(\sigma A)$, where $\mathcal{F}$ is the integrated flux and σ is the standard deviation of image intensities for a 3-sigma clipped copy of the image.
- Orientation (ψ): Angle of semimajor axis orientation ($\pm 90°$), where $0°$ corresponds to horizontal.
- Length (semimajor deviation, σ_a): one-sigma standard deviation along the semi-major axis of a 2D Gaussian w/same 2nd-order moments as the source.
- Width (semiminor deviation, σ_b): one-sigma standard deviation along the semi-minor axis of a 2D Gaussian w/same 2nd-order moments as the source.
- Elongation (η): σ_a/σ_b
- Ellipticity (ε): $(\sigma_a - \sigma_b)/\sigma_a$; near zero for radially-symmetric objects
- Area (A): Area of the segment in pixels.
- Equivalent radius (R): Radius of a circle of area A.
- Gini coefficient (G): Gini coefficient of intensities in the segment. This is near 0 for uniform illumination and near 1 if brightness is concentrated in a few pixels.
- Maximum intensity (p): Maximum intensity of pixels inside the segment. (The Gini coefficient has applications studies of galaxy morphology: see e.g., Lisker (2008).)
- Taper (Υ): We define the "taper" as the ratio of the FWHM of the minor axis of the segment ($\sim 2.35 \times \sigma_b$) to the "seeing FWHM" reported in the FITS meta data. For point sources and straight-line streaking point sources, $\Upsilon \sim 1$.

For all detections, we also tabulated $d_{\rm edge}$, the distance in pixels from the edge of the field, where many linear artifacts tend to reside.

(iii) **Labeling unmatched objects**: object centroids were estimated and then the angular distances calculated to the nearest object in the Pan-STARRS (Panoramic Survey Telescope and Rapid Response System, catalog PS1 DR2; Kaiser et al. (2002); Flewelling et al. (2020)) and SDSS (Sloan Digital Sky Survey; citeyork2000sloan) catalogs residing in the field-of-view ($d_{\rm cat}$). As discussed later, a threshold is applied to $d_{\rm cat}$ to identify "unmatched" objects.

(iv) **Counting revisits**: We tallied the number of times ZTF captured an image (of each filter type) that overlapped the position of each unmatched detection ($n_{\rm r}, n_{\rm g}, n_{\rm b}$). This was used later to filter out transient detections whose positions were captured only a few times. For example, the celestial coordinates of an unmatched detection having $n_{\rm g} = 7$ was captured 7 times by the g filter. A detection with a low revisit count may simply be a variable astronomical source that happened to dim below the detection threshold. A detection with a high revisit count and no proximate neighbors is more likely to be a genuine transient.

(v) **Computing nearest neighbor distances**: We computed the nearest neighbor distance between each unmatched detection and all of the others ($d_{\rm nn}$). This was used later to filter out false positives: i.e., objects that could not be matched to catalog objects, but which appeared in multiple images at the same (or very proximate) location: these are likely to be slow-moving or unmapped/uncataloged sources. An undesirable consequence is that tightly-clustered transients are eliminated in this way.

(vi) **Filtering**: For ZTF samples B and C, we filtered the unmatched detections to create several subsets. The goal of the first filter pass (producing set I) was to identify all valid detections. The goal of the second filter pass (producing set II) was to remove likely artifacts like sensor noise and cosmic ray tracks. The third filter pass (set III) preserved bright, isolated objects. The fourth filter pass was used to identify elongated (streaking) objects. The conditions used to define each subset are defined in Tables 6 and 7. Note that c_7 is not used in the definition of subsets for the control sample C. In our discussion of results, we refer to the specific subset of detections obtained using a specific method from a specific ZTF sample as follows: `sample/subset`. For example, subset II of ZTF sample C is denoted "C/II". Note that we have also disregarded all images with INFOBITS $\geq$ 33554432, which ZTF has used to mark invalid data products.

For the present proof-of-concept study, we manually reviewed the detections to determine what kinds of objects do and do not appear in these samples, rather than produce an exhaustive catalogue of the results. For example, in Figure 7 we present a few examples from B/IV of streaking objects. Streaks resembling these may belong to one of several categories: (i) meteors; (ii) high-altitude aircraft lights; (iii) near-Earth asteroids located beyond the shadow cone; or (iv) light-emitting objects above the atmosphere and moving within the shadow cone. The estimated angular speeds based on streak length, exposure time (30 seconds), and the assumption of continuous emission, can be used to estimate altitude in the case of objects in circular orbits around Earth. This can be used estimate whether, granting these assumptions, they reside in the shadow cone. Confident assignment to (iv) is impossible, however, without estimating a parallax, which is a primary objective of planned future searches using ExoProbe (Villarroel & Marcy 2023).

"Flash trains" are linear alignments of point source flashes, sometimes with intermediate streaking, commonly associated with satellites but also conceivably produced by pulsing light sources. NEOrion found no flash trains in Sample B (in shadow). By contrast, flash trains were readily found in Sample C (near the ecliptic pole); we show typical examples in Figure 8. These exhibit angular speeds consistent with altitudes typical of Medium Earth Orbit (MEO) to geosynchronous orbit (GSO).

NEOrion was also able to find clusters of previously catalogued minor bodies, demonstrating the ability to find clusters of transient candidates in single images. Manual follow-up inspection was required to find displaced images of the same objects in time-adjacent images, in order to recognize them as planetesimals. For example, we found four previ-

[4] Neorion is an ancient Greek word for "shipyard"; Orion was a hunter; NEOs are Near Earth Objects.

Table 6. Conditions used to filter unmatched detections from ZTF samples B and C into subsets; see also Table 7.

Condition	Definition	Purpose
c_1	$p < 3 \times 10^4$	not saturated
c_2	$d_{\rm nn} > 10$ as	separation from nearest unmatched detection
c_3	$d_{\rm cat} > 5$ as	separation from nearest catalog objects
c_3'	$d_{\rm cat} > 20$ as	highly separated from nearest catalog objects
c_4	$d_{\rm edge} > 20$ pix	at least 20 pixels from edge
c_5	$(n_{\rm r} > 3) \vee (n_{\rm g} > 3) \vee (n_{\rm b} > 3)$	location visited at least 10 times
c_6	$q > 5$	high S/N
c_6'	$q > 10$	very high S/N
c_7	$\rho < 6°$	within dark full shadow (DFS)
c_8	$(\varepsilon < 0.15) \vee ((\lvert\psi\rvert > 5°) \wedge (\lvert\psi\rvert < 85°))$	not a vertically- or horizontally-oriented elongated object (typical of many artifacts caused by telescope exposure and tracking errors)
c_9	$G > 0.1$	removes uniform-intensity artifacts
c_9'	$G > 0.2$	removes uniform-intensity artifacts
c_9''	$G > 0.5$	removes uniform-intensity artifacts
c_{10}	$10 < A < 1000$	removes tiny and very large objects
c_{11}	$\eta > 10$	elongated objects (aspect ratio larger than 10)
c_{12}	$0.3 < \Upsilon < 1.3$	removes cosmic rays and uniform-intensity artifacts
c_{12}'	$0.3 < \Upsilon < 1$	removes cosmic rays and uniform-intensity artifacts

Table 7. Definitions of subsets of unmatched detections.

Subset	Definition	N detections (Sample B)	Description
I	$c_3 \wedge c_5 \wedge c_7$	3,734,423	All valid dections
II	$c_1 \wedge c_3 \wedge c_4 \wedge c_5 \wedge c_7 \wedge c_6 \wedge c_8 \wedge c_9 \wedge c_{10} \wedge c_{12}$	614,556	Most artifacts removed
III	$c_1 \wedge c_2 \wedge c_3' \wedge c_4 \wedge c_5 \wedge c_6' \wedge c_7 \wedge c_8 \wedge c_9' \wedge c_{10} \wedge \wedge c_{12}'$	16,693	Bright and isolated
IV	$c_1 \wedge c_2 \wedge c_4 \wedge c_5 \wedge c_6 \wedge c_7 \wedge c_8 \wedge c_{11} \wedge c_{12}'$	5,940	Bright and elongated

ously catalogued minor bodies in a single ZTF image; these are listed in Table 8. To find multiple transient candidates similar to those presented in Villarroel et al. (2021); Solano et al. (2024), however, one needs to search for clusters of transients in time-adjacent images corresponding to approximately one hour of total exposure time. We have so far not automated this follow-up confirmation process but have plans to do so in future: that is, to download temporally adjacent images of the same field and then search for comparably bright objects that have been displaced in a westward direction. This enhancement would also permit us to search for candidate transients that are clustered in time.

4 DISCUSSION

In this paper, we described techniques that can be used to search for extraterrestrial artifacts in the Solar System near Earth. We discussed the utilization of pre-Sputnik images, space-borne telescopes, the analysis of reflectance spectra of space debris, and using the Earth's shadow as a filter to facilitate the detection of such objects. Previous studies (Villarroel et al. 2022b) have employed pre-Sputnik images to identify transients, yielding intriguing results. In the present work, we focused on the Earth shadow filter, evaluating the effectiveness of the methods for detecting fast transients and flash trains using existing data from the Zwicky Transient Facility (ZTF).

Our first analysis focused on Sample A of 678 images,

Table 8. Cluster of previously catalogued minor bodies detected using the automated search in the shadow, Sample B (all objects were found within 5.7° of the Earth shadow center). All were found in `ztf_20230917395197_000445_zr_c04_o_q4_sciimg.fits`, captured at 2023-09-17T09:29:06.489 (J.D. 2460204.8951968). Displaced images of these objects were found in temporally adjacent scenes.

Cluster of four catalogued minor bodies		
R.A. (J2000)	Dec. (J2000)	Object ID
345.58864	-5.91241	6459 Hidesan (1992 UY5)
345.19842	-5.78249	18555 Courant (1997 CN4)
345.50169	-5.55202	29453 (1997 RU6)
345.68042	-5.62310	625124 1997 GK23)

encompassing a small subset ($N = 262$) of candidate transients in Earth's shadow from a total of 11,029 one-off candidate transients with clear PSFs observed in single ZTF images (shared by Igor Andreoni). These candidates were constrained to durations shorter than 30 seconds, as given by the time difference between the previous or subsequent image captures (i.e., taken immediately before or after the given exposure). Among these cases, manual follow-up inspection has revealed at best several fast transients. Of special note is an uncatalogued object or set of objects shown in Figure 4 and described in Table 3. Although the objects

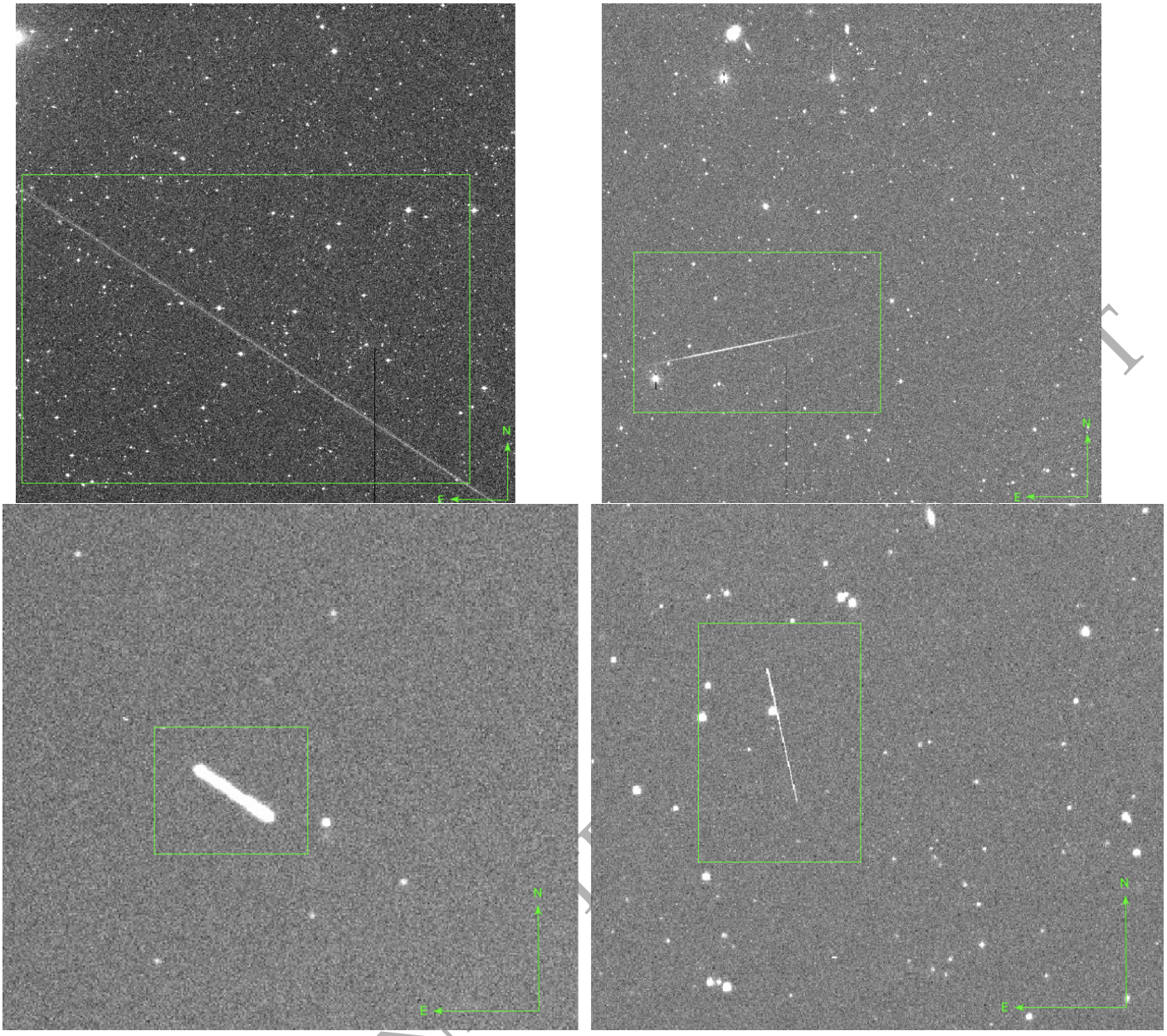

Figure 7. Examples of streaks found near the shadow center, from B/IV. The box sizes in the upper panels are (a) 46.3 × 31.9 arcmin, and (b) 25.2 arcmin × 16.6; in the lower panels: (c) 1.7 × 1.4 arcmin and (d) 2.6 × 3.8 arcmin. The first three images (a) through (c) are believed to be observations of real objects, while the fourth (d) is likely a cosmic ray due to the narrowness (FHWM of ~1 arcsecond) and uniform width of the track in spite of brightness fluctuations. Given the 30 second exposure time and assuming that the objects are gravitationally bound to Earth, the object in (a) is moving at angular speeds consistent with orbits lower than < 14,000 km, while object (b) corresponds to ~ 20,000 km altitude. Both objects are instead probably meteors (see text). (c) This uncatalogued object (not in MPC database as of April 2025) was 4.5° from the shadow center, and is probably an unknown heliocentric asteroid. If instead this were in a circular geocentric orbit, the streak length implies an altitude of almost 200,000 km, where the shadow radius is only about 2°. Refer to Table 9 for the ZTF data product filenames.

are located within a few degrees of the ecliptic, they do not appear in JPL's list of small bodies in the Solar system or the Minor Planet Center catalog as of April 2025. Moreover, if either pair of three detections represent an asteroid, then it moves across the sky at about 4 arcseconds per minute, which is several times faster than a main belt asteroid at opposition.

This leaves two possible interpretations. First, this case may be similar to the multiple clustered transient cases of unknown origin presented in (Villarroel et al. 2021; Solano et al. 2024). A second possibility is that these detections represent a single object in motion (e.g., a remote-controlled human spacecraft or asteroid). This is a good illustration of why triangulation is necessary to disambiguate events of this kind.

We estimated the detection rate of one-off candidate

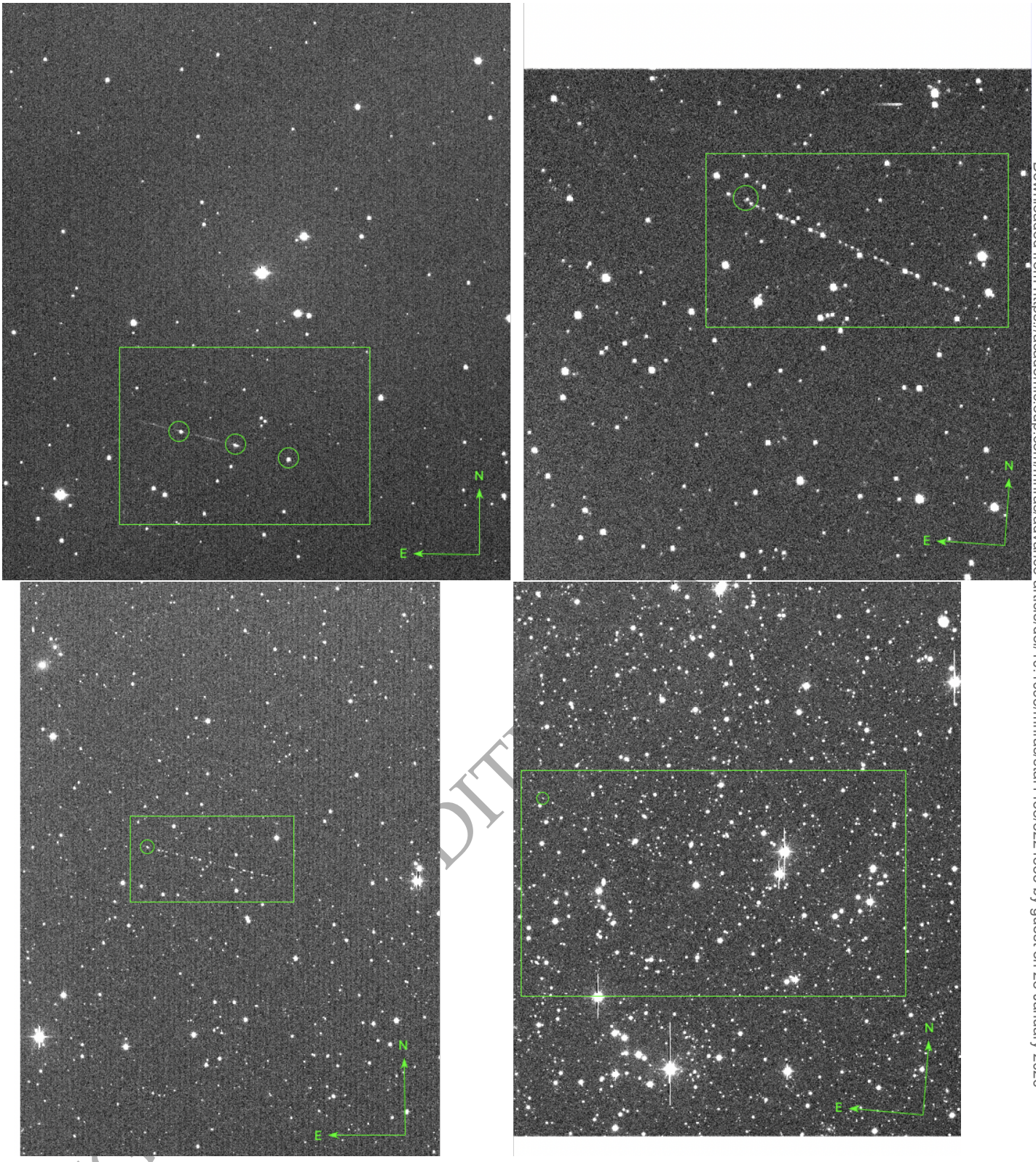

Figure 8. Examples of flash trains caused by satellite glints near the ecliptic pole. The box sizes for the upper panels are (a) 8.6 × 5.7 arcmin, and (b) 8 arcmin × 4.6; for the lower panels: (c) 7.5 × 3.9 arcmin, and (d) 21.2 × 12.4 arcmin. Given the 30 second exposure time and assuming that the objects are gravitationally bound to Earth, these objects are moving at angular speeds consistent with medium Earth orbits to geosynchronous orbits. Refer to Table 9 for the ZTF data product filenames.

Table 9. Table of filenames used in figure components, with distance from center of detected objects to center of Earth shadow.

Figure	Component	Shadow center distance	FITS filename
3	(a) left	4.6°	ztf_20191004297708_000447_zr_c02_o_q1_sciimg
	(b) right	3.0°	ztf_20191004351042_000447_zg_c02_o_q1_sciimg
4	(a) upper left	5.9°	ztf_20210211239062_000570_zr_c02_o_q3_sciimg
	(b) upper right	4.8°	ztf_20210211278912_000570_zg_c02_o_q3_sciimg
	(c) lower left	4.3°	ztf_20210211309618_000570_zg_c02_o_q3_sciimg
	(d) lower right	4.5°	ztf_20210211359132_000570_zg_c02_o_q3_sciimg
5	(a) left	7.5°	ztf_20210319353982_000473_zr_c04_o_q2_sciimg
	(b) right	8.2°	ztf_20210319378912_000473_zr_c04_o_q2_sciimg
6	(a) upper left	1.0°	ztf_20190729312951_000287_zg_c02_o_q2_sciimg
	(b) upper right	1.6°	ztf_20190729329120_000287_zg_c02_o_q2_sciimg
	(c) lower left	2.1°	ztf_20190729338495_000287_zr_c02_o_q2_sciimg
	(d) lower right	2.8°	ztf_20190729339398_000287_zr_c02_o_q2_sciimg
7	(a) upper left	4.9°	ztf_20190210285995_000467_zr_c09_o_q1_sciimg
	(b) upper right	4.4°	ztf_20191027260613_000504_zr_c16_o_q4_sciimg
	(c) lower left	4.5°	ztf_20191011385475_001494_zg_c03_o_q4_sciimg
	(d) lower right	3.3°	ztf_20180912341435_000394_zi_c02_o_q1_sciimg
8	(a) upper left	79.4°	ztf_20190326382303_000825_zg_c10_o_q2_sciimg
	(b) upper right	85.2°	ztf_20190326515729_000825_zr_c09_o_q2_sciimg
	(c) lower left	85.8°	ztf_20190408450498_000826_zr_c11_o_q1_sciimg
	(d) lower right	81.8°	ztf_20190411421551_000825_zr_c09_o_q3_sciimg

transients. According to the IPAC server, a total exposure time of 6,415,320 seconds (approximately 1800 hours) resulted in the identification of 11,029 candidate transients. Of this, only 2.4%—about 43 hours—was spent in the Earth-âĂŹs shadow, during which the observations covered 67,492 square degrees (including overlapping fields). During this interval, we detected one candidate case for multiple transients in Figure 4, corresponding to a rate of $\sim 3 \times 10^{-7}$ cases per hour per square degree, or ~ 0.01 cases per hour across the whole sky. This estimate is based on a single event and should be interpreted with caution due to small-number statistics.

This is a factor of 10^6 less than the number of fast flashes coming from reflections of space debris that has been measured previously (Nir et al. 2021b; Corbett et al. 2020). The multiple transient cases in Villarroel et al. (2021) were estimated to occur at a rate of ~ 0.07 transients hour^{-1} sky^{-1} and ~ 0.27 transients hour^{-1} sky^{-1} in Villarroel et al. (2022b).

This small detection rate is not unexpected if the multiple transient candidates are attributed to solar reflections from artificial objects in geosynchronous orbits around the Earth, as suggested in Villarroel et al. (2021) and Villarroel et al. (2022b). Further, the independent automated transient survey (sets B-C) carried out in Section 3.2 (see total detections listed in Table 7) suggests that there might be many more transients than were covered by the candidate transient alerts described in Section 3.1.

Nevertheless, severe methodological limitations affect the detection rate. Multiple transients were observed in images with 50 minutes of exposure in previous studies (Villarroel et al. 2021; Solano et al. 2024), whereas ZTF images typically only able to capture one-off transients, often in sets containing a few consecutive 30-second exposures of the same field. Unfortunately, the time spent on exposure per field is typically only 2–3 minutes before the telescope moves to a very different part of the sky, which makes it difficult to capture a process that could be spread out over an hour or more. Therefore, the likelihood of observing multiple transients with the ZTF is not high. The previous findings of multiple transients in the Palomar survey used approximately 50 minutes – 1 hour of exposure (Villarroel et al. 2021; Solano et al. 2024). To obtain a reasonable chance of detection in ZTF, but also of distinguishing between the effects of "multiple transients" versus the movement of an asteroid, an equally long time window would need to be necessary, resulting in hundreds of consecutive exposures of 30 seconds each—a condition not met in this study.

The automated survey of Samples B–C using *NEOrion* made possible the detection and study of many other interesting objects. We detected thousands of point sources of interest (as potential flashes), but also many streaks, which could form the focus of a follow-up study. The streaks shown in Figure 7 are within several degrees of the shadow center (Table 9). Streaks that cross the entire image, such as the one in the upper left of Figure 7, are probably meteors. The example shown in the upper right is contained entirely within a single image frame. The most likely explanation is a meteor striking the atmosphere at a steep angle. The FWHM of the cross-section is consistent with stellar psfs in the scene, suggesting an envelope of ionized gas measuring less than 0.5 m in diameter if located in the upper atmosphere. Alternatively, this could be a luminous object in Earth's shadow orbiting at an elevation of approximately

20,000 km. Without an estimate of the parallax, we cannot say for sure whether the estimated distance based on the angular speeds matches expectations consistent with the more prosaic explanation. With the help of instantaneous spectra as described by e.g. Marcy et al. (2022b), we could determine whether the luminosity derives from reflection or emission (and if so, what kind).

The methodological limitations of this study will be mitigated by the new ExoProbe project, see Villarroel & Marcy (2023). The project aims to build a network of telescopes with high-resolution Complementary Metal Oxide Semiconductor (CMOS) cameras to search for ET artifacts and probes in the inner Solar System, in search of short flashes (subsecond – second) associated with technological objects of potential extraterrestrial origin. A series of short exposure images (1s) will be taken at multiple telescopes simultaneously during an hour at a time, searching for any flash that appears in several telescopes, so that we instantly obtain a parallax (and hence the location) of such short transients. The parallax information is absolutely essential in order to estimate true distance. This will tell us whether objects like those in Figures 4, 7 and 8 are at the distances indicated by the angular speeds. The ExoProbe project enables us to search for, locate, and instantly validate and verify the results of such detections.

Searches within the Earth's shadow offer an exciting opportunity as they filter out solar reflections from most human-made objects. In the ExoProbe project, we will also search for elongated streaks in the shadow. With the exceptions discussed earlier, human satellites are not expected to emit any intrinsic light in the optical band. Therefore, one of the most effective methods for identifying an ET artifact or probe is by thoroughly exploring the shadow in searches for pulsing and continuous light. Long-term follow-up study of any such objects may be necessary to rule out prosaic explanations like those earlier mentioned. The significance of any discovery will be further enhanced if any of the objects exhibit unusual spectra or unusual motion.

Studies that make use of instruments with significantly higher time resolution and a ranging capability, such as the new ExoProbe instruments that will search in Earth's shadow, are necessary to find and convincingly identify technological objects of ET origin in near-Earth space.

5 DATA AVAILABILITY

The ZTF image data underlying this article are publicly available from the IPAC Infrared Science Archive at `https://irsa.ipac.caltech.edu`.

6 ACKNOWLEDGMENTS

B.V. wishes to thank Geoff Marcy, Igor Andreoni and Guy Nir for kind and helpful discussions and suggestions doing the course of this work. The paper has further profited from helpful discussions with Peter McCullough, Kevin Krisciunas, Axel Brandenburg and Rudolf BÃd'r.

ExoProbe is supported by an anonymous donor, to whom we are deeply grateful.

B.V. is also funded by the Swedish Research Council (Vetenskapsrådet, grant no. 2024-04708) and supported by the The LâĂŹOréal - UNESCO For Women in Science International Rising Talents prize.

This work makes use of observations from the Zwicky Transient Facility project. ZTF is supported by the National Science Foundation under Grant No. AST-2034437 and a collaboration including Caltech, IPAC, the Weizmann Institute for Science, the Oskar Klein Center at Stockholm University, the University of Maryland, the University of Washington, Deutsches Elektronen-Synchrotron, the University of Wisconsin, Trinity College Dublin, Lawrence Livermore National Laboratories, IN2P3, the University of Warwick, Ruhr University Bochum, and Northwestern University.

REFERENCES

Andreoni I., Kool E. C., Sagues-Carracedo A., et al., 2020, The Astrophysical Journal, 904, 155
Arimatsu K., Tsumura K., Usui F., Ootsubo T., Watanabe J.-i., 2021, The Astronomical Journal, 161, 135
Arkhipov A. V., Graham P. B., 1996, in Proc. SPIE. pp 150–161
Bellm E. C., Kulkarni S. R., Graham M. J., et al., 2019, Publications of the Astronomical Society of the Pacific, 131, 018002
Benford J., 2019, AJ, 158, 150
Bialy S., Loeb A., 2018, The Astrophysical Journal Letters, 868, L1
Bracewell R., 1973, Astronautics and Aeronautics, 11, 58
Bradley L., et al., 2024, astropy/photutils: 2.0.2, doi:10.5281/zenodo.13989456, `https://doi.org/10.5281/zenodo.13989456`
Bursov N. N., Filippova L. N., Fillipov V. V., et al., 2016, Technosignature Prospects with RATANâĂŘ600, Slides presented at IAA SETI Permanent Committee meeting
Carlotto M. J., Stein M. C., 1990, Journal of the British Interplanetary Society, 43, 209
Cocconi G., Morrison P., 1959, Nature, 184, 844
Corbett H., Law N. M., Soto A. V., et al., 2020, The Astrophysical Journal Letters, 903, L27
Davies P. C. W., Wagner R. V., 2013, Acta Astronautica, 89, 261
Domine L., et al., 2025, Sensors, 25, 783
Duev D. A., Mahabal A., Masci F. J., et al., 2019, Monthly Notices of the Royal Astronomical Society, 489, 3582
Enriquez J. E., Siemion A. P. V., Foster G., et al., 2017, The Astrophysical Journal, 849, 104
Flewelling H. e., et al., 2020, The Astrophysical Journal Supplement Series, 251, 7
Freitas R. A. J., 1980, Journal of the British Interplanetary Society, 33, 95
Freitas R. A. J., 1981, Cosmic Search, 3, 16
Freitas R. A., Valdes F., 1980, Icarus, 42, 442
Garrett M. A., Siemion A. P. V., 2022, Monthly Notices of the Royal Astronomical Society, 519, 4581
Gertz J., Marcy G., 2022, Journal of the British Interplanetary Society, 75, 142
Gillum E., 2023, Personal Communication, Cited with permission
Graham M. J., Kulkarni S. R., Bellm E. C., et al., 2019, Publications of the Astronomical Society of the Pacific, 131, 078001
Hapke B., 2001, Journal of Geophysical Research: Planets, 106, 10039
Haqq-Misra J., Kopparapu R. K., 2012, Acta Astronautica, 72, 15
Hippke M., 2018, Journal of Astrophysics and Astronomy, 39, 73
Hippke M., 2020, The Astronomical Journal, 159, 85
Howard A., Horowitz P., Mead C., et al., 2007, Acta Astronautica, 61, 78

Kaiser N., et al., 2002, in Survey and Other Telescope Technologies and Discoveries. pp 154–164
Kayal H., 2022, in Andresen J., Torres O., eds, , Extraterrestrial Intelligence: Academic and Societal ImplicationsĊambridge Scholars Publishing, pp 87–111
Kayal H., Greiner T., Kaiser T., Oehme S., 2023, in AIAA AVIATION 2023 Forum. p. 4100
Knuth K. H., 2024, in Proceedings of the KavliâĂŞIAU Symposium 387.
Lacki B. C., 2019, A Shiny New Method for SETI: Specular Reflections From Interplanetary Artifacts, arXiv:1903.05839, doi:10.1088/1538-3873/ab1304, https://arxiv.org/abs/1903.05839
Li D., Gajjar V., Wang P., et al., 2020, Research in Astronomy and Astrophysics, 20, 78
Lisker T., 2008, The Astrophysical Journal Supplement Series, 179, 319
Loeb A. A., Laukien F. H., 2023, Journal of Astronomical Instrumentation, 12, 2340003
Loeb A., et al., 2024, Chemical Geology, 670, 122415
Lubin P., 2016, Journal of the British Interplanetary Society, 69, 40
Maire J., et al., 2020, in X-Ray, Optical, and Infrared Detectors for Astronomy IX. pp 670–682
Marcy G. W., 2021, Monthly Notices of the Royal Astronomical Society, 505, 3537
Marcy G. W., et al., 2022a, Optical Technosignature SurveyâĂŤAll-Sky Pilot Program, Manuscript accepted by *MNRAS*âĂŤfinal citation details not yet assigned
Marcy G. W., Tellis N. K., Wishnow E. H., 2022b, Monthly Notices of the Royal Astronomical Society, 509, 3798
Marcy G. W., Tellis N. K., Wishnow E. H., 2022c, Monthly Notices of the Royal Astronomical Society, 515, 3898
Montebugnoli S., et al., 2001, in Ehrenfreund P., Angerer O., Battrick B., eds, Proceedings of the First European Workshop on Exo/Astro-Biology. ESA SP-496. pp 281–284
Nir G., 2024, Earthshadow: `Python` Tools for Astronomical Shadow-Tracking, https://github.com/guynir42/earthshadow
Nir G., et al., 2021a, Publications of the Astronomical Society of the Pacific, 133, 075002
Nir G., Ofek E. O., Ben-Ami S., Segev N., Polishook D., Manulis I., 2021b, Monthly Notices of the Royal Astronomical Society, 505, 2477
Papagiannis M. D., 1978, Quarterly Journal of the Royal Astronomical Society, 19, 277
Pearce E. C., Weiner B., Krantz H., 2020, Journal of Space Safety Engineering, 7, 376
Planck Collaboration 2014, Astronomy & Astrophysics, 571, A16
Price D. C., Enriquez J. E., Brzycki B., et al., 2020, The Astronomical Journal, 159, 86
Reines A. E., Marcy G. W., 2002, Publications of the Astronomical Society of the Pacific, 114, 416
Richmond M. W., Tanaka M., Morokuma T., et al., 2020, Publications of the Astronomical Society of Japan, 72, 3
Rose C., Wright G., 2004, Nature, 431, 47
Sagan C., 1963, Planetary and Space Science, 11, 485
Schwartz R. N., Townes C. H., 1961, Nature, 190, 205
Shostak S., 2020, International Journal of Astrobiology, 19, 456
Solano E., Marcy G. W., Villarroel B., Geier S., Streblyanska A., Lombardi G., Bär R. E., Andruk V. N., 2024, MNRAS, 527, 6312
Steel D., 1995, The Observatory, 115, 78
Stone R. P. S., Wright S. A., Drake F., Muñoz M., Treffers R., Werthimer D., 2005, Astrobiology, 5, 604
Szydagis M., Knuth K. H., Kugielsky B., Levy C., 2025, Progress in Aerospace Sciences, p. 101099
Tarter J., 2001, Annual Review of Astronomy and Astrophysics, 39, 511
Tellis N. K., Marcy G. W., 2017, The Astronomical Journal, 153, 251
Valdes F., Freitas R. A., 1983, Icarus, 53, 453
Vallee J., Aubeck C., 2010, Wonders in the sky: Unexplained aerial objects from antiquity to modern times. Penguin
Vasile M., Walker L., Campbell A., Marto S., Murray P., Marshall S., Savitski V., 2024, Scientific Reports, 14, 1570
Villarroel B., Marcy G., 2023, A New Era of Optical SETI: The Search for Artificial Objects of Non-Human Origin, The Debrief, February 2023
Villarroel B., et al., 2021, Scientific Reports, 11, 12794
Villarroel B., Solano E., Guergouri H., et al., 2022a, Is There a Background Population of High-Albedo Objects in Geosynchronous Orbits around Earth?, arXiv:2204.06091, doi:10.48550/arXiv.2204.06091, https://arxiv.org/abs/2204.06091
Villarroel B., et al., 2022b, Universe, 8, 561
Villarroel B., Mattsson L., Guergouri H., Solano E., Geier S., Dom O. N., Ward M. J., 2022c, Acta Astronautica, 194, 106
Watters W. A., Loeb A., Laukien F., Cloete R., Delacroix A., Dobroshinsky S., et al., 2023, Journal of Astronomical Instrumentation, 12, 2340006
Wright S. A., Horowitz P., Maire J., Werthimer D., Antonio F., Aronson M. e. a., 2018, in Proc. SPIE 10702, *Ground-based and Airborne Instrumentation for Astronomy VII*. , doi:10.1117/12.2314268, https://doi.org/10.1117/12.2314268
Zuckerman B., 1985, Acta Astronautica, 12, 127